

**'Computer Modelling Techniques for Industrial and  
Marine Cyclo-converter Drives'**

by Roger D. White, BSc

Thesis submitted to The University of Nottingham for  
the Degree of Doctor of Philosophy, May 1992.

<u>Contents</u>	Page
Abstract	i
Acknowledgments	iii
List of figures	iv
List of abbreviations	vii
 <b>Chapter 1: Introduction:-</b>	 <b>1</b>
1.1 General introduction	1
1.2 Review of industrial and marine drives	2
1.2.1 Marine drives	2
1.2.2 Industrial drives	4
1.3 Power control for ac drives	5
1.3.1 Pulse width modulated inverters	6
1.3.2 Synchro-converter drives	6
1.3.3 Cyclo-converter drive	7
1.4 Cyclo-converter operation	8
1.5 Synchronous/induction machines	12
1.6 Control system design	14
1.6.1 Vector control techniques	15
1.7 The supply network	16
1.8 Current research into cyclo-converter drives	18
1.9 Aims of this research work	19
 <b>Chapter 2: Literature review:-</b>	 <b>22</b>
2.1 Introduction	22
2.2 Mathematical analysis of cyclo-converters by Pelly	22
2.3 Modelling a steady state system	24

2.4	Models including current discontinuities	25
2.5	Models including overlap in the converter	26
2.6	Models analysing supply side harmonics	27
2.7	Modelling of the reverse blocking of thyristors	27

### **Chapter 3: Modelling of the Cyclo-converter Machine Drive:-**

3.1	Description of the computer system	29
3.2	Computer model flow charts	30
3.3	Runga Kutta 2nd, and 4th, order routines	30
3.4	Modelling the cyclo-converter	33
3.4.1	Modelling the cyclo-converter switching sequence	34
3.4.2	Modelling the supply system and decoupling reactance	35
3.4.3	Modelling the cyclo-converter interbridge delay and motor phase current discontinuities	36
3.4.4	Modelling overlap within the cyclo-converter	38
3.5	Modelling the machines	43
3.5.1	Introduction to generalised machine theory	44
3.5.2	Synchronous machine modelling	44
3.5.3	Induction machine modelling	46
3.5.4	Zero sequence components of current in the machine windings	50
3.5.5	Voltage to frequency control	50
3.6	Operation of the computer model	51
3.6.1	Introduction	51
3.6.2	Test 1a The effect of varying the time interval in the computer program	52
3.6.3	Test 1b The accuracy of numerical integration in the computer program	55
3.6.4	Time constants within the machine being	57

modelled and the reverse blocking of thyristors

3.6.5 Fourier analysis subroutine	58
3.6.6 Test 1c Characteristic performance of the Fourier analysis subroutine	61
3.6.7 Assumptions made within the simulation	61

#### **Chapter 4: Test results from CEGELEC, Newcastle University, and Pelly's analytical work:-**

4.1 Description of cyclo-converter drive installed at Wearmouth Colliery	65
4.1.1 Test 2 Comparison with results obtained at Wearmouth Colliery	66
4.2 Description of the cyclo-converter at Newcastle University	72
4.2.1 Test 3 Comparison with results obtained at Newcastle University	73
4.3 Description of Pelly's analytical work	73
4.3.1 Harmonic analysis of the output voltage of the cyclo-converter	73
4.3.2 Harmonic analysis of the input current of a cycloconverter	77
4.3.3 The results of Pelly's analytical work	78

#### **Chapter 5: The Cyclo-converter, machine and supply operational ratings and characteristics:-**

5.1 Cyclo-converter device losses and ratings	81
5.2 Motor winding losses and ratings	82
5.3 High voltage network electrical operating characteristics and cyclo-converter output characteristics	83
5.3.1 RMS ratings	84
5.3.2 Distortion factor	84
5.3.3 Power factor	86
5.3.4 Power and efficiency calculations	88

5.3.5 Voltage regulation	89
5.3.6 Torque ripple factor	90

## **Chapter 6 Testing of system characteristics and complete systems**

6.1 The power system to be analysed	92
6.2 The synchronous machine load	93
6.2.1 Control system effects	94
6.3 The characteristic behaviour of the basic model	95
6.3.1 Test 4: Monitoring of the system behaviour from 4-22 Hz	95
6.4 System characteristics and their effects	97
6.4.1 Test 5: The effect of interbridge delay	97
6.4.2 Test 6: The effect of overlap	102
6.4.3 Test 7: The effect of the supply reactances	109
6.4.4 Test 8: The effect of the decoupling reactances	113
6.5 The modelling of complete systems	117
6.5.1 Test 9: Comparison of Pelly's analytical model and the computer model with a sinewave output	119
6.5.2 Test 10 Comparison of Pelly's analytical model and the simplified converter and the dq axis model	123
6.5.3 Test 11 Comparison of the simplified model 1 and the complex model 5	128
6.5.4 Test 12 Comparison of the simplified converter and supply reactance model 3, and the complex model 5	133
6.5.5 Test 13: Comparison of the typical industrial model 4, and the simplified model 1	137
6.5.6 Test 14: Comparison of the simplified converter model 1 and the Thevenin motor model 2	141

## **Chapter 7 Effect of system parameters on simulated results**

<b>7.1</b>	<b>Introduction</b>	<b>147</b>
<b>7.2</b>	<b>Test 5 Interbridge changeover delay</b>	<b>147</b>
<b>7.2.1</b>	<b>Input current harmonics</b>	<b>149</b>
<b>7.2.2</b>	<b>Output phase voltage</b>	<b>151</b>
<b>7.2.3</b>	<b>Output voltage harmonics</b>	<b>152</b>
<b>7.2.4</b>	<b>Output phase current</b>	<b>152</b>
<b>7.2.5</b>	<b>Output current harmonics</b>	<b>153</b>
<b>7.3</b>	<b>Test 6 Overlap within the cyclo-converter</b>	<b>153</b>
<b>7.3.1</b>	<b>Input supply voltage</b>	<b>154</b>
<b>7.3.2</b>	<b>Input voltage harmonics</b>	<b>155</b>
<b>7.3.3</b>	<b>Input current and output current harmonic content</b>	<b>156</b>
<b>7.3.4</b>	<b>Output phase voltage</b>	<b>157</b>
<b>7.3.5</b>	<b>Output voltage harmonics</b>	<b>158</b>
<b>7.3.6</b>	<b>Output phase current</b>	<b>160</b>
<b>7.4</b>	<b>Test 7 Supply system reactance (including overlap)</b>	<b>160</b>
<b>7.4.1</b>	<b>Input supply voltage</b>	<b>161</b>
<b>7.4.2</b>	<b>Input current harmonics</b>	<b>161</b>
<b>7.4.3</b>	<b>Output phase voltage</b>	<b>162</b>
<b>7.4.4</b>	<b>Output voltage harmonics</b>	<b>162</b>
<b>7.5</b>	<b>Test 8 Decoupling reactance (including overlap)</b>	<b>162</b>
<b>7.5.1</b>	<b>Supply voltage harmonics</b>	<b>163</b>
<b>7.5.2</b>	<b>Output phase voltage</b>	<b>163</b>
<b>7.5.3</b>	<b>Output voltage harmonics</b>	<b>163</b>

## **Chapter 8 The computational analysis of various system models**

<b>8.1</b>	<b>The system models commonly used</b>	<b>165</b>
<b>8.1.1</b>	<b>Introduction</b>	<b>165</b>
<b>8.1.2</b>	<b>The base model</b>	<b>167</b>
<b>8.1.3</b>	<b>The system models to be examined</b>	<b>167</b>
<b>8.2</b>	<b>Test 9 Comparison of Pelly's analytical Model with sinewave output current produced computationally</b>	<b>169</b>
<b>8.2.1</b>	<b>Input current harmonics</b>	<b>169</b>
<b>8.2.2</b>	<b>Output voltage harmonics</b>	<b>170</b>
<b>8.3</b>	<b>Test 10 Comparison of Pelly's analytical Model and the simplified converter and the dq axis Model 1</b>	<b>170</b>
<b>8.3.1</b>	<b>Input current harmonics</b>	<b>171</b>
<b>8.3.2</b>	<b>Output voltage harmonics</b>	<b>171</b>
<b>8.3.3</b>	<b>Output phase voltage</b>	<b>171</b>
<b>8.3.4</b>	<b>Output phase current</b>	<b>172</b>
<b>8.4</b>	<b>Test 11: Comparison of results for simple and complex modelling of the synchronous motor: models 1, 5</b>	<b>173</b>
<b>8.4.1</b>	<b>Input voltage harmonics</b>	<b>174</b>
<b>8.4.2</b>	<b>Input current harmonics</b>	<b>174</b>
<b>8.4.3</b>	<b>Output phase voltage</b>	<b>175</b>
<b>8.4.4</b>	<b>Output voltage harmonics</b>	<b>176</b>
<b>8.4.5</b>	<b>Output phase current</b>	<b>176</b>
<b>8.4.6</b>	<b>Output current harmonics</b>	<b>177</b>
<b>8.5</b>	<b>Test 12: Comparison of the results for the complex Model 5 and Model 3 this models the supply reactance and the effects of overlap</b>	<b>178</b>
<b>8.5.1</b>	<b>Input voltage harmonics</b>	<b>178</b>
<b>8.5.2</b>	<b>Input current harmonics</b>	<b>179</b>
<b>8.5.3</b>	<b>Output voltage harmonics</b>	<b>179</b>

8.5.4	Output current harmonics	179
8.6	Test 13: Comparison of results for the simple and industrial, Model 1, 4	180
8.6.1	Input voltage harmonics	180
8.6.2	Input current harmonics	180
8.6.3	Output phase voltage	181
8.6.4	Output voltage harmonics	181
8.7	Test 14: Comparison of the simple Thevenin Model 2 and the complex dq axis model for the synchronous motor Model 1	181
8.7.1	Motor load angle and its behaviour	181
8.7.2	Motor torque ripple and its behaviour	182
8.7.3	Motor efficiency and its behaviour	183
8.7.4	Cyclo-converter waveforms	184
<b>Chapter 9 Discussion of results</b>		
9.1	Introduction	185
9.2	Interbridge delay	185
9.3	Commutation overlap	187
9.4	Supply reactance	188
9.5	Decoupling reactance	190
9.6	Pelly's model	191
9.7	Simplified model 1	193
9.8	The Thevenin model 2	194
9.9	Simplified model 3 with supply reactance	195
9.10	Industrial model 4	196
9.11	The complex model 5	196
9.12	Influence of the cyclo-converter on the auxiliary supply	198
<b>Chapter 10 Conclusions</b>		199



- A1 Synchronous motor characteristics as used in Tests 10-15.**
- A1.1 Rated motor characteristics.**
- A1.2 Motor parameters.**
- A1.3 Per unit notation.**

**Appendix B****Table B.1**

Results from Pelly's mathematical analysis and details of the relationship between the drive frequency and the percentage harmonics of the input current of a 6 pulse cyclo-converter.

**Table B.2**

Results from Pelly's mathematical analysis and details of the relationship between the drive frequency and the percentage harmonics of the output voltage of a 6 pulse cyclo-converter.

**Appendix C**

The commutation process within the converter:

- C1 The positive converter:**
  - Commutation process from C1 to A1,  
Calculation of the currents during overlap,  
Fig's 3.2a 3.2b: commutation process.
  - Commutation process from B2 to C2  
Calculation of the currents during overlap,  
Fig's 3.3: commutation process.
- C2 The negative converter:**
  - Commutation process from C2' to A2',  
Calculation of the currents during overlap,  
Fig's 3.4: commutation process.
  - Commutation process from B1' to C1',  
Calculation of the currents during overlap,  
Fig's 3.5: commutation process.

**Appendix D**

Cyclo-converter characteristic waveforms for models 1 to 5:

- (a) Input voltage and current waveforms,
- (b) Harmonic analysis of input voltage and current waveforms.

**Limits for harmonics in the United Kingdom  
Electricity Supply System**

**Table E1 Permitted harmonic currents for any one  
consumer at the point of common coupling**

**Table E2 Harmonic voltage distortion limits at any  
point on the system**

## Abstract

Large cyclo-converter drives using either synchronous or induction machines are found in a number of low speed high torque applications: these include steel mills, gearless cement mills, mine winders and ice breakers.

The cyclo-converter output frequency is synthesised from portions of the high voltage supply system. At low frequencies this produces an output current waveform which is reasonably sinusoidal, as the frequency increases the waveform become more distorted. There is concern for the level of current harmonics produced by the cyclo-converter in both the motor windings and the supply system. The waveform distortion is mainly due to the switching action of the cyclo-converter, this is modified by the effects of interbridge changover delay, commutation overlap, the supply and decoupling reactances.

Industrial drives are required to conform to the Electricity Council's regulations on input current harmonics and voltage waveform distortion. In marine drives the main generators feed the ship propulsion system and the ship's auxiliary supplies. The level of interference produced by the converter input line current on the supply network is of particular concern. High levels of voltage distortion may cause malfunction of the auxiliary equipment and produce large torque pulsations in the supply alternator.

The cyclo-converter generates unwanted harmonics in the output current waveforms, these are responsible for torque pulsations on the motor drive. With naval marine drives the torque pulsation is of particular interest, since this level must be minimised to increase the sensitivity of detecting instruments such as passive sonar.

To date, mathematical models and computer based models have not detailed all the aspects which are responsible for the distortion to the converter input and output waveforms. This thesis seeks to address this and identify the effects on the converter performance of, the converter interbridge delay, overlap and the supply parameters supply and decoupling reactance. Various motor models will also be examined.

The author has used the mathematical work by Pelly as a basis, and has identified the percentage errors in the level of harmonic currents which are likely to be introduced if his results are used in designing new systems.

Comparisons will be made with experimentally produced results obtained from a mine winder at the Wearmouth Colliery. Results from a lower powered cyclo-converter produced experimentally and computationally at Newcastle University will also be examined.

### Acknowledgements

The author wishes to express his sincere gratitude the following people:

- (1) To my project supervisor Dr. K. Bradley for his supervision of the project, guidance, technical support, and encouragement throughout the project,
- (2) To CEGELECT Projects for permission to publish the results from the Wearmouth Colliery tests, and for the provision of motor and power system data without which this research into high power systems could not have been possible,
- (3) Senior Electrical Engineers at CEGELEC and GEC Machines who have provided advice on cyclo-converters, synchronous and induction motor design and operating characteristics in the working environment,
- (4) To the operating staff in the Computing Centre at Derbyshire College of Higher Education, for all the time given in the operation of the computer system and in the preparation of the plots from the computer simulation.

### List of Figures

- Fig 1.1 3 phase cyclo-converter with isolation transformers  
 Fig 1.2 3 phase cyclo-converter with decoupling reactors

**Test 1a: Variation of computer modelling parameters**

- Fig 3.1a Characteristic performance of the time interval within the simulator

**Test 1b: Characteristic behaviour of the Runge Kutta Integration routines**

- Fig 3.1b Performance of the 2nd and 4th order numerical integration routines

**Test 1c: Characteristic behaviour of the Fourier analysis routines**

- Fig 3.1c Characteristic performance of the Fourier analysis routines

- Fig 3.2a Overlap positive converter devices C1 to A1  
 Fig 3.2b Equivalent circuit for overlap in the converter  
 Fig 3.3 Overlap positive converter devices B2 to C2  
 Fig 3.4 Overlap negative converter devices C2' to A2'  
 Fig 3.5 Overlap negative converter devices C1' to B1'  
 Fig 3.6 3 phase synchronous machine dq axis model  
 Fig 3.7 3 phase induction machine dq axis model  
 Fig 3.8 Computer model flow chart Thevenin Supply

**Test 2: Comparison with results obtained at Weirmouth Colliery**

- Fig 4.1a Cyclo-converter fed induction motor driving Koepe winder at Wearmouth Colliery  
 Fig 4.1b Converter output voltage and current waveforms at 5 Hz drive frequency Wearmouth Colliery  
 Fig 4.1c Spectrum of the voltage and current waveforms at 5 Hz drive frequency Wearmouth Colliery  
 Fig 4.1d Simulation results of voltage and current at 5 Hz drive frequency  
 Fig 4.1e Simulation results for spectrum of voltage and current at 5 Hz drive frequency

**Test 3: Comparison with results obtained at Newcastle University**

- Fig 4.2a Converter output voltage and current waveforms at 16.667 Hz (Newcastle paper)  
 Fig 4.2b Simulation of voltage and current at 16.667 Hz

**Test 4 Monitor of the system behaviour**

(The Figure number is designated with the Chapter number followed by the Test Number)

- Fig 6.4a Waveforms of system with sinewave output current  
 Fig 6.4b Harmonics of system with sinewave output current  
 Fig 6.4c Waveforms of system with Model 1  
 Fig 6.4d Harmonics of system with Model 1

Fig 6.4e Waveforms of system with Model 2

Fig 6.4f Harmonics of system with Model 2

Fig 6.4g Waveforms of system with Model 3

Fig 6.4h Harmonics of system with Model 3

Fig 6.4i Waveforms of system with Model 4

Fig 6.4j Harmonics of system with Model 4

Fig 6.4k Waveforms of system with Model 5

Fig 6.4l Harmonics of system with Model 5

Fig 6.4m Waveform of typical commutation process

Fig 6.4n Waveform of commutation with and without  
the decoupling reactor

#### 6.4 System characteristics and their effects

##### Test 5: The effect of interbridge delay

Fig 6.5a Input current harmonic ripple (%)  
Output current harmonic ripple (%)

Fig 6.5b Output voltage harmonic ripple (%)  
Output current harmonic ripple (%)

Fig 6.5c Output phase voltage (V)  
Output phase current (A)

##### Test 6: The effect of overlap

Fig 6.6a Input current harmonic ripple (%)  
Input voltage harmonic ripple (%)

Fig 6.6b Input Voltage Regulation (%)

Fig 6.6c Output phase voltage (V)  
Output phase current (A)

Fig 6.6d Output voltage harmonic ripple (%)

Fig 6.6e Output current harmonic ripple (%)

##### Test 7: The effect of supply reactance

Fig 6.7a Input current harmonic ripple (%)  
Input voltage harmonic ripple (%)

Fig 6.7b Output voltage harmonic ripple (%)

Fig 6.7c Output phase voltage (V)  
Output phase current (A)

##### Test 8: The effects of decoupling reactance

Fig 6.8a Input current harmonic ripple (%)  
Input voltage harmonic ripple (%)

Fig 6.8b Output voltage harmonic ripple (%)

Fig 6.8c Output phase voltage (V)  
Output phase current (A)

**Test 9: Comparison of Pelly's analytical Model and the computer model with a sinewave output**

**Fig 6.9a** Input current harmonic ripple (%)  
Output load power factor

**Fig 6.9b** Output voltage harmonic ripple (%)  
Output load power factor

**Test 10: Comparison of Pelly's analytical model and the simplified converter and dq axis model 1**

**Fig 6.10a** Input current harmonic ripple (%)

**Fig 6.10b** Output voltage harmonic ripple (%)  
Output load power factor

**Fig 6.10c** Output phase voltage (V)  
Output phase current (A)

**Test 11: Comparison of the simplified model 1 and the complex model 5**

**Fig 6.11a** Input current harmonic ripple (%)  
Input voltage harmonic ripple (%)

**Fig 6.11b** Input voltage regulation (%)

**Fig 6.11c** Output voltage harmonic ripple (%)  
Output current harmonic ripple (%)

**Fig 6.11d** Output phase voltage (V)  
Output phase current (A)

**Test 12: Comparison of the simplified converter and supply reactance model 3 ,and the complex model 5**

**Fig 6.12a** Input current harmonic ripple (%)  
Input voltage harmonic ripple (%)

**Fig 6.12b** Output voltage harmonic ripple (%)  
Output current harmonic ripple (%)

**Fig 6.12c** Output phase voltage (V)  
Output phase current (A)

**Test 13: Comparison of the typical industrial supply model 4, and simplified model 1**

**Fig 6.13a** Input current harmonic ripple (%)  
Input voltage harmonic ripple (%)

**Fig 6.13b** Output voltage harmonic ripple (%)  
Output current harmonic ripple (%)

**Fig 6.13c** Output phase voltage (V)  
Output phase current (A)

**Test 14: Comparison of the simplified converter and Thevenin motor model**

**Fig 6.14a** Motor efficiency (%)

**Fig 6.14b** Motor torque ripple factor (PU)

**Fig 6.14c** Input current harmonics (%)

**Fig 6.14d** Output current harmonics (%)



### List of Abbreviations

#### General abbreviations:

$i$	Instantaneous current
$I_{av}$	Average current
$I_{ph}$	Output phase current
$I_{pk}$	Peak current
$I_{rms}$	rms current
$p$	$d/dt$
$V_m$	Maximun voltage
$V_{rms}$	rms voltage
$v$	Instantaneous voltage

#### Supply Abbreviations:

$I_s$	Supply line current
$L_s$	Supply inductance
$L_s(\text{overlap})$	Supply inductance (overlap process)
$L_d$	Converter decoupling inductance
$L_d(\text{overlap})$	Converter decoupling inductance(overlap process)
$V_s$	Supply line voltage
$V_l$	Voltage lost due to supply reactance
$V_l(\text{overlap})$	Voltage lost due to supply reactance(overlap process)
$V_{ph}$	Supply phase voltage
$X_s$	Supply reactance
$X_d$	Converter decoupling reactance

#### Converter Abbreviations:

$I_{ph}$	Phase current
$I_{ov}$	Current during overlap
$V_{ov}$	Voltage lost due to overlap
$d$	Modulation depth
$R_b$	Reverse blocking resistance for thyristor
$P_d$	Power dissipation

#### Motor Abbreviations:

$[I]$	Current matrix
$[G]$	Resistive matrix derived from inductance variation
$[L]$	Inductance matrix
$[R]$	Resistance matrix
$[V]$	Voltage matrix
$L_a$	Load angle between the stator and rotor
$L_{st}$	Motor sub-transient time constant
$PP$	Pole pairs
$Q$	Angle between stator and rotor field
$R_a$	Stator resistance
Slip	Operating slip of the machine
tor	Instantaneous torque
Tor	Motor torque

Tor(av)      Average motor torque  
 Tor(rms)     RMS motor torque  
 Tor(rated)   Motor torque rated  
 T<sub>m</sub>          Motor Time constant  
 ω<sub>m</sub>          Angular velocity

P<sub>sc</sub>          Stator core loss  
 P<sub>scu</sub>        Stator copper loss  
 P<sub>rcu</sub>        Rotor damper bar loss  
 P<sub>f</sub>          Rotor field loss

#### Synchronous Motor Abbreviations:

##### D axis inductances:

I<sub>d</sub>    d axis stator current  
 I<sub>kd</sub>   d axis damper current  
 I<sub>f</sub>    Field current

L<sub>ad</sub>   Mutual inductance  
 L      Leakage inductance  
 L<sub>d</sub>    d axis inductance ( $L_{ad} + L$ )  
 L<sub>kd</sub>   d axis inductance damper winding  
 M<sub>dd</sub>   Mutual inductance D axis / d axis damper ( $L_{ad} + L$ )  
 M<sub>ddf</sub>   Mutual inductance d axis damper / field axis ( $L_{ad} + L$ )  
 M<sub>df</sub>   Mutual inductance d axis / motor field ( $L_{ad}$ )  
 L<sub>f</sub>    Field inductance ( $L_f + L_{ad}$ )  
 R<sub>c</sub>    Resistance of core  
 R<sub>d</sub>    d axis stator resistance  
 R<sub>dd</sub>   d axis damper resistance  
 R<sub>f</sub>    Field resistance

##### Q axis inductances:

I<sub>q</sub>    q axis stator current  
 I<sub>kq</sub>   q axis damper current

L<sub>aq</sub>   Mutual inductance  
 L<sub>q</sub>    q axis inductance ( $L_{aq} + L$ )  
 M<sub>qq</sub>   Mutual inductance Q axis /q axis damper ( $L_{aq}$ )  
 L<sub>kq</sub>   q axis inductance damper winding ( $L_{kq} + L_{aq}$ )  
 R<sub>q</sub>    q axis stator resistance  
 R<sub>qq</sub>   q axis damper resistance

#### Induction motor abbreviations:

L<sub>d</sub>    d axis inductance  
 M<sub>dd</sub>   Mutual inductance D axis / d axis damper  
 R<sub>d</sub>    d axis stator resistance  
 R<sub>dd</sub>   d axis damper resistance

L<sub>q</sub>    q axis inductance  
 M<sub>qq</sub>   Mutual inductance Q axis /q axis damper  
 R<sub>q</sub>    q axis stator resistance  
 R<sub>qq</sub>   q axis damper resistance

## Chapter 1

### Introduction

#### 1.1 General introduction

It is increasingly important to be able to predict the operational performance of power systems and thereby enable designers to minimise design faults and poor operational performance prior to manufacture. A computer model of a complete power system provides a mechanism whereby the behaviour of the system may be analysed in detail so that the operational performance can be optimised.

Cyclo-converters are used in a variety of industrial and marine applications, the operational and system characteristics are required by design engineers to make an accurate prediction of the required ratings and characteristics of the converter, motor and supply network. Power converters have disadvantages in that they are responsible for the generation of harmonics and subsequent disturbance to the supply network and the machine load. In the design stage the level of harmonics likely to be produced by a converter should be known, since it will produce undesirable torque pulsations in the motor and the supply alternator

## 1.2 Review of industrial and marine drives

Marine and industrial cyclo-converters are limited normally to high power levels with high torque at low speed. Cyclo-converters are not able to operate at high speeds due to the commutation process. The cost of converters for low speed high torque applications make the cyclo-converter a viable option.

### 1.2.1 Marine Drives

A ship propulsion system designed with fixed pitch propellers requires a reversible variable speed drive in order that there can be control of the ship speed and direction. It is now common place for a ship to use an ac generator system with a form of electronic power converter to provide controlled power to the ac/dc motors. This arrangement allows the same generators to supply the ship propulsion and provide for auxiliary services using separate transformers. Alternatively a motor generator set may be used to ensure that there is complete electrical isolation between the power and auxiliary circuits.

Marine generators and drive systems are a compromise which endeavour to maximise availability, reliability, performance, fuel economy and minimise weight, space, and cost. The normal mode of drive is therefore direct coupling between the motor and the propeller shaft to avoid gearbox

vibration. The application of the electrical drive is well established due the advantages that it provides to the ship designer Ref.4:-

The flexibility of the construction and the ease of control of the drive system.

Ease of control of the propulsion system provided by computer or microprocessor control.

A considerable saving in the size of the propulsion equipment reducing the length of the propeller shaft, making it less subject to torque pulses from the drive.

The level of torque pulsations of an electrical drive has been long established as being significantly lower than a mechanical drive. A fundamental requirement in naval ship propulsion design is low noise operation. This has been brought about because of the increasing sensitivity of detecting instruments such as passive sonar. The main purpose of anti submarine warfare is to use a passive sonar towed behind the frigate. it is essential therefore that the ship provides a quiet platform to maximise the effectiveness of the detection equipment.

Submarines have used a battery supply feeding dc motors with a smooth current for many years, surface ships however are designed to avoid the cost, complexity and

space required for such a system. Power converters do not produce a smooth output and therefore filtering is required on dc motors or harmonic elimination maybe required on ac drive systems.

Drives for frigates require that the ship must be capable of stopping and reversing quickly. This can be best achieved with electrical drives which have a certain overload capability.

Perhaps the most important aspect of marine propulsion systems is that the system fault levels are usually very low due to the fact that the ship generators invariably have a high source impedance. The effect of this is to produce relatively large overlap angles which have to be allowed for in any assessment of the converter performance. Overlap angles of 20% are not uncommon and their effect on the supply system is significant.

#### 1.2.2 Industrial drives

The cyclo-converter has been known about since the development of the grid controlled mercury arc rectifiers in the 1930's. The system was developed to produce the 16.66 Hz power for traction applications from the 50 Hz supply system. Since that time it has been used in a variety of applications including induction heating, low frequency arc furnace for slag refining, and motor drives. During the late

1940's there was development of motor drives in the area of slow speed high power applications in roller table drives in steel mills, gearless cement mill drives, winder drives for colliery pit heads and, laterly reverse rolling mills with extremely high dynamic requirements for torque and speed reversal.

The drive can be produced at any power level and uses the least sophisticated switching element the thyristor. The converter can be used to supply either a synchronous or asynchronous motor. For simple applications like pumps and fans the asynchronous motor is normally used since precise control is not essential. However, where more accurate control of the dynamic load is required as in the case of a steel mill, it is more preferable to use the synchronous motor. With the synchronous motor the excitation can be controlled from a separate independent source. The motor flux can be set more precisely allowing finer control over the torque.

### 1.3 Power control for ac drives

There are basically three types of power converter that can be considered for ship propulsion, pulse width modulation (pwm), synchro-converter drive (synchronous machine only), and cyclo-converter.

### 1.3.1 Pulse width modulated inverters

The development of the high power gate turn off thyristor (GTO) and the micro processor has had a significant effect on the development and application of this form of converter with both synchronous and asynchronous motors. The elimination of the commutation circuits has made this converter attractive however it still has to face up to the high costs of these devices when used in high power applications. The development of the micro processor has enabled the control strategy to be developed with a high degree of complexity and sophistication. The design of systems capable of dealing with harmonic elimination have enabled engineers to ensure that the operational characteristic of the converter are maximised.

### 1.3.2 Synchro-converter drive

This is a dc link converter which uses the ac machine generated back emf's to effectively line commute the inverter feeding the machine. The inverter produces a stepped rotation of the stator mmf wave as the convertor commutates from one thyristor to another. This clocking of the stator mmf produces a pulsating torque superimposed on the mean torque. It is therefore considered that the synchro converter drive is not suitable for marine applications due to the level of vibration it will produce in the propulsion

KE2



system. The synchro drive naturally lends itself to a high speed drive, propellers operate at low speed and gearboxes are not acceptable in drives requiring low vibration levels.

### 1.3.3 Cyclo-converter drive

The cyclo-converter is a line commutated converter system which can be used to provide a low frequency ac supply. A low frequency supply is used to provide a slow speed drive as this means fewer poles on the motor which, in turn make the motor design easier. It can be used to supply both synchronous and induction motors in industrial and marine applications. For ship propulsion duty, the synchronous motor is preferred because it can be provided more easily with the long air gaps, which are desirable on large machines on ships. Although the cyclo-converter can provide a voltage and current output which is closer to a sinewave than is possible with a synchro-converter, it is still rich in harmonics. The dominant harmonics produced by the six pulse bridge are based around the 6th and 12th etc. (of the supply frequency); due to the modulation process used to provide the low frequency waveform there are side bands of the harmonic base frequency.

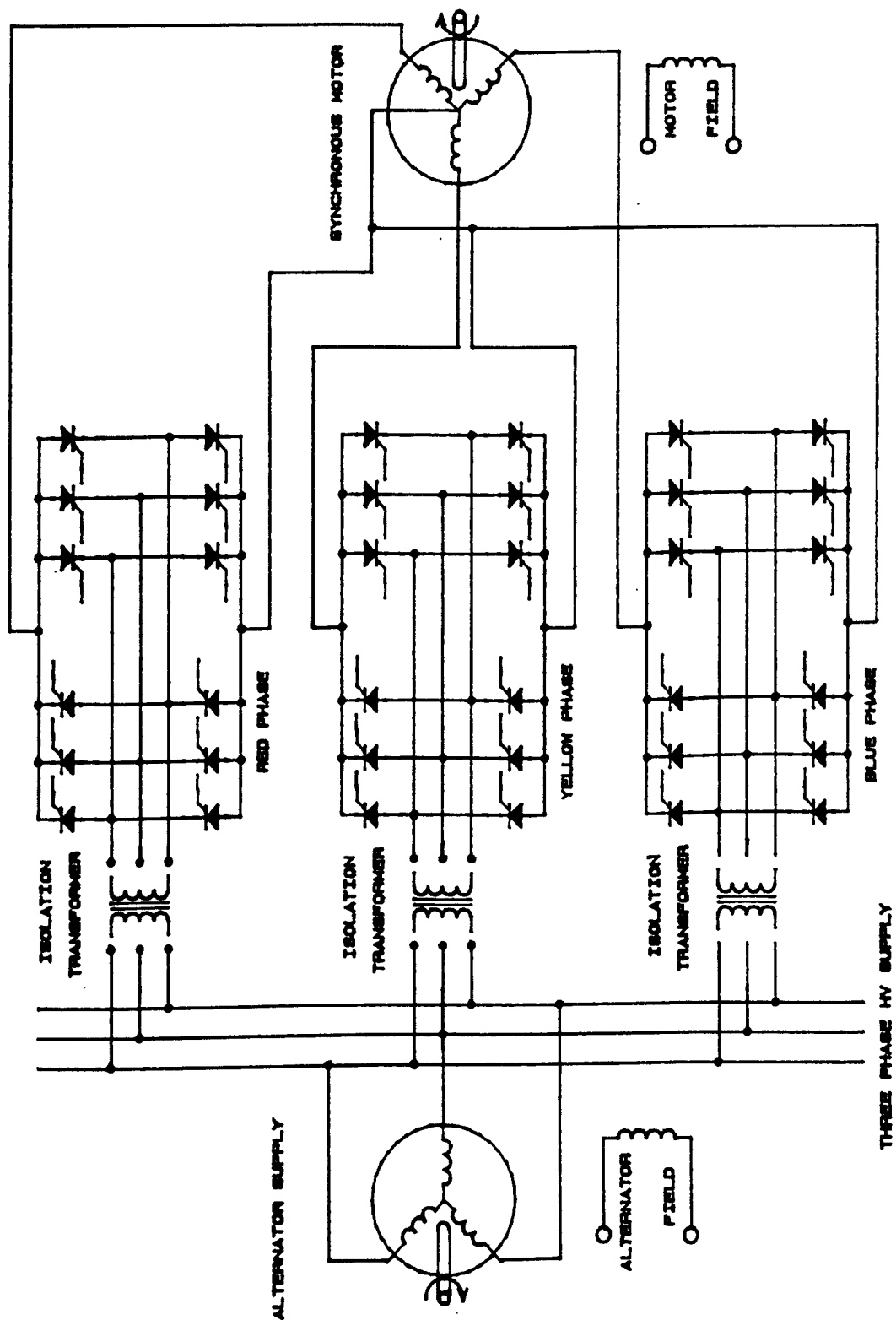
#### 1.4 Cyclo-converter operation

Speed control of squirrel cage induction motors and synchronous motors requires a drive that is capable of regulating both voltage and frequency. This may be achieved with cyclo-converters with naturally commutated devices or a forced commutated inverter with an intermediate d.c. link. However, the cost of the commutation equipment, smoothing circuits and two stages of power conditioning for the inverter drive has to be compared with the great number of thyristors needed for cyclo-converters. With cyclo-converters the required device ratings concerning turn-off time, current rise time and rate of change of voltage ( $dv/dt$ ) are considerably less arduous than for devices required with an inverter drive system. The cyclo-converter is a frequency changer and as such, is concerned with the conversion of energy by synthesising a low frequency wave from the appropriate sections of a higher frequency source. Cyclo-converters operate at frequencies below the supply source frequency and applications are normally restricted to low speed high power drives as in large industrial or marine applications.

A cyclo-converter consists of a pair of fully controlled thyristor bridges connected in a back to back arrangement, as shown in Fig 1.1. The converter is basically the same unit as used in a naturally commutating dc rectifier with

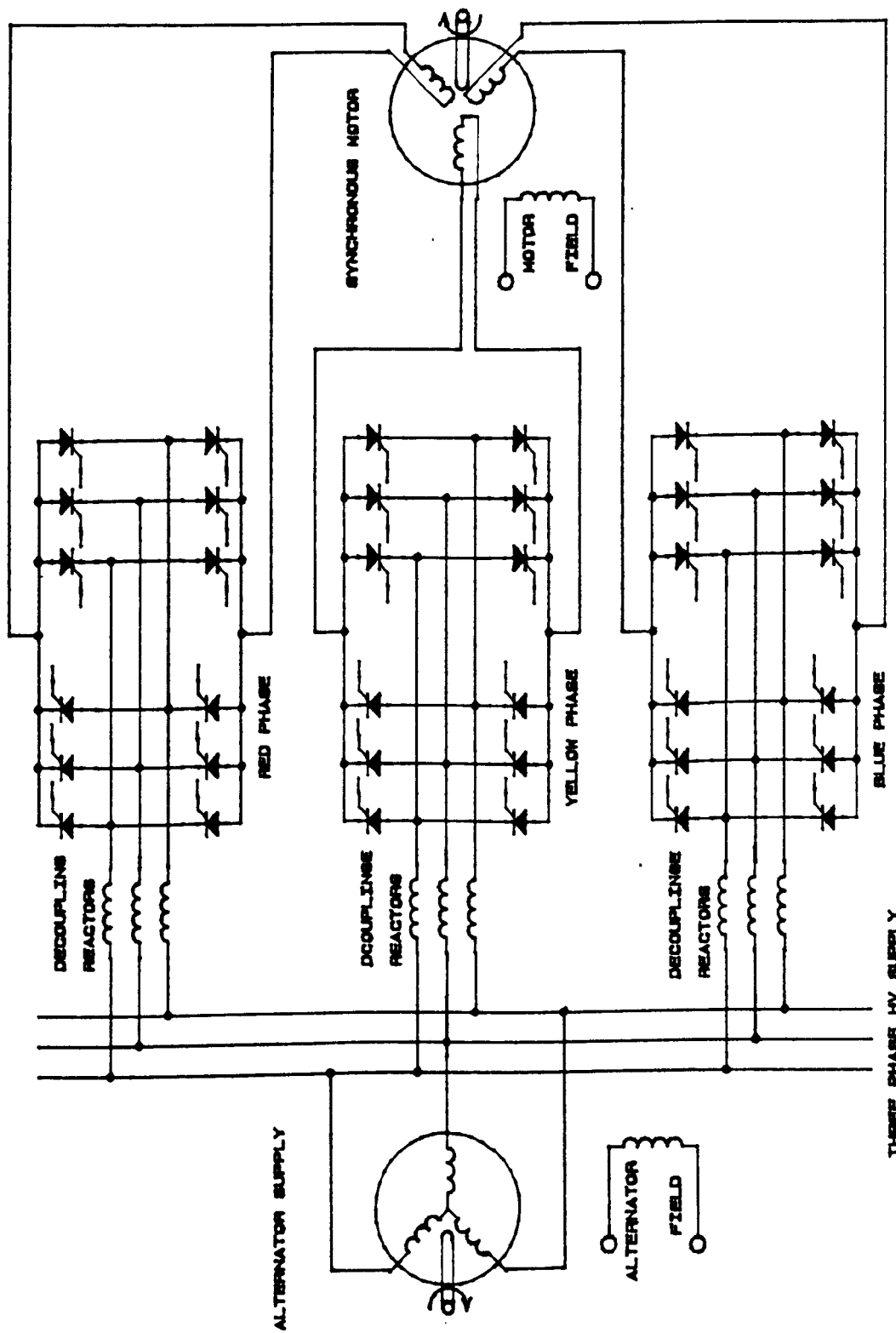
the positive rectifier supplying the positive current to the load, whilst the negative rectifier supplies negative half cycle to the load. Each half of the converter therefore consists of six naturally commutating thyristors controlling one direction of load current. The synthesised cyclo-converter output voltage supplied by a 6 pulse supply is directly related to the cosine of the delay of the firing angle and as such cosine time waves are compared to the reference sine wave to establish the delay angle for each device in the cyclo-converter. With a.c. motor drives it is necessary to provide voltage to frequency control, this can be simply achieved by reducing the reference sine wave compared with the cosine timing waveforms.

Three converter units are required to produce a three phase supply for the induction motor. The synthesised output voltage produces a low frequency wave from the high frequency 50 Hz supply system. This is achieved by the sequential switching of the supply terminals to the induction motor terminals. The motor terminal voltage is synthesised from portions of the supply line voltages. At low output frequencies the output voltage contains many portions of the supply waveform and produces a reasonably sinusoidal output current waveform. Output frequencies greater than one third of the mains frequency produce a converter output voltage and current distorted by the beating effect between the supply and load frequency. This



3 PHASE CYCLO-CONVERTER WITH ISOLATION TRANSFORMERS

FIG 1.1



3 PHASE CYCLO-CONVERTER WITH DECOUPLING REACTORS

FIG 1.2

produces a significant level of harmonic content in the converter output current, and consequently harmonic torque pulsations.

To provide accurate results it is necessary to model the supply system for the converter. This can prove to be quite complex since it may be necessary to model the supply from individual feeds isolated by transformers or reactors, or in the case of marine drives a high voltage alternator. The computer modelling of the power supply is extremely complex if it is to be modelled accurately. It is possible to simplify the power supply arrangements from a high voltage supply network using, conventional circuit theory and per unit notation prior to inclusion in the computer simulation.

### 1.5 Synchronous and induction machines

Large marine or industrial drives are moving towards synchronous or asynchronous motors and away from dc drives. The size of the dc motor is limited by the ability of the commutator to work effectively at high power levels ( high voltage is limited by insulation, high current and speed by the commutation process). The limitation of the output power of the dc motor increases the number required to provide a given output power and increases the consequential cost and

installation costs. The maintenance of the commutators is costly and is particularly difficult in the marine environment.

The design and construction of the synchronous motor is more complex than the induction motor, the synchronous machine has one main advantage in that the rotor field can be independently controlled and therefore provide power factor correction to the supply network. On every other count; simplicity of construction, robustness of the rotor, no insulation required on the rotor windings, no rotor excitation, no slip rings, lower temperature rise for the same performance, the asynchronous machine is better than or equal to the synchronous machine. The asynchronous machine has less active material than each of the other variable speed machines, and is therefore inherently the lowest cost machine in material costs.

A good power factor can be obtained with the induction motor however, the process is more complex compared to the synchronous machine, and is today a matter of industrial confidentiality. However a good power factor is assured if a machine is chosen with a high pole-circumferential length to air gap ratio, and the rotor is designed with a low reactance winding.

## 1.6 Control System Design

Drive control systems are required to satisfy a number of operating requirements to ensure that the power supply system is not inadvertently affected and that the load is not placed under undue stress. The control system should provide a high performance control of the load torque over the required speed range, this should also include a desired torque at standstill.

The design of the power and control systems should be to ensure a minimum disturbance to the power supply network and limit the generation of harmonics related to multiples of the supply frequency and associated side-bands. The output voltage distortion should be controlled such that the load current and hence motor load torque pulsations are minimised to reduce harmonic currents which could stimulate mechanical resonance of the output shaft. This is of particular importance to marine applications where the torque pulsations may have an effect upon the operation of the anti submarine warfare equipment.

The basic control strategy is the same for both induction and synchronous motors. The ac drive must provide a variable ratio of motor voltage to motor frequency in order to maintain a constant magnetic flux. Voltage boost is commonly used at low frequency to compensate for the stator



resistance voltage drop. ac cyclo-converter drives can now be designed with a superior performance to dc drives with the use of vector control.

#### 1.6.1 Vector Control Techniques

An ac motor produces a torque by the interaction between the rotating magnetic fields on the stator and the rotor. With any machine the two fields must be in synchronism in the air gap to develop a non zero mean component of torque. The torque developed will be dependent on the magnitude and phase relationship between the fields. With an ac machine there is no commutator as in a dc machine to keep the fields at right angles and deciding maximum torque. Hence it is necessary to control both the amplitude of the stator and rotor fields as well as their phase relationships to produce maximum torque. This mode of control is commonly called Vector Control. A convenient method to relate the stator field vector to the rotor field vector is to transform the 3-axis, 3 phase stator currents to 2-axis, 2 phase currents mutually orthoganol.

The control system on an industrial or marine drive is normally designed to provide closed loop control over the speed of the machine. This circuit basically compares the actual speed with the ramped speed reference to produce an amplified speed error signal to drive the machine. Closed loop torque control is derived from the torque algorithm

which is a function of the machine equivalent circuit parameters. Closed loop current control is necessary to set the the firing pulses for each motor phase bridge in the cyclo-converter and provide a current limit for the converter devices and the armature windings.

### 1.7 The supply network

To provide accurate results it is necessary to model the supply system for the converter. This can prove to be quite complex since it may be necessary to model the supply from individual feeds isolated by transformers or reactors, or in the case of marine drives a high voltage alternator. The reactor, or transformer in the supply lines to the converter is expected to perform a number of functions and its reactance is selected to be a compromise between a number of conflicting requirements. Line reactances may be needed for the following reasons:

To avoid interaction between converters on the same supply.

To limit the fault current at the converter and thus provide satisfactory protection.

To ensure that  $di/dt$  during commutation is within the limits of the converter devices and the converter design.

The main elements of the power circuit are shown in Fig 1.2, the power supply system has been simplified as detailed above to accommodate any power supply arrangement that could be used in practice. Three bi-directional bridges are fed through decoupling reactors, the power supply could also be designed using delta/star transformers to simulate the electrical isolation of the converter. The converter is a non circulating current type and as such the star point of the converter output is connected to the to the star point of the motor stator. With this connection and with the level of converter output unbalance, it is necessary to consider zero sequence components of currents which may appear in the motor phase windings. This type of connection does produce a higher kVA rating for the input supply transformers, however it does have the added advantage of being able to test each converter individually during commissioning or maintenance

A supply impedance common to two or more converters is liable to create undesirable interaction effects. Commutation notches produced in the supply of the same or remote converter can have an effect on the auxiliary supplies for the firing circuits.

If the two or more converters are capable of operating ,even momentarily at the same firing angle then the depth of the notch produced at the point of common coupling of the power circuits would be given by:-

$$d = \frac{L_s}{L_s + L_d}$$

where

$L_d$  is the parallel combination of the converter line inductances

$L_s$  is the supply inductance

Commutation disturbances due to remote converters will result in a lower voltage being available for commutation of the other converters connected to the same system, and this will result in increased overlap angles.

#### 1.8 Current research into cyclo-converter drives

Nottingham Polytechnic: are developing ASIC devices for cyclo-converter control schemes. The cyclo-converter is a three phase three pulse bridge arrangement and uses a vector control strategy for control of the ac motor.

Two ASIC have been designed to implement a new control strategy based on the cosine wave pulse crossing method. Partitioning of the circuits allowed duplicate use of one of the ASICS to provide both positive and negative gate firing delays for the thyristor drive circuits. The ASICS were produced using Mentor Graphics Electronic Design Automation (EDA) for design, simulation and layout.

P. J.

University of Aberdeen: have developed a time domain computer model to analyse cyclo-converters using a proprietary software package. The work to date has shown that they are able to model the installation at Wearmouth Colliery using induction machines with interbridge delay. The main thrust of their work appears to be directly related to the Ministry of Defence and the harmonic torque pulsations which are produced from different arrangements of cyclo-converters 3,6,9,12 Pulse, and motors which either have a conventional stator winding or are doubly fed. *Ref.*

GEC Alsthom: are a major manufacturer of cyclo-converter drives in the UK, and have developed a variable speed drive system producing a fast dynamic performance, low amplitude torque pulsation, low noise and low vibration levels. Applications include rolling mills, ball mills, mine winders and ship propulsion, with ratings as 3730kW 40 rpm for an induction machine rolling mill drive and 9700kW 60 rpm for a synchronous machine ship propulsion drive.

### 1.9 Aims of this research work

The main aim of this research is to investigate the principles involved in computer modelling of complex power systems, and specifically that of cyclo-converter drives supplying asynchronous or synchronous machines. It is intended to assess the performance of computer models with

results obtained from actual test rigs. Data has been obtained from tests of cyclo drives at CEGELEC and Newcastle University, this will enable waveforms and characteristic behaviour to be compared.

Modelling in the past has been piecemeal, computer models have only taken into account some of the system parameters, this has been due to the complexity of the modelling process. This work intends to show the relevance of these parameters in the modelling process and how they effect such things as supply harmonics, load harmonics, waveforms, and machine performance.

Pelly has developed a theoretical analysis for the behaviour of the cyclo-converter under fictitious operating conditions, This work will indicate that Pelly analysis is very limited in that it makes numerous assumptions and chooses to ignore certain aspects of the system which cannot be modelled by his mathematical techniques e.g. current discontinuities. To date industrial and machine designers use the data he has developed along with an educated assessment and experiential knowledge to predict the performance of the cyclo-converter drive under varying load conditions. It is intended that this work will provide a more precise prediction of system characteristic behaviour, and show the effects of interbridge change over delay,

overlap, supply reactance, decoupling reactance, and machine modelling on the overall performance of the cyclo-converter drive and the supply system.

## Chapter 2

### Literature Review

#### 2.1 Introduction

This review has been conducted by a literature search of papers presented at conferences in the USA and Great Britain, the search was conducted through the services of the Library at Derbyshire College.

#### 2.2 Mathematical analysis of cyclo-converters by Pelly

Pelly <sup>17</sup> produced a mathematical analysis of the harmonics content for a simple cyclo-converter with passive load. This theory assumes that the load current waveform is sinusoidal, this is very limited in that the effects of an ac motor with or without damper windings will produce a current determined by the converter output voltage and its harmonics. Pelly's theory also contains simplifications in respect of the power source and converter operational characteristics, providing no understanding of the effect of source impedance, overlap and inter-bridge delay on the converter output voltage and input current waveforms.

Clearly the marine drive operates well away from these ideal conditions, and Pelly's mathematical model therefore will provide limited information to the design engineer.



The Mathematical analysis by Pelly covers two main areas: the harmonic analysis of the output voltage of the cyclo-converter, and the analysis of the input current of the cyclo-converter.

Harmonic analysis of the output voltage:

The analysis covers both the circulating and non circulating current designs of the converter. The analysis models an open loop control system with cosine wave crossing control and a continuous load current waveform.

The analysis of the output voltage waveform of the phase-controlled converter is derived by expressing this wave as the mathematical sum of the voltage segments generated by each of the individual thyristors within the converter. Each individual voltage segment is expressed mathematically as the product of the appropriate sinusoidal input voltage and a switching function, this being represented as a harmonic series.

Harmonic analysis of the input line current:

The analysis covers the circulating current free mode of operation of the converter and it assumes that the output current waveform of the cyclo-converter is a pure sinusoid, which is displaced from the fundamental component of the

output voltage by the displacement angle of the load. It assumes that switching from the positive to negative converter bank takes place with no discontinuities . The internal impedance of the power source, as well as the winding resistance and leakage reactance of the input transformer (if used), are assumed to be negligible.

The analysis models an open loop control of the cyclo-converter, with the firing instants being determined by the cosine wave crossing control method

### 2.3 Modelling a steady state system

It is not infrequent when modelling machines in computer analysis for the steady state condition to be assumed, i.e. the synchronous motor at steady state is represented by three e.m.f.'s with series resistance and inductance. This is the method chosen by Doruff and Sidibe <sup>8</sup>, and Tadakuma and Tamura <sup>12</sup> the main advantage of this method is that the modelling technique is simple, the disadvantage is that it does not take into consideration the transient nature of the cyclo-converter supply or machine load under a variety of operating conditions.

## 2.4 Models including current discontinuities

Current discontinuities in devices and the supply waveforms occur in a number of ways within the converter; interbridge changeover delay, current zeros and overlap between devices which are commutating.

Doruff and Sidibe <sup>8</sup> do include interbridge but give no indication as to how it is achieved, Chattopadhyay and Jabardhanarao <sup>6</sup> deal with discontinuities by modification of the stator voltage prior to the integration process. I feel that this may be a better method since it is more precise and does not entail extended calculation time due to the reverse resistance of the device. However the method adopted by the author is more simple requiring only two modes whereas this paper has to consider 5 separate modes and transformations. The time step interval for the integration process, in this paper was 0.1 ms for an operating frequency of 16.666 Hz. , this does seem rather a large interval, (600 intervals per cycle). An interesting feature of this simulator is that the model calculates by interpolation the point of discontinuity, this is necessary due to the rather large time interval used.

In Doeuff Iung and Gudefin's paper <sup>9</sup> interbridge delay was included and to achieve this and reduce the computational time, a further transformation was introduced during

periods of discontinuity. This required four different models depending on the number of stator phases supplied by the cyclo-converter. In the paper they state that the voltage fed to the motor during a discontinuity cannot be calculated until the currents are known i.e. at the end of the integration step. This is true, however I do not agree that this negates the use of the dq transformation on the stator voltages.

Niiranen <sup>11</sup> has developed a new method based on the equivalent voltage source, this method allows the simulation to be made with the usual two-axis model of the machine. the equivalent voltage source is based on the idea of using the voltage instead of high impedance to force a phase current to zero during the periods of current discontinuity or interbridge delay. The main advantages are that no shortened integration step is required to cope with the reduced machine time constant.

## 2.5 Models including overlap in the converter

Overlap is a system parameter which can only be included if decoupling reactance and source reactance are modelled within the program. Tadakuma and Tamura <sup>11</sup>, included overlap in the simulation process with the inclusion of the phase source impedance. However no decoupling reactance was used as would be necessary in a large converter system. This

model would produce large notches on the supply waveform and hence produce an increase in the harmonic content on both converter input and output waveform characteristics.

## 2.6 Models analysing supply side harmonics

Doruff and Sidibe <sup>8</sup> have mainly considered the line side effects and performed a comparison between the computer simulation and Pelly's theory for harmonic content ignoring source impedance, interbridge delay, and assuming a simplified Thevenin synchronous motor load. The paper then details the effects of load impedance, supply impedance, and interbridge delay upon the harmonic content in supply lines, it does not indicate the effects that the converter may have on the load. They concluded that the simulation provided an accurate determination of the mains current harmonics, and since Pelly's theory has been developed solely with passive loads, this work provided a more accurate prediction.

## 2.7 Modelling of the reverse blocking of thyristors

The integration time size does seem to cause universal problems. Tuncay, Alan, Brown <sup>13</sup> decided to overcome this problem, which is associated with the device reverse blocking resistance by decreasing the integration step when

this caused the computation time to become excessive. A second approach was to write a program using ideal switches details of how this was achieved were not explicit.

## Chapter 3

### Modelling of the cyclo-converter and machine drives

#### 3.1 Description of the Computer system

The computer system which has been used for the simulation is a VAX cluster comprising three MICRO VAX 2 with 16 MB computer on board memory and a VAX 4000-200 with 24MB computer on board memory, a clock rate of 114 MHz. A number of peripherals including line printers, plotters, graphics terminals, standard keyboard terminals and terminals connected via a telecommunications 'grape vine'.

The current version of the operating system is VAX VMS 5.4/2. The simulation has been written entirely in VAX Fortran 77 version 5.6, using the scientific subroutines installed in the computer library to manipulate and solve the machine matrix equations and to provide the fourier analysis for the system and converter waveforms. The disk capacity is 560 MB and the program is allocated 77MB. The size is necessary to be able to store at least one version of every file generated by the programme plus a backup. There are then three sub directories which enabled the program to be run in parallel at week-ends without the disk quota being exceeded.

Connected to the main frame cluster are a number of graphics terminals and a Houston Instruments DMP50 plotter, this has been used extensively to provide visual images of the waveforms obtained in the process of developing the program. All of the waveforms presented in this document have been produced using this facility. It has been necessary for the author to develop specific subroutines to enable the data to be displayed on both the graphics terminals and the plotter.

The simulation has been run mainly by the use of the batch facility, this has enabled a high utilisation factor of the computer system and allowed the author to run a complete set of drive frequencies 4-22.5 Hz (13 runs), over a twelve hour period.

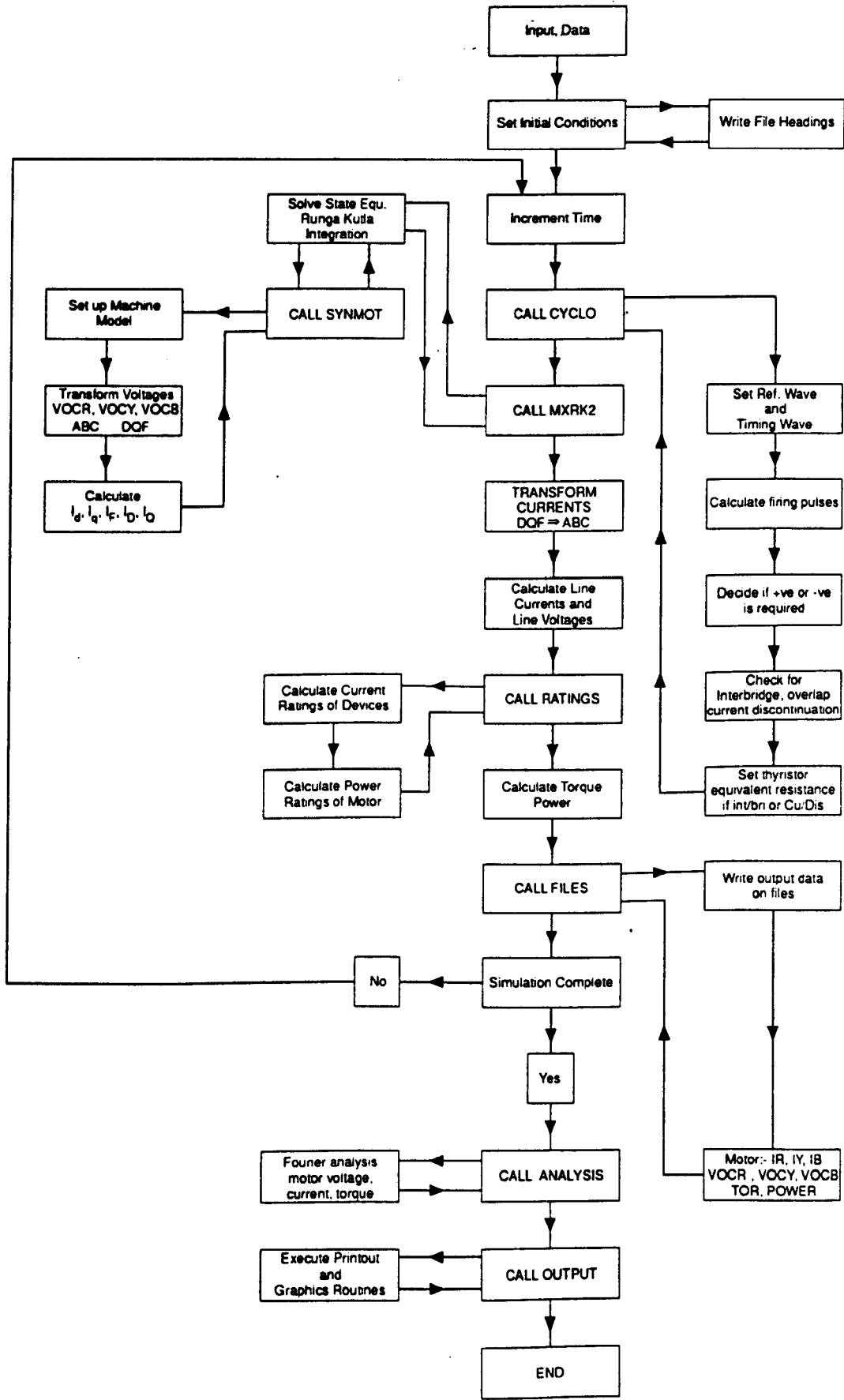
### 3.2 Computer model flow charts

See Fig 3.8

### 3.3 Runge Kutta 2nd and 4th order routine

The computer program has been written with numerical integration at the centre of the process. The machine has been represented by the conventional two axis dq equations. This entailed a 4x4 matrix for an induction motor without zero sequence components, and a 5x5 matrix where zero sequence components are considered. With the synchronous





machine a 5x5 matrix is necessary for the machine without zero sequence components and a 6x6 where they are to be considered. It is then necessary by matrix manipulation to rearrange the equations so that they are presented in the conventional stator form, that is with the  $di/dt$ 's as the subject as shown below:-

$$[V] = ( [L]s + [R] + [G] ) [I]$$

[L] Inductance matrix (emf's due to  $di/dt$ )

[G] Resistance matrix derived from inductance variation (emf's due to rotation)

[R] Resistance matrix

$$p[I] = [L]^{-1} \times ( [V] - ( [R] + [G] ) [I] )$$

The Runge Kutta integration process is able to calculate out the  $di/dt$ 's for each equation and hence calculate the change in the machine currents due to the change in voltage over the time interval. It is not possible to stop the integration process should a discontinuity occur ie, a commutation of two devices, interbridge, or current discontinuity. This would inevitably make the results more accurate however, the author does not feel that the increase in the complexity of a programme capable of achieving this, and the fact that the time interval is already very small, would make this complexity justified.

Both 2nd and a 4th order Runge Kutta integration subroutine has been used in the development of the simulation.

### 3.4 Modelling the cyclo-converter:-

Fig.3.1 shows in simplified schematic form the marine drive system to be examined. A normal marine system would comprise two or more generators with two or more cyclo-converters and propulsion motors. The 6 pulse version shown here would not be common due to the relatively high harmonic ripple introduced into the supply. 12 pulse converters, or possibly 6 pulse converters with 6 phase motors would form a more practical scheme.

The system of Fig 1.1 however, forms a practical, simplified model for evaluation of the detailed effects of the system operation such as interbridge delay and overlap. Although the multiple drives are not simulated individually, their lumped effect represents the worse case condition from the harmonic current generation viewpoint.

It is important to be able to predict, with some degree of accuracy, the operational performance of the drive and its effect on the power system to enable the designer to provide the optimum operational performance at a competitive price. Vector control of the synchronous machine and cyclo-converter drive is not difficult and provides the rapid

response which may be required for applications such as ice breakers. A Computer model of a complete power and drive system has been developed to provide this information.

The cyclo-converter used in this model has a circulating current free (or blocked group) type. The mode of control is such as to block the firing of one group of thyristors until the current in the other group has ceased.

#### 3.4.1 Modelling the cyclo-converter switching sequence

The simulator uses a step by step method to determine the output voltage of the cyclo-converter. Initially the supply system parameters and the converter arrangement are defined, this determines the number of thyristors which are required in the cyclo-converter. For this work a 6 pulse or bridge configuration has been used. The timing waves are generated internally and are related to the specific phase of the supply, the point of firing therefore is determined for each thyristor by comparing the reference waveforms with the timing waveform. If the point of intersection occurs when the slope of the timing waveform is positive then the firing pulse is for the positive group, whereas if the slope is negative the pulse is for the negative group. The output voltage for the positive and negative group of one output phase is determined for each time increment, and the simulator decides whether the phase current is positive or

negative and which of the output bridges of the converter should be used, whether there is a period of interbridge delay. This whole process is repeated for each phase.

The output of the negative group will differ in waveform to that of the positive group when the output waveform is not composed of an integral number of input cycles, since successive output half cycles will start at different instances relative to the input supply waveform. This condition means that the motor will operate under a virtually continuous transient condition. It is vital therefore that the model is able to deal with the transient solution, so that these effects can be examined.

#### 3.4.2 Modelling the supply system and decoupling reactances

The supply system is a vital part of the model if overlap and supply regulation is to be considered. The supply parameters, which in a typical large marine or industrial application consist of a source impedance, high to low voltage transformer or decoupling reactance have to be defined. The distortion of the supply system voltage created by overlap in the converter can be excessive with commutation notches in excess of  $20^\circ$  of supply frequency are not uncommon. The level of distortion is significant in that it modifies the harmonic content of the converter and

load waveforms, and adversely affects the operation of another converter or electrical equipment connected to the common supply point.

The alternator source impedances and decoupling reactor effect the output voltage of the converter due to the regulation produced by the line currents; the alternator and decoupling reactor are also responsible for the overlap which occurs as one device commutates to another. The operation is complex producing large commutation notches in the supply voltage. This is covered in detail in section 3.4.4.

The most attractive connection for marine applications is for the motor to have completely separate stator windings, since this allows the converters to be connected to the supply without the need for transformers. However with this arrangement decoupling reactors must be included if the harmonic distortion is to be controlled on the alternator bus bars. This research has assumed this winding arrangement.

#### **3.4.3 Modelling the cyclo-converter interbridge delay and motor phase current discontinuities**

There are a number of bridge arrangements which can be used in a cyclo-converter, the least expensive arrangement would be to use a suppressed, anti-parallel bridge connection. In

this arrangement both bridges are suppressed during interbridge. It is possible therefore for there to be a interbridge period of a minimum of 3 ms up to a maximum of 10 ms depending on the point of changeover with respect to the supply waveforms.

Interbridge changeover delay causes one phase of the motor stator to be disconnected from the three phase supply. The simplest method of simulating this condition is to increase the stator resistance, causing one phase of the motor to have a high resistance. For this it is necessary to transform the new stator(abc) resistances to the machine(dq) resistances each time a discontinuity takes place. The main disadvantage of this approach is that the time increment must be reduced for the modified stator time constant is now much less.

Under low load conditions it is possible for the motor phase current to reduce to zero for a time. Operationally the thyristors would go into reverse conduction and after a few milliseconds block all reverse current. This is simulated by increasing the phase resistance of the respective motor phase winding in the computer model and then transforming the stator (abc) resistances to the machine(dq) resistances as with interbridge changeover delay.

This modelling does not take into the leakage current in the thyristor switches, leakage currents of 100 mA may be considered negligible compared to the motor currents which are in excess of 300A in an industrial drive. This assumption would have to be reconsidered if smaller loads were to be investigated.

#### 3.4.4 Modelling overlap within the cyclo-converter

Overlap is the time taken for the current to commute from one converter device to another, in the same bank within the converter. The current is not transferred instantaneously due to the supply reactance which controls the rise and fall of currents in the commutating devices. The simulation initiates overlap when the firing sequence indicates that the next device in the bridge should commence conduction.

The computational analysis assumes the system  $di/dt$ 's from the previous time interval and this is adequate if the time interval is small, and the current being calculated is not discontinuous. During overlap the current is discontinuous since it is being forced to pass from one device to another by the supply phase voltages. The  $di/dt$  in the device during overlap is used to calculate the voltage drop in the alternator reactors  $L_s(1)$  and  $L_s(3)$ , therefore because of the current discontinuity it is necessary to provide the correct initial  $di/dt$  for commutation to commence correctly.



$$\text{initial } di/dt(\text{device}) = ( V_{ph(1)} - V_{ph(3)} ) / ( L_d + L_s )$$

$V_{ph}$  phase supply voltage

$L_d$  decoupling reactance

$L_s$  supply reactance

Once the commutation process has been initiated the rate of rise of current in the device turning on and hence the rate of fall of current in the device turning off are calculated. Since there is more than one converter connected in parallel across the supply, therefore the equations to establish the device currents will be dependent upon the voltage drops in the supply system due to these currents as well.

For the positive Converter:

(a) Commutation from devices C1 to A1 positive output of converter:

(See Fig 3.2 for diagramtic representation of overlap for equation given)

At the point of commutation the red phase voltage  $V_{ph(1)}$  is more positive than the yellow phase voltage  $V_{ph(3)}$ , therefore a current is driven around as shown turning C1 off and bringing A1 on. At the same time the phase supplies are required to provide the current to the other converters as indicated.

Circuit equations:

Instantaneous values

$V_{ph}$  phase voltage

$V_1$  voltage across supply reactance

$V_d$  voltage across decoupling reactance

$I_{ph}$  phase current

$I_{ov}$  overlap current

$L_d$  decoupling reactance

$$V_{ph}(1) - V_{ph}(3) = V_1(1) - V_1(3) + V_d(1) - V_d(3) \quad -(1)$$

$$I_{ov}(3) = I_{ph}(1) - I_{ov}(1) \quad -(2)$$

From 1,2

$$V_{ph}(1) - V_{ph}(3) = V_1(1) - V_1(3) + L_d * p(I_{ov}(1)) - \\ L_d * p(I_{ph}(1) - I_{ov}(1))$$

$$V_{ph}(1) - V_{ph}(3) = V_1(1) - V_1(3) - L_d * p(I_{ph}(1)) + \\ 2 * L_d * p(I_{ov}(1))$$

$$p(I_{ov}(1)) = (V_{ph}(1) - V_{ph}(3) - V_1(1) + V_1(3) + L_d * p(I_{ph}(1))) / \\ (2 * L_d)$$

It was found however that this modelling was not adequate, this was due to the fact that the  $di/dt$ 's of the converter were not correct for the first step in the overlap period. The  $di/dt$ 's under normal conditions were relatively small

compared to the expected value during overlap, therefore if these reduced values are placed into the overlap equations the resultant current flow could be quite inaccurate. The effect of this was to produce a larger than normal change in current which in turn produced a large  $di/dt$  and hence a large voltage spike on the supply system. The outcome of this was that the system invariably went into oscillation sometimes causing the program to run into numerical overflow, otherwise the programme would find its way out and continue.

To overcome this problem it was necessary to include an initial line to predict the initial  $di/dt$  for that particular overlap. This proved to be reasonably successful reducing the oscillations and preventing all but a few discontinuities of current and hence large  $di/dt$ 's.

$$P(I_{ov}(1)) = (V_{ph}(1) - V_{ph}(3)) / (2 \cdot L_d + 2 \cdot L_s) \quad -(3)$$

This equation was also found to be too simplistic and did not deal with all of the characteristics of the system during overlap. The current of the outgoing device had associated with it two components, the current due to start to commute and the currents for the other converters, the voltage drop due to this current had to be taken into consideration. To establish the rate of the  $di/dt$  of the

commutating current it became necessary to separate these two effects, and therefore the principle of superposition was used Fig 3.2b

I<sub>so</sub> current in the supply reactance due to overlap  
I<sub>s</sub> supply line current

$$V_{ph(1)} - V_{ph(3)} = (p(I_s(1)) - p(I_{so}(3))) * L_s + \\ p(I_{ov}(1)) * (L_d + L_s) - p(I_{ov}(3)) * (L_d + L_s) \quad -(4)$$

$$I_{ov}(1) = I_{ph}(1) - I_{ov}(3) \quad -(5)$$

From 4,5

$$V_{ph(1)} - V_{ph(3)} = (p(I_s(1)) - p(I_{so}(3))) * L_s + \\ p(I_{ov}(1)) * (L_d + L_s) - (p(I_{ph}(1)) - p(I_{ov}(1))) * (L_d + L_s)$$

$$p(I_{ov}(1)) = (V_{ph(1)} - V_{ph(3)} - (p(I_s(1)) - p(I_{so}(3))) * L_s \\ + p(I_{ph}(1)) * (L_d + L_s)) / (2 * L_d + 2 * L_s)$$

(b) Commutation from devices B2 to C2 negative output of converter:

See Appendix C1

Negative Converter:

(a) Commutation from devices C2' to A2' positive output of converter:

See Appendix C2

(b) Commutation from devices B1' to C1' negative output of converter:

See Appendix C2

### 3.5 Modelling the machines

Since the converter is selecting various parts of a supply waveform and therefore creating a transient after every commutation, during the overlap process, and after interbridge changeover, it is necessary to model the machine as a full dq axis model including the transient response. This requires a 5x5 matrix dq axis model including damper windings , for a synchronous machine, and a 4x4 matrix dq axis model for an induction machine.

A simulation using the simplified modelling of the synchronous machine would produce inaccurate results in the machine performance and losses. A steady state model (dq axis) not capable of responding to the transient solution would produce no useful information.

A Thevenin model will be examined, this does provide some characteristics of the machine but lacks information concerning the losses in the machine windings, and the effect of the damper windings.

### 3.5.1 Introduction to generalised machine theory

The analysis for the motor is achieved by applying the classical dq transformations to the machine parameters and operating variables. With the application of the correct transformation, the motor is represented by a two phase motor with windings fixed with respect to each other. The two phase transformation eliminates time varying mutual inductances, replacing them with speed-voltage terms, Mutual coupling between phases is also eliminated making the model considerably easier to handle in a digital simulation.

### 3.5.2 The Synchronous Machine Modelling

The three phase output voltages from the cyclo-converter are converted into dq form to provide the internal voltages for the three phase connected synchronous motor (See Fig 3.6). Two conversions are necessary the first converts the cyclo-converter output voltages (abc) to an equivalent two phase system, the second transformation converts the two phase system to stationary axes with respect to the rotor field (dq).

The synchronous motor is then modelled in terms of the first deviates for the motor currents, these being expressed in Fdq form. For a synchronous motor with dampers a 5 by 5 impedance matrix is obtained. Solution of this differential equation is possible using matrix mathematical techniques.

$$[V] = ([L]s + [R] + [G]) [I] \dots \dots \dots (1)$$

[L] - inductance matrix (EMF's due to di/dt)

[G] - resistive matrix derived from inductance  
variation  
(EMF's due to rotation)

[R] - resistance matrix

$$s[I] = [L]^{-1} ([V] - ([R] + [G]) [I]) \dots \dots \dots (2)$$

The solution of the simultaneous differential equation can be achieved using a Runge Kutta integration technique, whereby the di/dt is calculated for each discrete step in the program, knowing the time dependent voltages in Fdq form and the initial value of the currents in Fdq form.

From the solution of the internal motor currents in Fdq form it is possible to establish the torque :-

$$Tor = PP \times [L_{aq}(I_{kq} + I_q)I_d - L_{ad}(I_f + I_{kd} + I_d)I_q - (L_d - L_q)I_d \times I_q] \cdot (3)$$

PP - No. of Pole pairs

Since the model is capable of analysing the behaviour of the motor in the transient mode, it is possible to observe the effect on motor current and motor torque due to a step change in load on the output shaft of the motor. This step change is introduced into the simulation by changing the load angle between the stator abc axis and rotor field axis. Within the model this has the effect of changing the angle between the axis of the three phase stator and the axis of the rotor field hence

$$Q = (\omega_m \times t) + L_a$$

Q = Angle required to transform the three phase supply to an equivalent dq axis.

$\omega_m$  = Mechanical angular velocity

$L_a$  = Load angle of the rotor

### 3.5.3 Induction Machine modelling:

The induction machine used in the simulation is assumed to have windings located as shown in Fig 3.7 . The three phase output voltages from the cyclo-converter are converted into



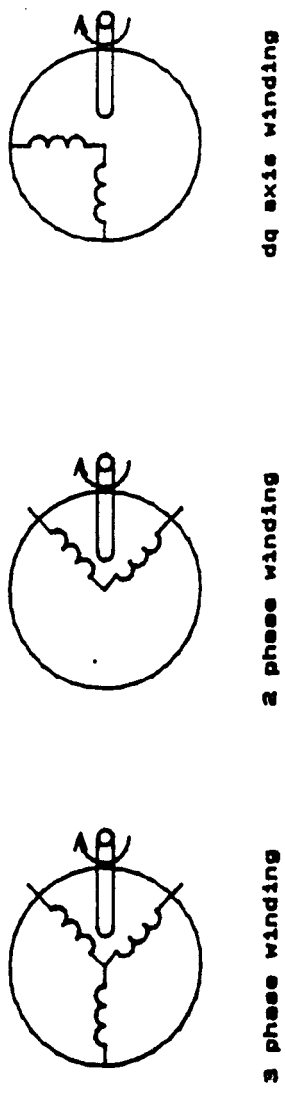
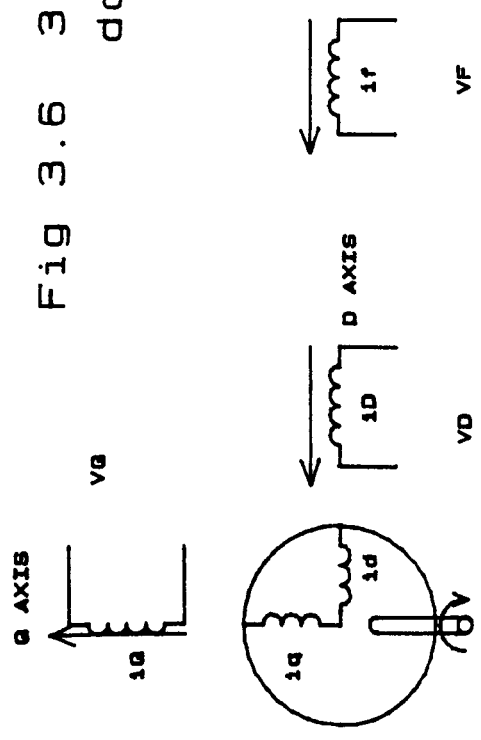
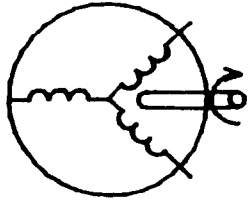


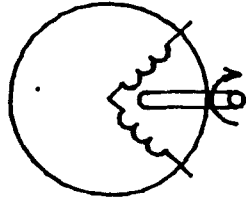
Fig 3.6 3 PHASE SYNCHRONOUS MACHINE  
dq AXIS MODEL



Balanced Synchronous Motor dq axis model



3 phase winding



2 phase winding

q AXIS STATOR

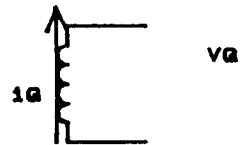
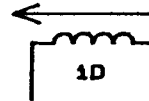
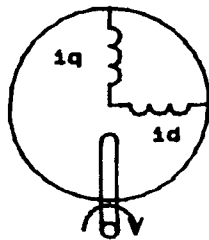


Fig 3.7 3 PHASE INDUCTION MACHINE  
dq AXIS MODEL



D AXIS STATOR

v\_D

Balanced Induction Motor dq axis model

dq form to provide the internal voltages for the three phase machine. The generalised machine transformation is achieved in one step by converting the rotor (abc) windings to a two phase system rotating at the same speed as the stator rotating field.

The induction motor is then modelled in terms of the first deviates for the motor currents, these being expressed in Fdq form. Solution of this differential equation is possible using matrix mathematical techniques.

$$[V] = ([L]s + [R] + [G]) [I] \dots \dots \dots (1)$$

[L] - inductance matrix (EMF's due to di/dt)

[G] - resistive matrix derived from inductance  
variation (EMF's due to rotation)

[R] - resistance matrix

$$S[I] = [L] ([V] - ([R] + [G]) [I]) \dots \dots \dots (2)$$

Solution of the simultaneous differential equation is achieved using a Runge Kutta integration technique, whereby the di/dt is calculated for each discrete step in the programme, knowing the time dependent voltages in dq form and the initial value of the currents in dq form. From the solution of the internal motor currents in Fdq form it is possible to establish the torque developed by the rotor:-

$$T_{or} = PP \times ( I_q \times I_d \times M_{dd} - I_d \times I_q \times M_{qq} ) \dots \dots \dots (3)$$

PP - No. of Poles pairs

#### 3.5.4 Zero sequence components of current in the machine windings

Zero sequence components of current will flow in machine windings which are connected to a common neutral point and if the phase voltages are unbalanced. Zero sequence currents are inevitable where a cyclo-converter produces the machine phase voltages from portions of the three phase supply waveforms, and the windings have a common neutral point.

If reactors are included to provide decoupling between each phase of the cyclo then the motor phase windings must be isolated, otherwise large fault currents would flow between different phases of the cyclo-converter. With this phase winding arrangement a 5 by 5 matrix is required for a Synchronous machine and a 4 by 4 matrix with an induction machine.

If the converter phases are isolated by input transformers then the motor phase windings can be connected to a common neutral point, assuming an inbalance in the phase voltages zero sequence components of currents will flow in the

machine windings. To model this the synchronous machine requires a 6 by 6 impedance matrix and the induction motor a 5 by 5 impedance matrix.

### 3.5.5 Voltage to frequency control

Synchronous and asynchronous machines are controlled by a frequency converter with voltage to frequency control. This allows the motor to be controlled at constant torque over the required speed range. At low frequencies the voltage to frequency control has to be modified with the introduction of voltage boost to take into consideration the effect of voltage drop due to the stator winding resistance. The stator resistance becomes more significant in relation to the applied voltage and a higher value of applied voltage is necessary to ensure the correct flux level. Without the voltage boost characteristic, the motor performance would deteriorate dramatically and the motor phase current, motor torque and supply currents would reduce in magnitude as the frequency reduced.

## 3.6 Operation of the computer model

### 3.6.1 Introduction

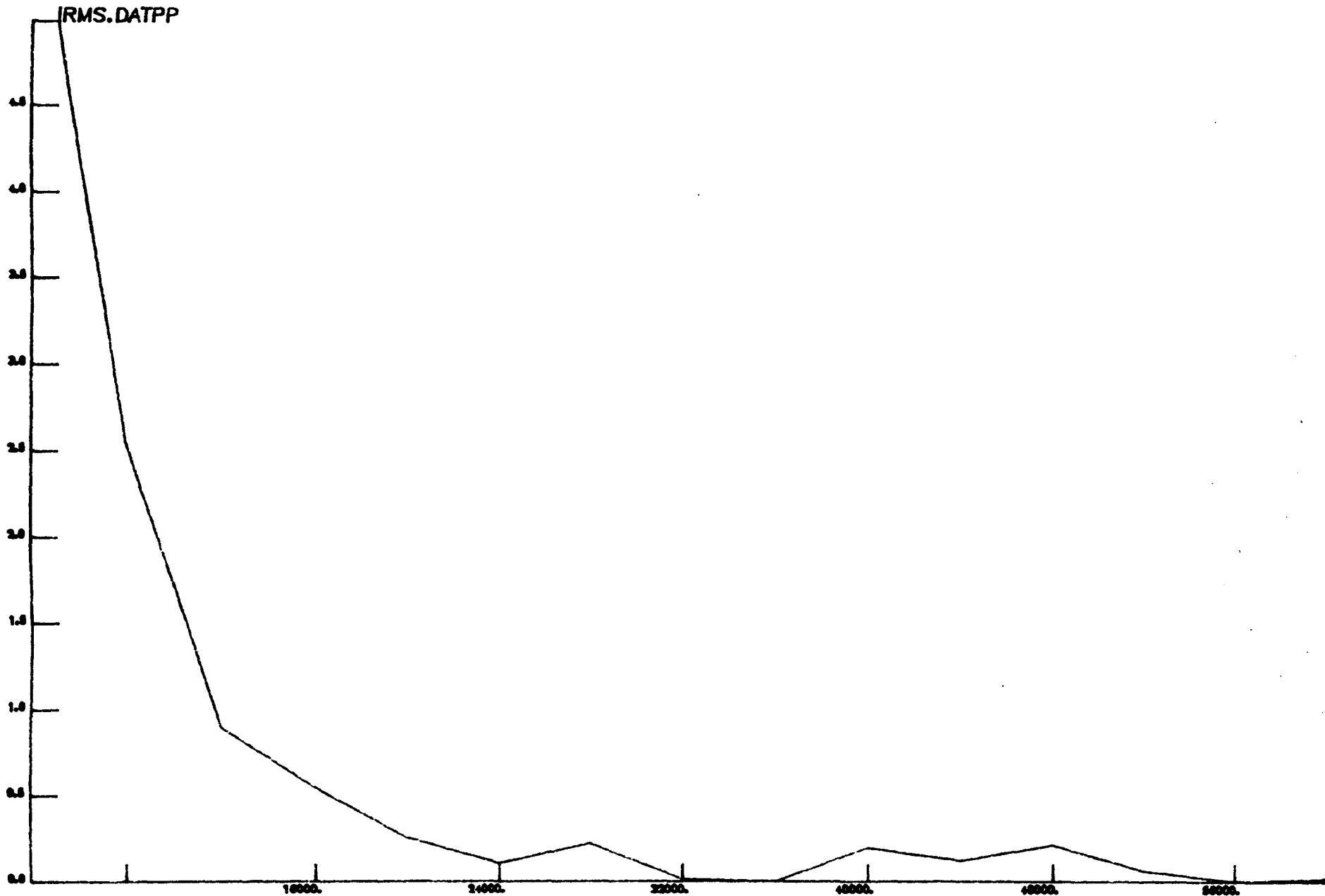
The computer model is a simulation of a real system. It has been designed to model the electrical behaviour of the complete power system. The results obtained will reflect what happens in the real world as long as the model is

operated within reasonable limits. These limits relate to the information which is made available to the computer system in terms of mathematical modelling, numerical integration techniques, time increments and time constants of the system being modelled. The accuracy does depend on all of these parameters and in the end the simulation can only provide an indication of the results that would be obtained in practice. The level of accuracy that can be expected can at present only be estimated unless a detailed set of results including the main system parameters are obtained from a known system.

#### 3.6.2 Test 1a: The effect of varying the time interval in the computer program

It was important to establish how the number of time steps per cycle of output supply affected the simulation, and hence to verify what was an optimum value to use for test results. The number of points was increased to investigate the effect on the precision of the program. It was found that the results became asymptotic with the program finally failing to operate past 60,000 points per cycle. Fig 3.1a shows how the number of points affected a number of system parameters. It can be seen that the precision of the model increased with the increase in the number of points, however it became necessary to compromise between the number of

PERCENTAGE



NO OF SAMPLES

Fig 3.1a Characteristic performance of the time interval within the simulator.

points to achieve the most precise results and the length of time for the computer program to run. The number of points taken for this work was chosen to be 8000 points, even though this would give an error of 1%, compared to 0.5% error with 16,000 points the saving in computational time became the deciding factor.

It is also important to realise that the the number of time step points does not only effect the output waveform but also the input waveforms:-

5 Hz drive frequency with 8000 points, produces 800 points on the 50Hz supply waveform,

10 Hz drive frequency with 8000 points, produces 1600 points on the 50Hz supply waveform

20 Hz drive frequency with 8000 points, produces 3200 points on the 50Hz supply waveform

It may therefore be expedient to modify the number of points as the load frequency falls to ensure that the supply waveform is adequately formed and that a Fourier analysis is obtainable up to a sufficiently high frequency.



### 3.6.3 Test 1b: The accuracy of numerical integration in the program

The solution of the matrix differential equations is dependent upon a numerical integration technique. Two models of the Runge Kutta integration technique were used and assessed for accuracy. The position in the flow chart of this process is given in Fig 3.9. It was found that when the routines were tested against an equation with a known solution that they both operated well providing a high degree of correlation. However it was established that the fourth order routine as expected was marginally more accurate than the second order routine and therefore it has been used throughout for this work. Fig 3.1b shows the graph of accuracy against the level of work required to achieve the result, it must be noted that the fourth order integration process takes approximately twice as long to compute as the second order integration process. Therefore 8000 points on the fourth order is equivalent to 16,000 points with the 2nd order routine for the same amount of work.

# TEST 1b

## INTEGRATION

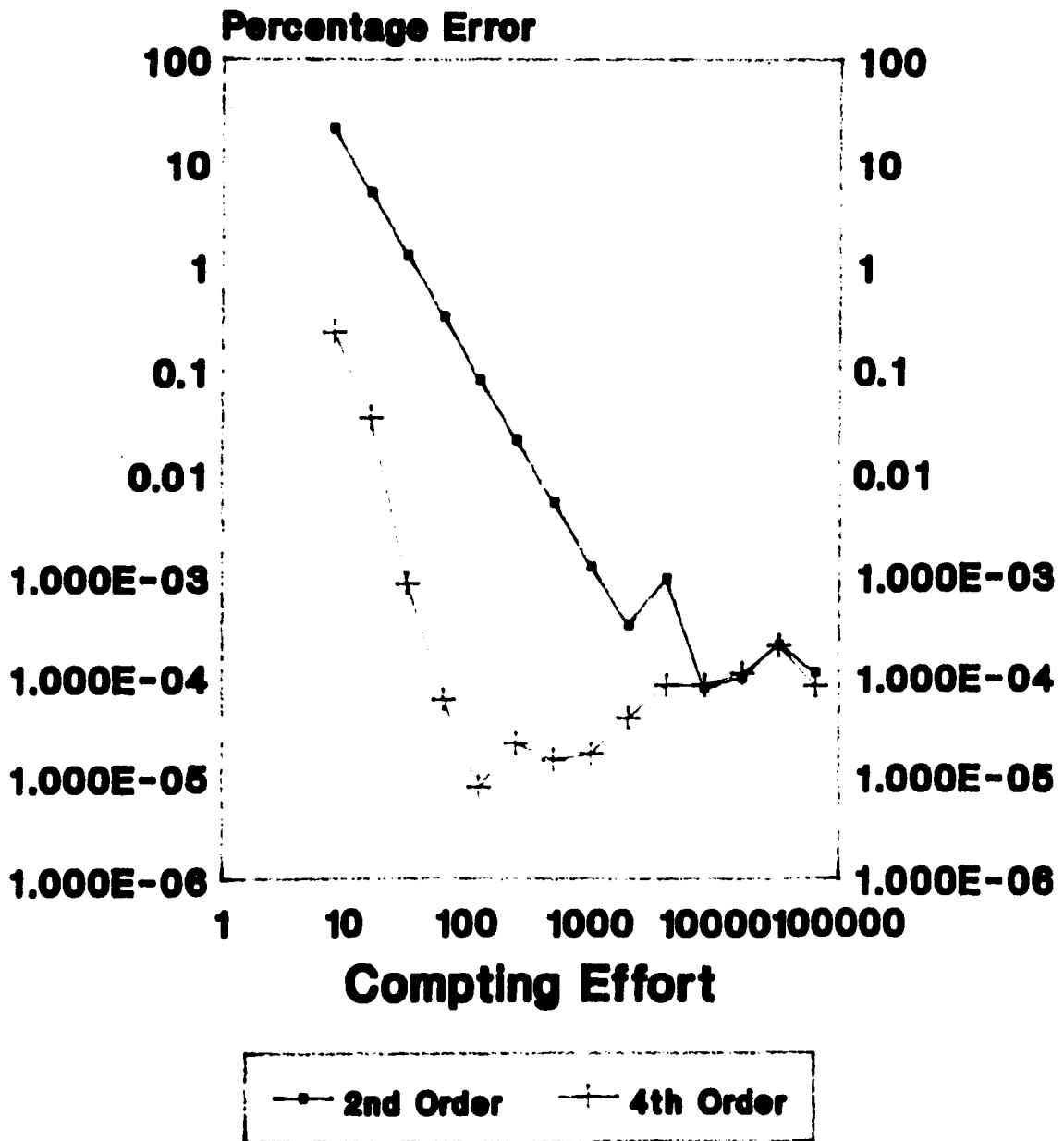


Fig 3.1b 2nd Order Runge Kutta  
4th Order Runge Kutta

### 3.6.4 Time constants within the machine being modelled and the reverse blocking of thyristors

The machine time constants are a deciding factor in the operation of the simulation. For the integration to take place the time increment must be much less than the time constant of the circuit being modelled. This was not normally a problem since the number of points was well in excess of the required, however under a period of current discontinuity or interbridge changeover this particular problem was highlighted as the machine time constant was increased by a factor of approx 1000. It therefore has become a feature of this programme that for these characteristics to be operative the number of points should not fall below a nominal value of 8000 points. The critical point is dependent on the operational frequency of the drive since at :

for 5 Hz the time interval is  $0.025 \text{ ms} (1/(5 \times 8000))$

for 10 Hz the time interval is  $0.0125 \text{ ms} (1/(10 \times 8000))$

for 20 Hz the time interval is  $0.00625 \text{ ms} (1/(20 \times 8000))$

The largest time increment will occur at the lowest frequency 4 Hz, this gives a time interval of;

$$\text{time interval} = \frac{\text{periodic time}}{8000} = \frac{0.2}{8000}$$

time interval = 0.000025 s

The normal time constant of the machine can be defined as the product of the sub transient reactance and the phase resistance for the machine.

$$t_m = L_{st} / R_a = 0.07295 \text{ s}$$

However under periods where the phase resistance is increased to simulate the cyclo-converter entering interbridge delay or a current discontinuity the machine time constant rises to the product of the sub-transient reactance and the blocking resistance of the thyristor.

$$t_m = L_{st} / R_b = 0.000023 \text{ s}$$

The time step was modified within the program so that the program became more accurate over the periods of discontinuity. This then allowed the programme to run faster at other times. It was found that with a high values of supply reactance and decoupling reactance that the converter was spending up to 30° in overlap and with the interbridge period of 3 ms . This meant that the time available for operation at the longer time step was minimal.

It was necessary to run the simulation at the time interval defined by the time constant of the machine  $t_m$ , and the accuracy of the Runge Kutta integration process, see section 3.6.3.

### 3.6.5 Fourier analysis routines

The drive frequency of operation and the number of points per cycle of the drive frequency had a direct effect upon the Fourier analysis and the ability to obtain an accurate spectrum of the waveforms under analysis. To compare the results obtained from the computer simulation and those obtained from theory (Pelly), and practice (Weamouth) it became necessary to consider harmonics of the supply frequency 300 Hz, 600 Hz, 900 Hz. To achieve this it was decided to analyse all waveforms up to at least 1000 Hz with the minimum order of harmonics set to 100:

Drive output fourier analysis:

Drive 5 Hz, frequency range 5-1000Hz, Harmonic order 200

Drive 10 Hz, frequency range 10-1000Hz, harmonic order 100

Drive >10 Hz, frequency range > 1000Hz, harmonic order 100

Supply side Fourier analysis:

To make the Fourier analysis valid it is essential that the number of points per cycle is at least equal to the maximum order of harmonics being considered. The worst case for this must be at the lowest frequency of operation of the cyclo-converter. This is adequate for the frequency range which is specified to be compared with Pelly's work and the test results from CEGELEC Weamouth.

It was found however that the accuracy of the Fourier analysis on the input line currents and the supply voltages was affected by the number of points taken as well as the number of cycles analysed. To increase the accuracy further it was decided to make the harmonic analysis for the input supply current and the input supply voltages different to that for the load waveforms:-

- (a) The first Fourier analysis was to establish the level of the harmonics in the load current and voltage waveforms. This was taken over the drive frequency's periodic time.
- (b) The second Fourier analysis was to establish the level of harmonics in the supply side waveforms. This analysis was taken over 5 cycles of the mains frequency as the analysis had to cover a multiple number of cycles of the supply waveform. This gave the analysis a greater degree of accuracy particularly at the lower drive

frequencies.

### **3.6.6 Test1c: Characteristic performance of the Fourier analysis subroutine**

A test was conducted on the Fourier analysis routine to ensure that it was working correctly and that there was no aliasing being produced by the analysis.

Fig 3.1c Characteristic performance of the fourier analysis routines .

### **3.6.7 Assumptions made within the simulation**

Within the program it was necessary to make assumptions, either to make the program function, or to reduce the computational time. The effect of each assumption has to be justified to ensure that the effect on the results are minimal:-

- (a) The supply voltages are modelled by a Thevenin source except where an alternator model was used. This produces errors in that the effect of the machine dampers could not be modelled. The damper bars in the real machine contain resistance and inductance and they are responsible for reducing the mechanical oscillations of the machine, and produce losses which reduce the efficiency of the supply system. The mutual

coupling between the rotor and stator of the machine has the effect of modifying the stator induced voltages.

- (b) The thyristors are ideal and therefore provide no voltage drop when conducting or delay in the switching process. The inclusion of the device voltage drop is not difficult, however with a voltage of 1-2 volts depending on device characteristic and a supply voltage of 3000-4000 volts the error is insignificant.
- (c) The synchronous motor is considered to be an ideal machine in that the magnetisation is considered linear, ignoring saturation, and that the airgap MMF is sinusoidally distributed in space. These assumptions enable the direct and quadrature axes voltages and MMF's to be resolved.
- (d) The motor is assumed to operate at a constant angular velocity. This is necessary if results are to be obtained from the simulation within a reasonable period of time. It is possible to include the modelling of the rotational performance of the machine however the time taken by the program to achieve a steady state condition would be too large, hence it was decided that only the electrical conditions under constant speed would be considered. The simulation is run for twenty



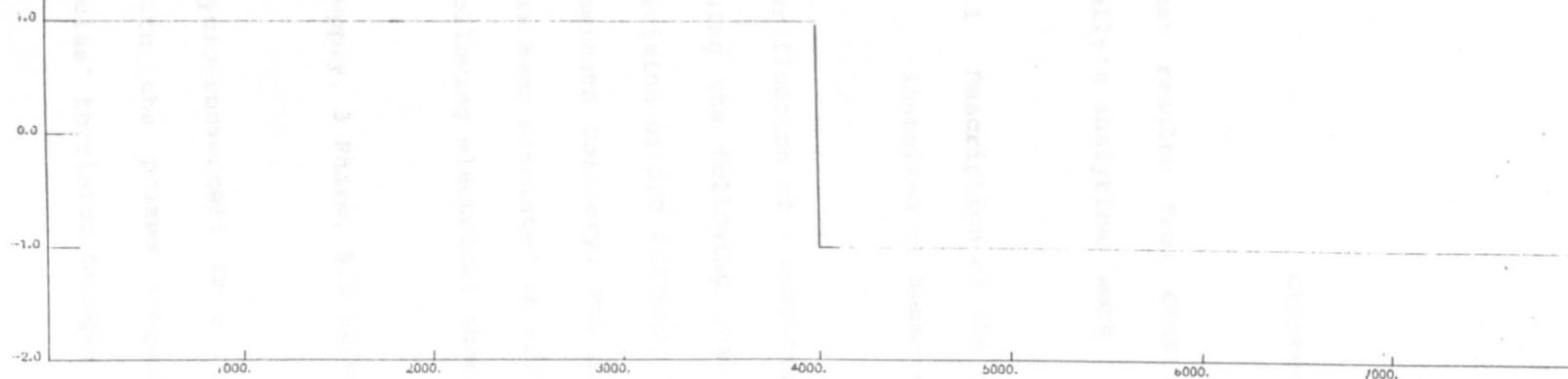
cycles to allow electrical disturbances to die away leaving the results under steady state conditions. The simulation does not respond to any mechanical oscillations that would be produced by the loading or control system for the motor.

- (e) The control system of the cyclo-converter in a real system would normally be closed loop. The computer simulation has been designed to operate at a constant voltage to frequency ratio for each drive frequency. This typical control system will produce a constant current characteristic however, if there is supply regulation due to supply reactances or decoupling reactance, the control system will compensate and keep the current constant. However when these reactances are included in the open loop control system, the simulation does not modify the firing circuits to keep the current at a constant level.

JENG505

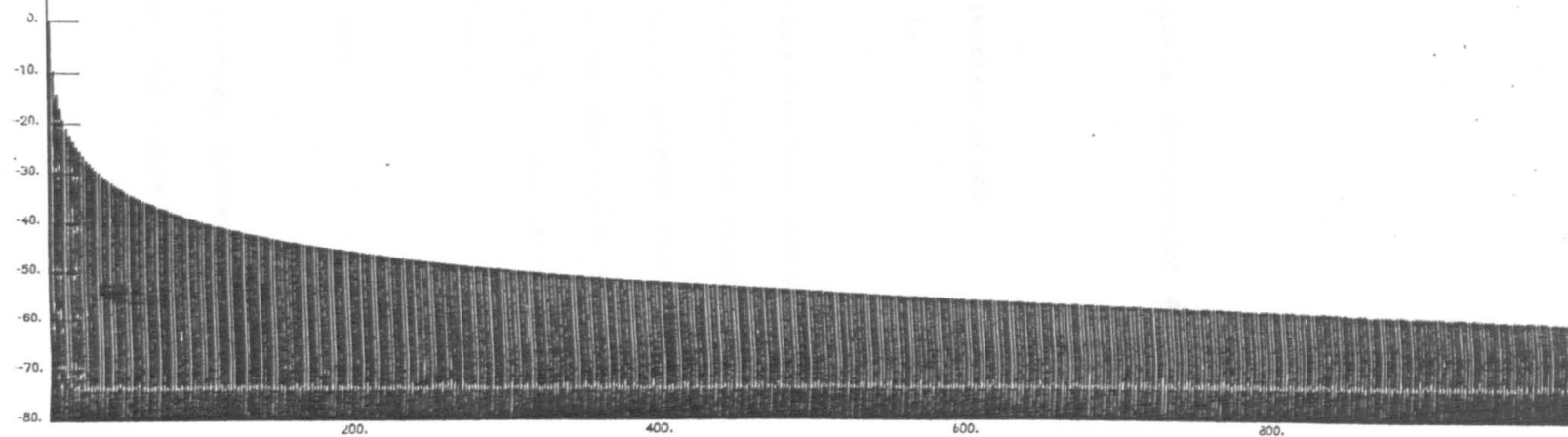
SPCUR.DATPP

100



SPCUR

TIME



HARMONICS

b

Fig 3.1c Characteristic performance of the fourier analysis routines

## Chapter 4

Test results from CEGELEC, Newcastle University and  
Pelly's analytical work

### 4.1 Description of the cyclo-converter drive installed at Weamouth Fig 4.1a

Verification of a computer simulation has been obtained using the following results from GEC Marine Drives a division of GEC ALSTHOM, for a cyclo-converter drive at Weamouth Colliery. The arrangement of the drive which has been simulated is shown in Fig 4.1a the drive has following electrical characteristics:-

Supply: 3 Phase, 5.5 kV/550 V, 50 Hz;

Cyclo-converter: is a "non circulating current" type with the phases comprising two anti-parallel "six pulse" thyristor bridge;

The induction motor: 373 kW machine designed for 412 V RMS at maximum frequency of 20 Hz, with a full load current of 355 A at a full load slip of 1.89% ;

Motor speed 587 rpm, 4 Pole machine.

#### 4.1.1 Test 2 Comparison with results obtained at

Wearmouth: Fig 4.1b, 4.1c, 4.1d, 4.1e

To validate the program a series of tests were conducted on the simulation program where the frequency was varied from 2.5 Hz to 20 Hz and the results compared to those obtained experimentally. The comparison of the waveforms obtained for cyclo-converter output voltage and current at a frequency of 5.0 Hz are shown in Fig 4.1d, ; as can be seen there is a good degree of correlation between the results obtained experimentally and those produced by the computer simulation.

Comparison of the "harmonic spectrum" for the input line current, cyclo-converter output voltage and cyclo-converter output current are shown in Fig 4.1e . The general shape obtained does shows a high degree of correlation. It should be noted that the harmonics obtained at levels below 30 Db cannot be taken as significant, since this is well into noise level for the equipment under consideration. The variation of output frequency does effect the harmonics produced in all three characteristics shown above, the line current harmonics will vary in accordance with the theoretical analysis by Pelly 16. It should be noted that Pelly's

# GEC Electrical Projects Limited

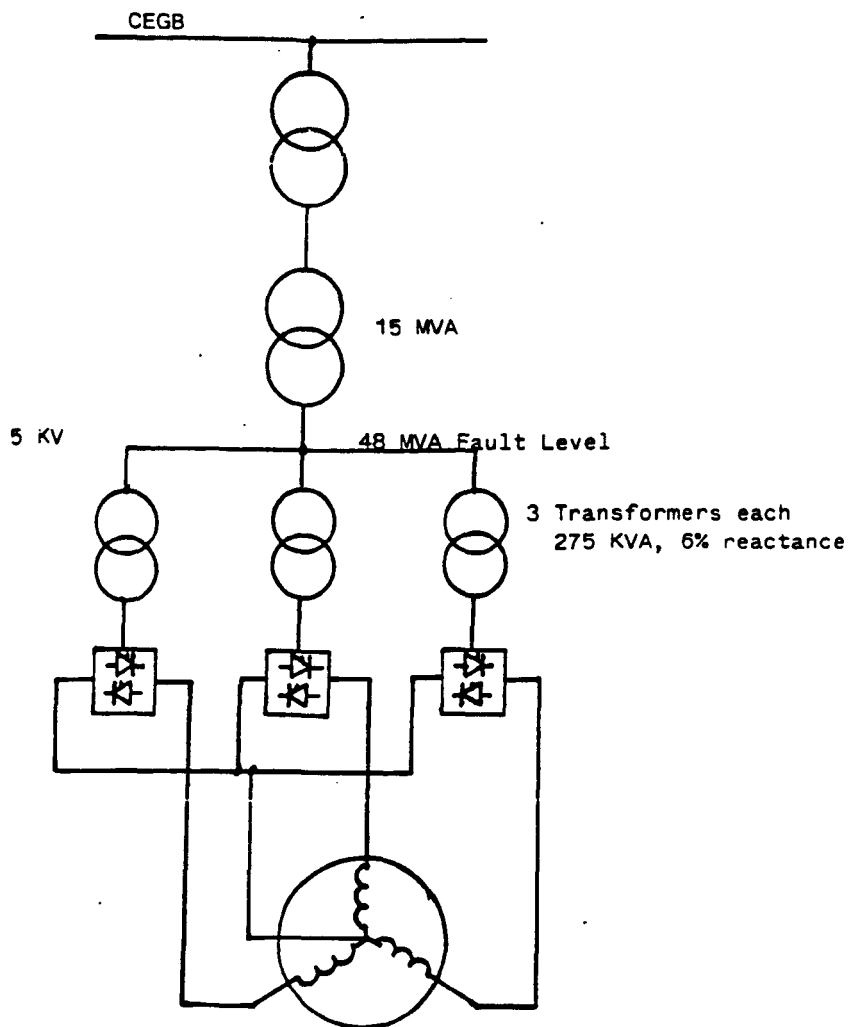
Reference

Section

Sheet

Conn.

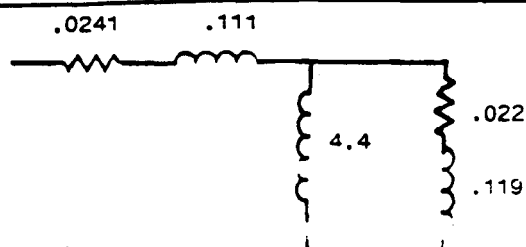
CYCLO-CONVERTOR DRIVE (WEARMOUTH)



## Motor

500 HP  
714 volts  
20 Hz

## SYSTEM CONNECTIONS FOR FACTORY TESTS



Circuit constants in ohms  
at 20 Hz

Motor supply 412 volts/ph  
at 20 Hz

Full load current 355 amp

Full load slip 1.89%

## MOTOR EQUIVALENT CIRCUIT

Fig 4.1a Cyclo-converter fed induction motor driving Koepe winder at Wearmouth Colliery

Issue

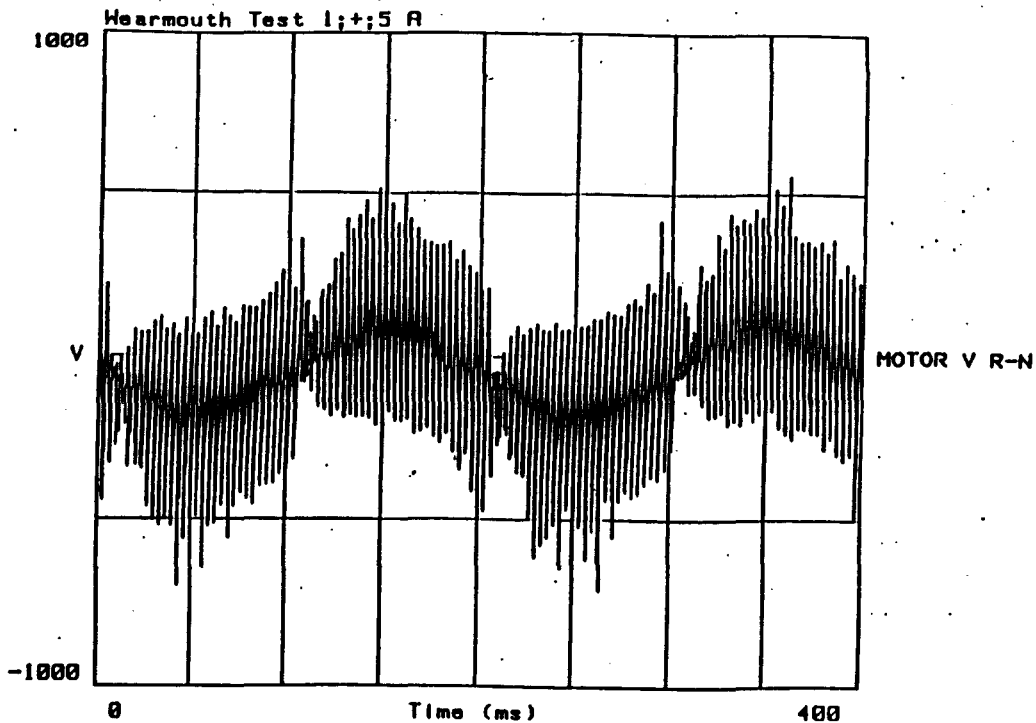
Date

Author

**GEC**

18FUIA

FIG. 4.4.2. MOTOR VOLTAGE WAVEFORM (V<sub>m</sub>) (f<sub>o</sub> = 5Hz)



18FUIA

FIG. 4.5.2. MOTOR CURRENT WAVEFORM (I<sub>r</sub>) (f<sub>o</sub> = 5Hz)

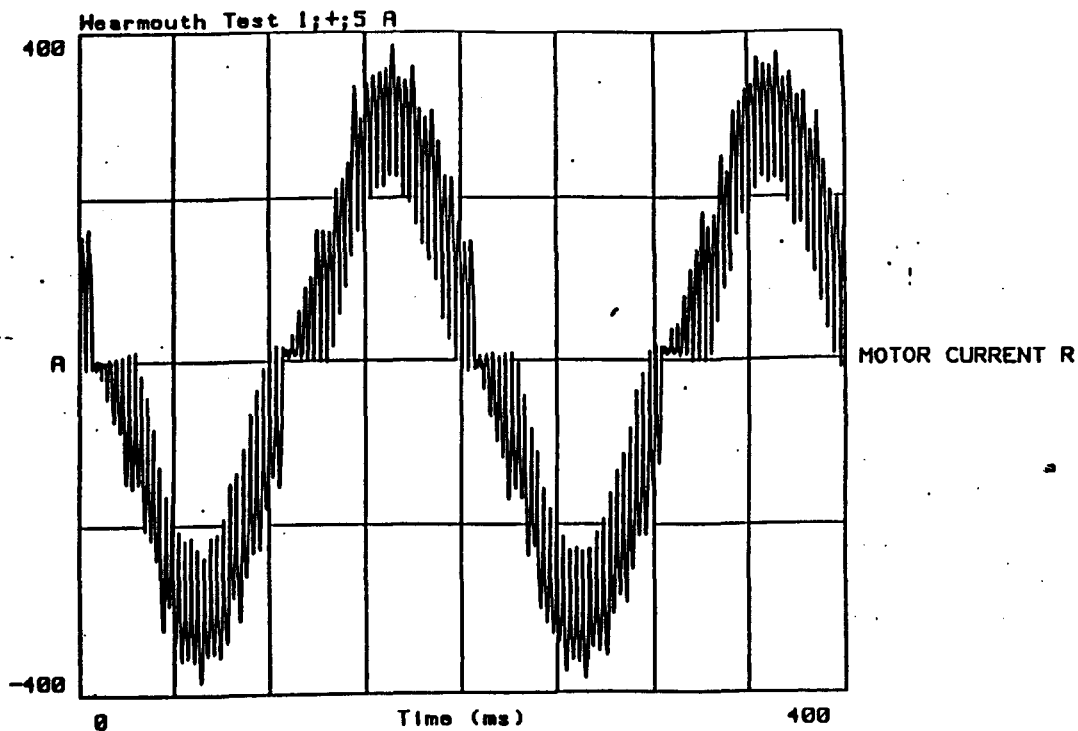


Fig 4.1b Converter output voltage and current waveforms at 5 Hz drive frequency (Wearmouth Colliery)

FIG. 4.4.7 MOTOR VOLTAGE SPECTRUM (V/r) (fo = 5Hz)

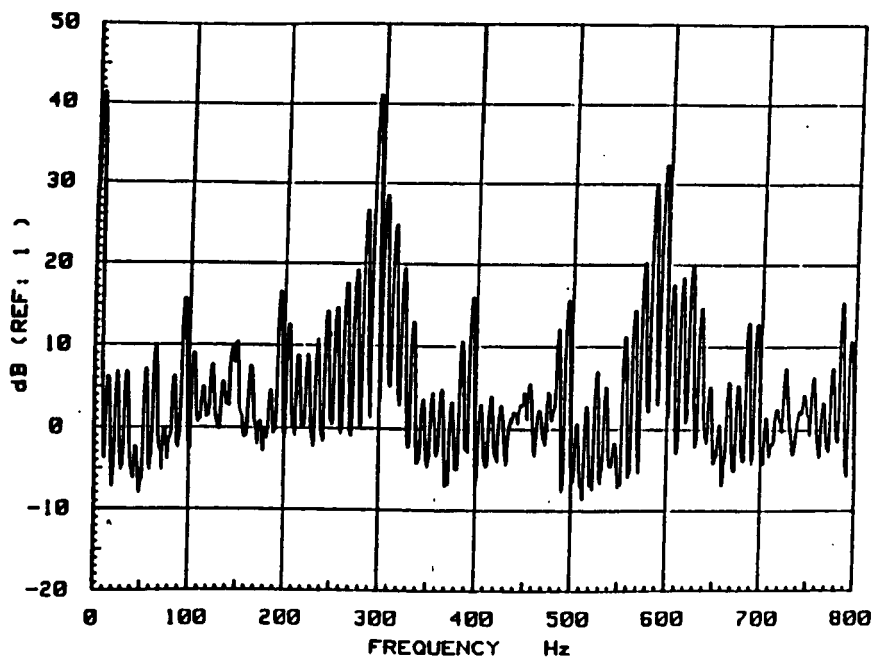


FIG. 4.5.7 MOTOR CURRENT SPECTRUM (I/r) (fo = 5Hz)

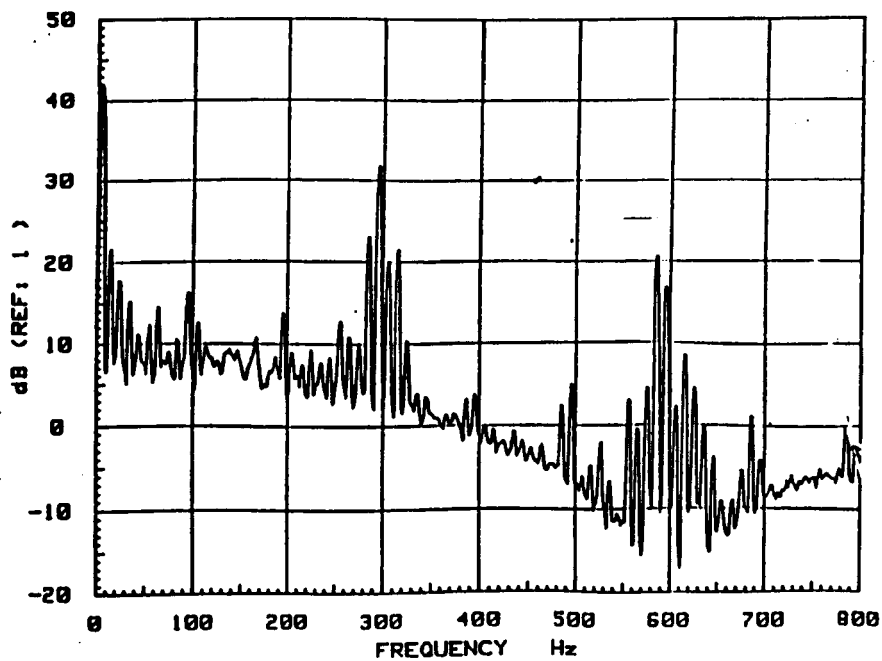
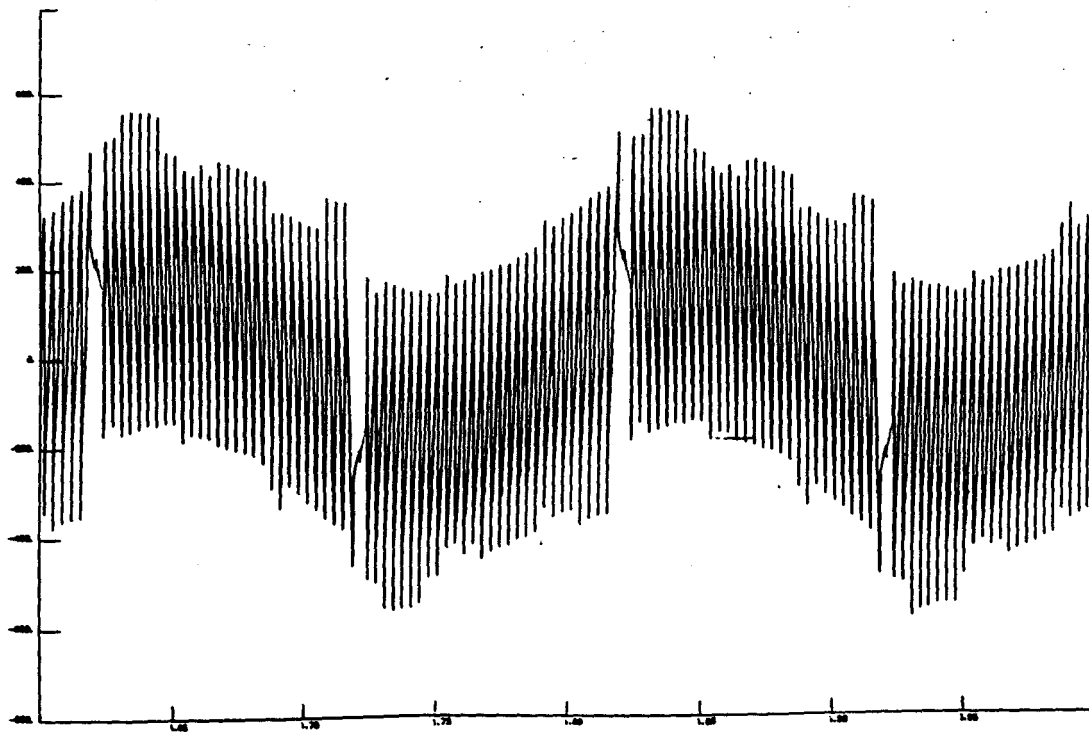


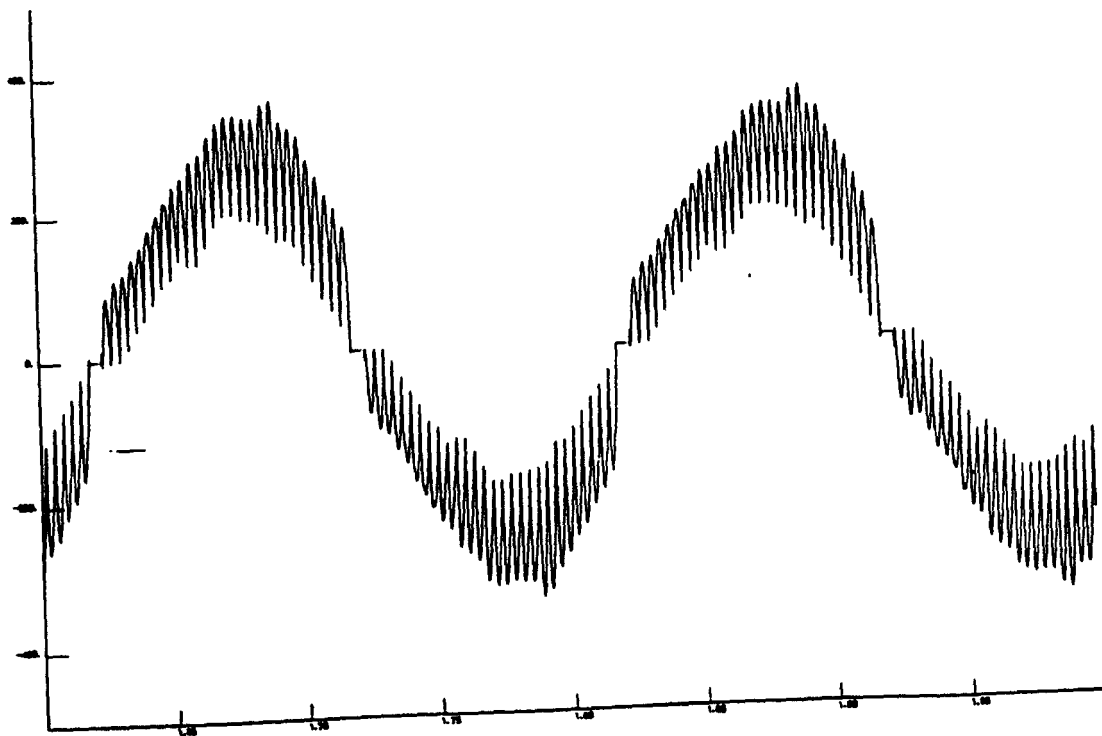
Fig 4.1c Spectrum of the voltage and current waveforms at 5 Hz drive frequency (Wearmouth Colliery)

JENG505

V  
X  
C

TIME(SECONDS)

JENG505

I  
A

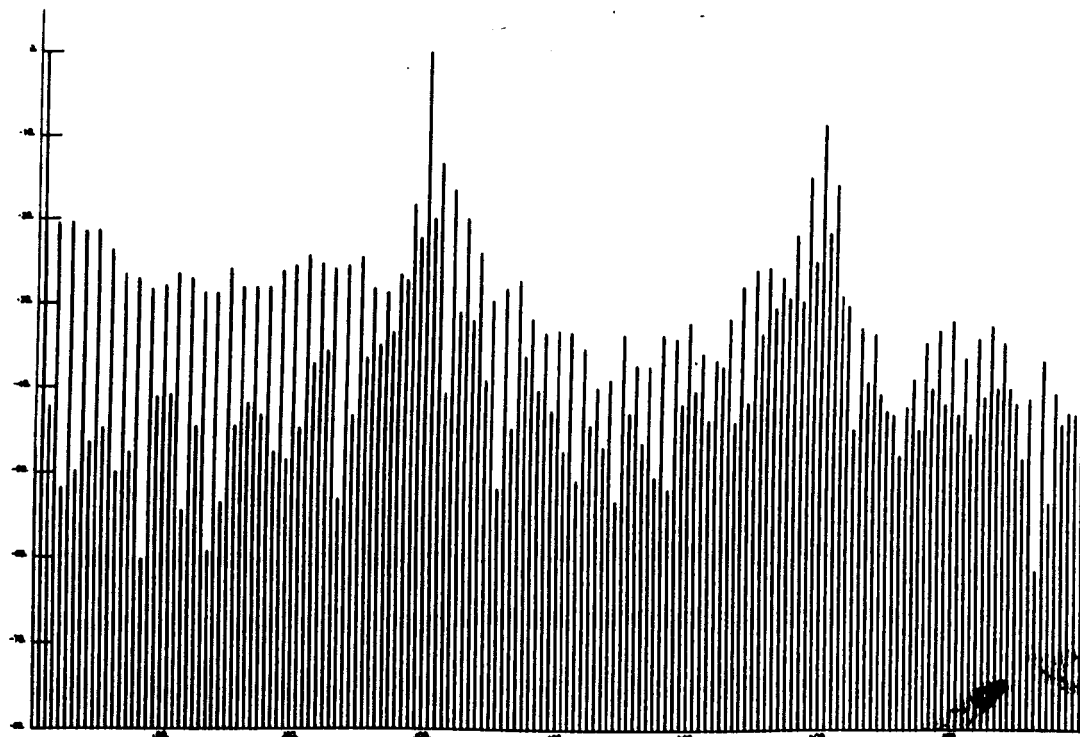
TIME(SECONDS)

Fig 4.1d Simulation results of voltage and current at 5 Hz drive frequency



JENG505

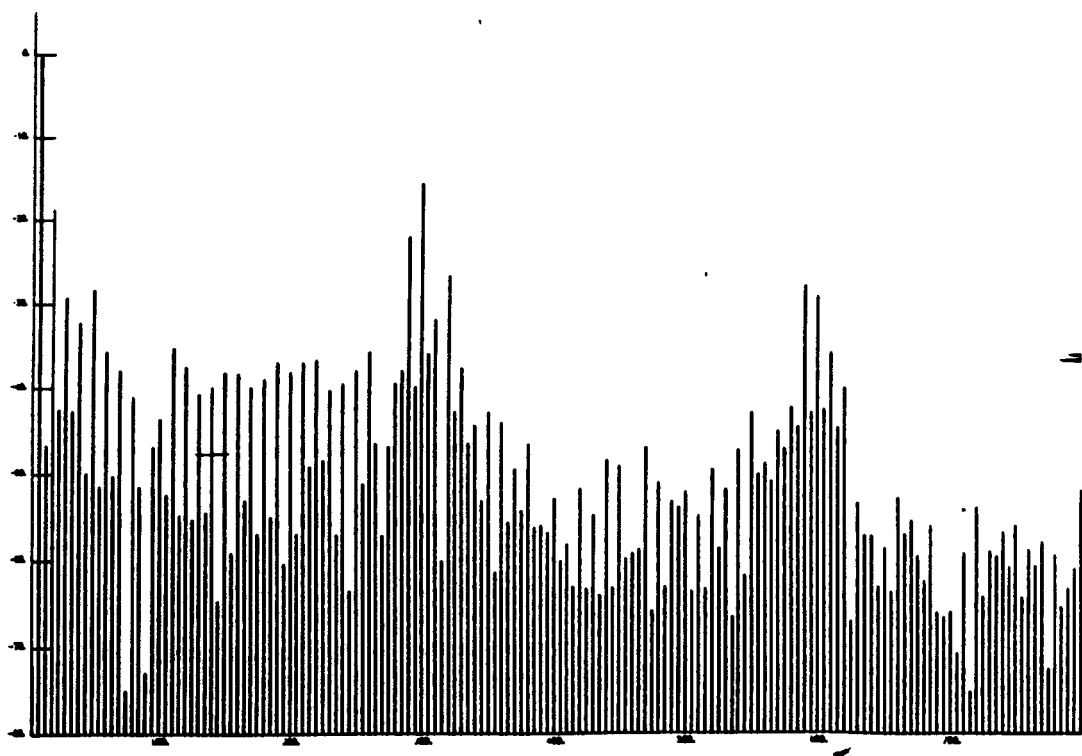
VOLT



HARMONIC NUMBER

JENG505

CURR



HARMONIC NUMBER

Fig 4.1e Simulation results for spectrum of voltage and current at 5 Hz drive frequency

analysis is limited in that it only considers static loads and does not include interbridge delay, decoupling reactance, or supply system impedance.

#### 4.2 Description of the cyclo-converter at Newcastle University

A test was simulated to see if the results of Newcastle University could be replicated ignoring interbridge delay, source impedance, decoupling reactance, and overlap. The second test was to assess the effects of including these system and converter parameters.

The test was conducted on the following cyclo-converter drive:-

The Supply: 3 Phase 243V at 50Hz;

Cyclo-converter: a "non circulating current" type with the phases comprising two anti-parallel "6 pulse" thyristor bridge;

The induction motor parameters:

$R_d = R_q = 0.8060$ ,  $R_{dd} = R_{qq} = 0.759$ ,  $L_d = L_q = 0.12$  H,  $M_{dd} = M_{qq} = 0.112$  H, pole pairs = 2, slip = 0.09,

modulation depth = 0.4, output frequency = 16.67 Hz

#### **4.2.1 Test 3 Comparison with experimental results**

obtained at Newcastle: Fig 4.2a, 4.2b

The first test results are shown in Fig 4.2b. This shows that it was possible to reproduce the results produced at Newcastle University.

With the authors simulation it is possible to include system parameters supply, decoupling reactance, interbridge and overlap. A much higher degree of correlation can therefore be obtained compared to the results taken on the Newcastle test rig. The simplified simulation results indicate that it is unwise to over simplify the power system or converter in any computer modelling exercise.

#### **4.3 Description of Pelly's analytical work**

##### **4.3.1 Harmonic analysis of the output voltage of the cyclo-converter**

The cyclo-converter can be operated with circulating current between the two bridge converters or in the circulating free mode. Pelly has chosen primarily to analyse the latter as this is used in most practical systems. The analysis and quantitative data presented are applicable to an 'open loop' cosine wave crossing

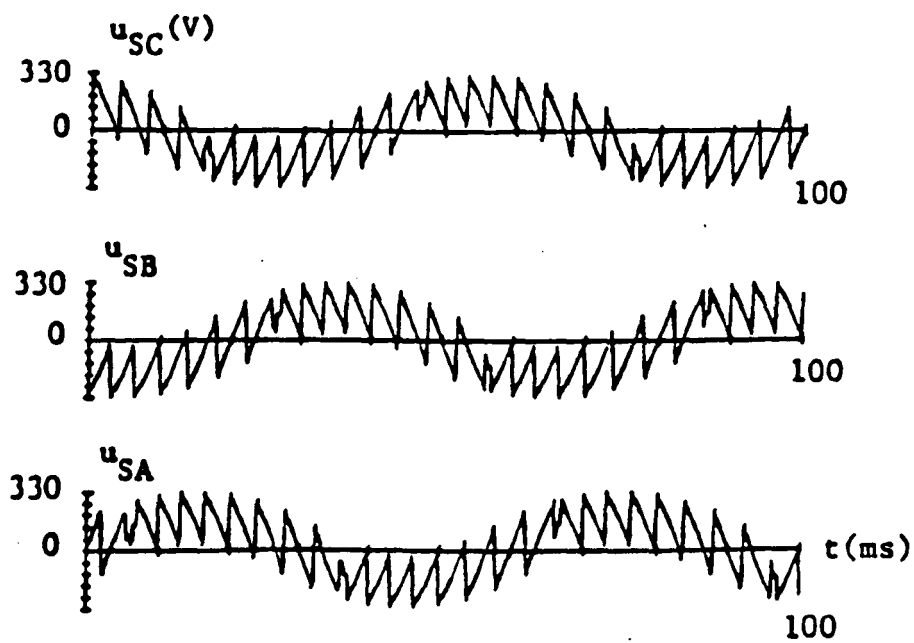


Fig. 5 Cycloconverter Output Voltages

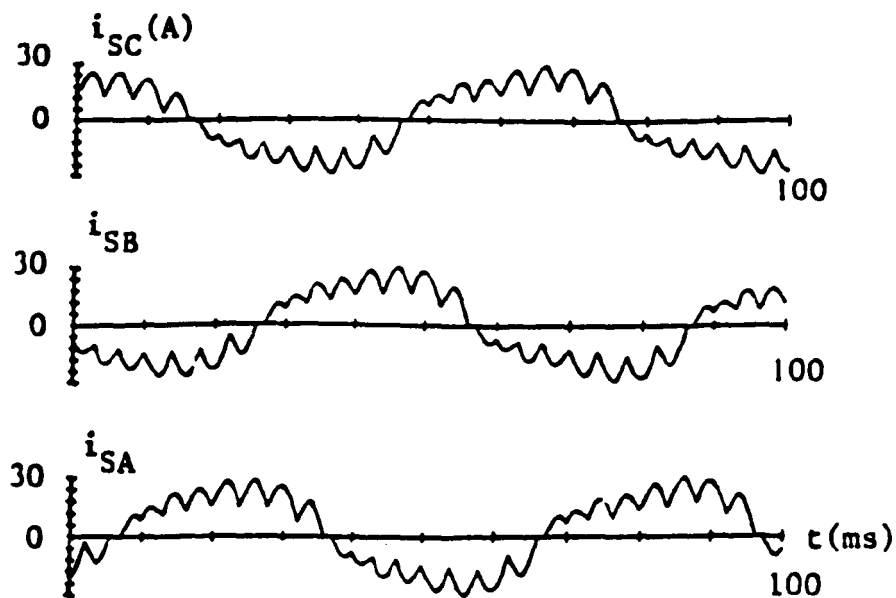


Fig. 6 Motor Phase Currents

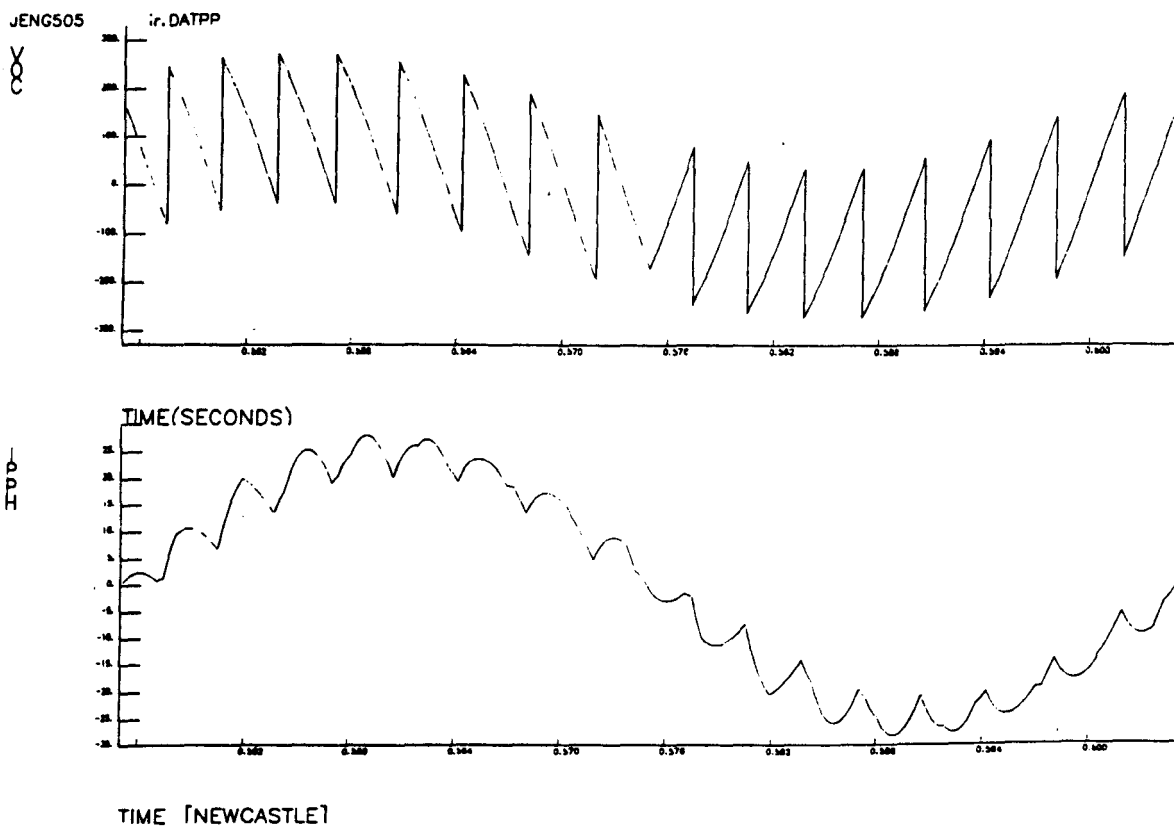


Fig 4.2b Simulation of voltage and current at 16.667 Hz

firing angle control, where a continuous sinusoidal load current waveform has been assumed. In other words, Pelly has assumed that the load has the ability to suppress all harmonic voltages of the load voltage waveform and hence ensure that the converter does not enter discontinuous current mode. The analysis also does not take into consideration the delay of change over from positive to negative bridge. Since the results of the harmonic analysis assume 'open loop' firing angle control they can only be very closely representative of the waveforms to be found with a closed loop control system.

Pelly's analytical approach enables the harmonic series for the output voltage to be expressed, quite generally in terms of each of the independent variables. The output voltage waveform may be expressed as the mathematical sum of the voltage segments generated by each of the individual thyristors within the converter. Each individual voltage segment is expressed as the product of the appropriate sinusoidal input voltage and a 'switching function'; this function assumes unit amplitude when the thyristor is conducting and zero when the thyristor is non-conducting. The switching function is then expressed as a 'phase modulated

harmonic series' thus arriving at a general harmonic series for the output voltage waveform in terms of each of the independent variables.

#### 4.3.2 Harmonic analysis of the input current of a cyclo-converter

In calculating the harmonics generated in the supply current to the 3 phase cyclo-converter, Pelly made the following assumptions:

As with the output voltage analysis the cyclo-converter is considered to be primarily circulating-current free, and the control is 'open loop' with the firing instants calculated by the cosine crossing control method.

The output current waveform of the cyclo-converter is assumed to be a pure sinusoid, which is displaced from the wanted component of the output voltage by the displacement angle of the load. Pelly ignores the characteristic current ripple produced by the cyclo-converter by assuming that the load is able to suppress all harmonics other than the fundamental itself.

The internal impedance of the supply system and the transformer feeding the converter is considered to be negligibly small. This may be a reasonable assumption with hard industrial supplies connected to parts of the grid system, however where the converter is installed in a self contained system as in a marine application the source impedance is not negligible.

#### 4.3.3 The results of Pelly's analytical work

Pelly produces a detailed breakdown of the harmonics to be found in the output voltage waveform and the input current waveform. The harmonics are related to a number of factors including, the pulse number, whether the load is single phase or balanced three phase, the displacement factor of the load current, and the modulation depth of the control system.

A small computer programme was written based on Pelly's work to calculate the distortion factor and the percentage harmonic content for both the output voltage waveform and the input line current waveform.



The results of Pelly's analysis of the output voltage distortion factor are given in Appendix B Table B2. The results given are for a 6 pulse converter at frequencies of 5,10,15,20 Hz with displacement factor of 0, 0.5, and 1 .

The results of Pelly's analysis of the input current distortion factor are given in Appendix B Table B1, for the same conditions defined above.

The results produced by Pelly's mathematical analysis show the overall trend that will be seen in most of the results obtained computationally.

**The output voltage distortion factor: Fig 6.9a**

This is the relationship which exists between the component of the fundamental output voltage and associated harmonics. As the output frequency approaches the frequency of the supply network ( $f > 10$  Hz) larger portions of the supply line voltages are used to produce the synthesised output voltage, it is not surprising that the voltage distortion reduces. As the frequency reduces below 10 Hz the output voltage is synthesised from a larger number of portions of the line voltage, increasing the distortion. The constant

ratio between the output frequency and voltage will have the effect of increases the distortion to the output voltage waveform.

As the drive frequency varies from 4-22 Hz, the percentage of output voltage harmonics can be seen therefore to reduce from 80-20% .

**The input current distortion factor: Fig 6.9b**

This is also related to the frequency of the drive, and can be seen not to change so significantly over the range of drive frequency. The input current is affected by the output drive frequency since the load current is responsible for modifying the waveshape of the 3 phase input line currents. The only part of input line current waveform which is modified by this process is the top portion, the sides of the input line current are not modified due to the fact that there is no source reactance in Pelly's model.

## Chapter 5

The Cyclo-converter, machine and supply operational ratings and characteristics

### 5.1 Cyclo-converter device losses and ratings

The computer model has a subroutine which calculates the current and power ratings within the cyclo-converter and motor. The calculations are normally taken over a few cycles of the reference frequency so that a precise results may be obtained.

The cyclo-converter device ratings are of particular interest. Each device may only conduct for a short period of time compared to the periodic time of the frequency being generated, yet at times it must pass the full load motor current. Those ratings which are computed include:-

$I_{av}$ :- The device forward current averaged out over a complete cycle,

$I_{rms}$ :- The rms rating of the device this is responsible for the rise in temperature of the junction.

$I_{pk}$  This may occur every cycle and as such has to be taken as the worst case peak current,

$P_d$       The power dissipated in the device this is  
             necessary to establish the required heat sink  
             for the thyristor.

## 5.2    Motor winding losses and ratings

The motor ratings have been calculated to establish the total heat losses within the motor. It is then possible to compare these losses with the cyclo-converter operating at different frequencies. The motor losses which have been computed are:-

$P_{sc}$    - Stator core loss

$P_{scu}$    - Stator copper loss

$P_{rcu}$    - Rotor damper bar copper loss

$P_f$     - Rotor field losses

To establish the stator core losses, it is necessary to calculate the back e.m.f. or magnetising voltage of the machine from the dq axis model. It is inevitable therefore that the core losses ( $P_{sc}$ ) will be dependent on any fluctuations in the field current

$$P_{sc} = \frac{(EMF)^2}{R_c} \dots\dots\dots(4)$$

The stator copper losses ( $P_{scu}$ ) and rotor bar copper losses are calculated from the stator current and rotor bar current, these are computed from the dq axis model. The level of copper losses will be dependent on the rms value of these currents.

$$P_{scu} = (I_{rms})^2 \times R_a \quad \dots\dots\dots(5)$$

The rotor field losses ( $P_f$ ) are computed from the rms currents in the field (rotor) of the synchronous motor. These losses will vary due to the induced emf from the stator windings which in turn will modify the rotor field currents.

$$P_f = (I_f)^2 \times R_f \quad \dots\dots\dots(6)$$

### 5.3 High voltage supply network electrical operating characteristics and cyclo-converter output characteristics

The performance of the supply network is affected not only by the machine load characteristic but also by the cyclo-converter and the control system.

The level of disturbance to the supply network is evaluated to enable the design engineers to ensure that the network is of adequate strength and that other consumers are not adversely affected by the harmonic distortion. The supply line currents are calculated from the three input currents

of the individual phases of the cyclo-converter. These abc currents are then summed together to give the total supply current. The supply voltages are modified by the cyclo-converter currents and the commutation process within the cyclo-converter. Fourier analysis is used to obtain a spectrum of the harmonic content of the voltages and currents in the supply network.

### 5.3.1 RMS Ratings

The rms values of the following system voltages and currents are calculated in the classical way over the same period.

$$V_{rms} = \sqrt{\frac{\text{sum (instan. voltage)}^2 \times dt}{\text{Total time}}}$$

The rms values (including the harmonics) :-

$I_{ph}$  (rms) phase currents

$V_{ph}$  (rms) phase voltages

$I_s$  (rms) line currents

$V_s$  (rms) line voltages

### 5.3.2 Distortion factor

The harmonics associated with supply currents are responsible for producing distortion of the supply voltage on the network. If the supply is obtained from a HV or EHV supply point, the supply authorities will normally specify

the amount of distortion which can be tolerated at that particular point in a supply network, (see Appendix E Electricity Regulation G5/3), to ensure that other customers connected at the point of common coupling are not adversely affected. The distortion factor is defined as the ratio between the fundamental rms component and the total rms component of the waveform. To obtain these components it is necessary to apply the Fourier analysis to the waveform concerned and then extract the fundamental component. The rms total component can be obtained by the sum of the squares of the individual components, this value can then be compared with the rms value obtained in section 5.3.1 .

$$\text{Distortion factor} = \frac{\text{rms fundamental component}}{\text{rms total component}}$$

The percentage harmonic component of a particular waveform is calculated from the distortion factor:

$$\text{Percent. Harmonic} = (1 - \text{distortion factor}) \times 100$$

The distortion factor is calculated in the computer simulation for the input and output line voltages and currents. Pelly, in his theory, calculates analytically the output voltage distortion factor and the input line current distortion factor. He also makes the assumption that the output current waveform is perfectly sinusoidal, in other

words the output current distortion factor is 1.0. This is far from the truth and causes the input current distortion factor to be in error, the input line current contains harmonics related to the load frequency which are therefore responsible for producing harmonic voltage drops in the supply voltage waveform. Pelly's model does not take into consideration the modification to the supply waveform due to the harmonic content of the load.

### 5.3.3 Power factor

The definition of power factor for an electrical circuit , is the factor by which the voltamperes must be multiplied in order to give the average power. In the sinusoidal ac system where the current contains no harmonics, the power factor is conventionally defined as the cosine of the angle between the current and the voltage, this is more commonly known as the displacement factor. With low reactance supplies, the supply phase voltage can be taken as being sinusoidal, and hence there will be no power associated with the harmonic currents.

$$\text{power} = V_{\text{rms}} \times I_{\text{rms}} \times \text{displacement angle}$$

This however cannot be assumed in this instance as the supply waveform contains a significant quantity of harmonics and therefore a more precise calculation is required:



$$\text{power} = \frac{\sum (\text{instan. voltage} \times \text{instan. current}) \times dt}{\text{time period}}$$

The average power is calculated on an incremental basis over the last 3 cycles of the drive frequency, the power factor can now be calculated assuming that the total rms value of the voltage and currents are known:

$$\text{power factor} = \frac{\text{average power}}{V_{\text{rms}}(\text{total}) \times I_{\text{rms}}(\text{total})}$$

#### 5.3.4 Power and efficiency calculations

Losses in the drive can be calculated, this is to predict the motor efficiency and converter efficiency. As the converter is working at high voltage the devices in this instance have been modelled as perfect devices making them lossless. This means that there will be no difference between the input and output power to the converter.

The motor efficiency has been calculated by two methods, firstly by measuring the input and output power. The second method calculates the machine losses and compares that to the motor input power.

$$\text{input power} = \frac{\sum (I(\text{instant}) \times V(\text{instant})) \times dt}{\text{total time}}$$

$$\text{Ave. torque} = \frac{\sum (\text{torque}(\text{instant})) \times dt}{\text{total time}}$$

$$\text{output power} = \text{average torque} \times \omega_m$$

$$\text{Motor losses} = P_{sc} + P_{scu} + P_{rcu} + P_f$$

$$\text{Motor Eff(1)} = \frac{\text{output power}}{\text{input power}} \times 100$$

$$\text{Motor Eff(2)} = \left( \text{input power} - (P_{sc} + P_{scu} + P_{rcu} + P_f) \right) \times 100$$

---

input power

### 5.3.5 Voltage Regulation

The power supply system includes supply and decoupling reactances these are responsible for the regulation of the power supply network. This analysis considers the effects of these reactances on the supply network and load waveforms.

$$\text{Voltage regulation (1)} = V_{rms}(\text{supply}) - V_{rms}(\text{line})$$

---

$V_{rms}(\text{supply})$

$$\text{Voltage Regulation (2)} = V_{rms}(\text{supply}) - V_{rms}(\text{converter})$$

---

$V_{rms}(\text{supply})$

Voltage regulation (1) considers the regulation of the supply system reactance, whereas the voltage regulation (2) calculates the regulation of the supply system and the decoupling reactances.

### 5.3.6 Torque ripple factor

Torque pulsations are produced in the mechanical drives of synchronous machines by the chopping action of the power electronic drive on the current waveforms. The converter produces input and output currents which are rich in harmonics. These harmonics are responsible for producing torque pulsations which can produce damage to the machine windings and mountings, due to the equal and opposite reaction. In naval applications where passive sonar is used the production of harmonics by the ship propulsion system can produce significant levels of interference due to the torque pulsations produced and transmitted through the drive shaft and machine mountings.

The torque ripple factor is an indication of the percentage of harmonic torque pulsations which are being experienced by the synchronous motor or the alternator supply. It is important to realise that harmonic ripple should be related to the rated torque rather than the average torque. This is because the average torque on the alternator will vary with load conditions, and it is the ratio to the rated torque which is important for machine designers.

$$\text{Tor(rms)} = \sqrt{\frac{\sum ( \text{instant. torque} )^2 \times dt )}{\text{time period}}}$$

$$\text{Tor(av)} = \frac{\sum (\text{instant.torque}) \times dt}{\text{time period}}$$

$$\text{Ripple factor} = \frac{\sqrt{(\text{Tor(rms)}^2 - \text{Tor(av)}^2)}}{\text{Tor(rated)}}$$

## Chapter 6

### Testing of system characteristics and complete systems

#### 6.1 The power system to be analysed

Fig 1.1 shows a simplified schematic for a marine drive system it is a simplified model for the evaluation of the detailed effects of the system characteristics such as interbridge delay and overlap. Although the multiple drives are not simulated individually, their lumped effect represents a worse case condition from the harmonic current generation.

The converter is a circulating current free 6 pulse bridge cyclo-converter whose modulation depth is related to the frequency of the drive, unless specified separately.

The motor used for this study is taken from a marine application and comprised a 10 MW synchronous motor with a basic system voltage of 6.6 kV. The motor is fitted with damper windings and therefore can only fully be modelled with the dq axis motor model.

## 6.2 The synchronous machine load

The motor which is modelled in the following series of tests is defined in Appendix A. The motor data has been provided by CEGELEC, it represents a large synchronous machine which has a base frequency of 50 Hz. This will have the effect of producing a higher level of cyclo-converter output voltage harmonics than for a comparable machine with a lower base frequency. The machine dq axis equivalent circuit is provided with the machine not entering saturation.

The machine has been set up with an over excited field, this has been designed to enable the motor to operate at near unity displacement factor, and produces a power factor of 0.6 at a frequency of 20 Hz due to the distortion of both voltage and current waveform. With the motor operating at a load angle of 0.66 radians, model 1 produces rated output torque of 149 KN. The inclusion of system characteristics in the computer simulation reduce the torque that the motor can produce. It would be very interesting but very time consuming to examine the conditions to bring the motor back to this rated torque. These test therefore will only examine the change in performance of the drive due to the inclusion the supply and cyclo-converter characteristics.

The load current and input line current waveform are dependent on the load which is applied to the motor shaft. The load is defined by the load angle of the synchronous motor and is therefore not able to respond to mechanical transients or the dynamic behaviour of the ship's propeller.

The load angle and speed of the synchronous motor are fixed, the simulation is therefore not able to predict the performance of the converter and motor under closed loop control. The load conditions for each of the models will be the same, therefore any comparison will only strictly be valid for the model as described at the specified load angle.

#### 6.2.1 Control system effects

The results of this simulation are purely related to the 'open loop' firing angle control, and not strictly applicable to a practical control scheme which uses a negative feedback to provide current control.

The results obtained under the 'open loop' simulation for the output voltage will be very closely representative of the predominant harmonic components to be found in the output voltage. This is because the components inherently cannot be suppressed, and are therefore virtually unmodified by feedback.



This simulation weakness is that the 'closed loop control' in practical schemes is used to suppress the small amounts of objectionable distortion terms which would otherwise be present. Nevertheless it is possible to use the simulation to analyse the objectionable subharmonic components, obtained with an open-loop firing angle control, and the knowledge of these 'open loop' amplitudes of these components would enable an assessment of the feasibility, of suppressing them by means of corrective feedback. The simulation does not therefore highlight the disparity in results due to the different approaches to system modelling, but provides results which will indicate the importance of system and operational characteristics.

### 6.3 The characteristic behaviour of the basic model

#### 6.3.1 Test 4 Monitor of the system behaviour from 4-22 Hz

(see Appendix D)

To monitor the behaviour of the drive system over the required frequency range (4-22 Hz), a set of tests was undertaken. The main system parameters were plotted to ensure that the model performed correctly, and that there was no unusual system behaviour.

Typical waveforms for each of the models are also provided in Appendix D

Fig 6.4a Waveforms of converter with Sinewave output current

Fig 6.4b Harmonics of converter with Sinewave output current

Fig 6.4c Waveforms of converter with Model 1

Fig 6.4d Harmonics of converter with Model 1

Fig 6.4e Waveforms of converter with Model 2

Fig 6.4f Harmonics of converter with Model 2

Fig 6.4g Waveforms of converter with Model 3

Fig 6.4h Harmonics of converter with Model 3

Fig 6.4i Waveforms of converter with Model 4

Fig 6.4j Harmonics of converter with Model 4

Fig 6.4k Waveforms of converter with Model 5

Fig 6.4l Harmonics of converter with Model 5

#### 6.4 System characteristics and their effects

The first series of tests was designed to observe the system characteristics interbridge delay, decoupling reactance, supply reactance and overlap, and their effect on the performance of the cyclo-converter and the power supply network.

##### 6.4.1 Test 5 The effects of interbridge delay

The purpose of the test was to assess the effects of interbridge delay on the system behaviour and in particular the current distortion factor, using a delay 0.003 ms of interbridge delay.

##### Test conditions:

The computer simulation was operated over the range of drive frequency 4-22 Hz with the following system characteristics

Run A	Run B
Supply reactance 0%	Supply Reactance 0 %
Decoupling Reactance 0 %	Decoupling reactance 0 %
Interbridge Delay 0.00 mS	Interbridge delay 0.003mS
No overlap	No overlap
dq axis motor model	dq axis motor model

##### Test results:

The following system operational characteristics were plotted against the drive frequency :-

Fig 6.5a Input current harmonic ripple (%)

Output current harmonic ripple (%)

Fig 6.5b Output voltage harmonic ripple (%)

Fig 6.5c Output phase voltage (V)

Output phase current (A)

# TEST 5

## INTERBRIDGE

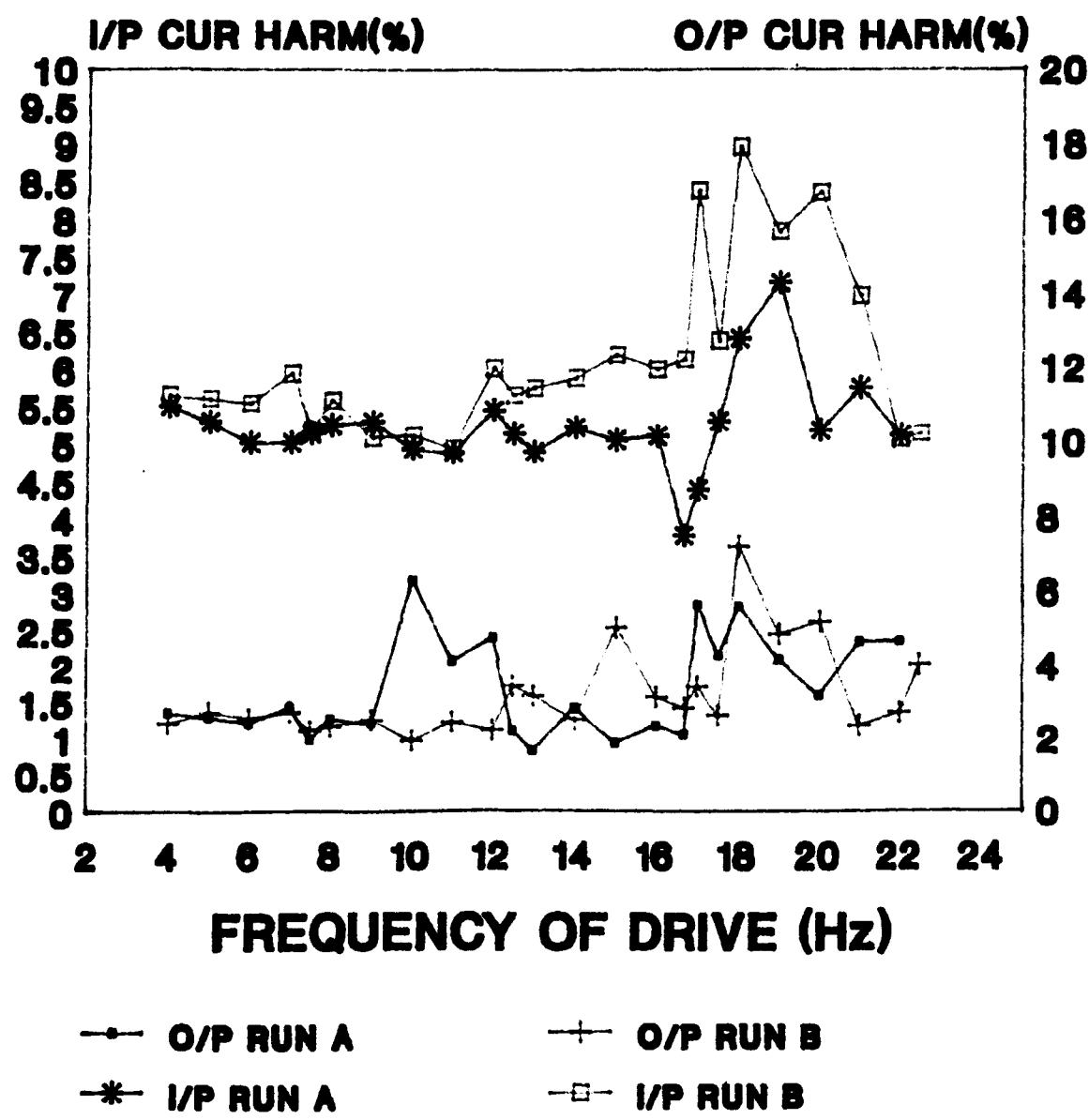
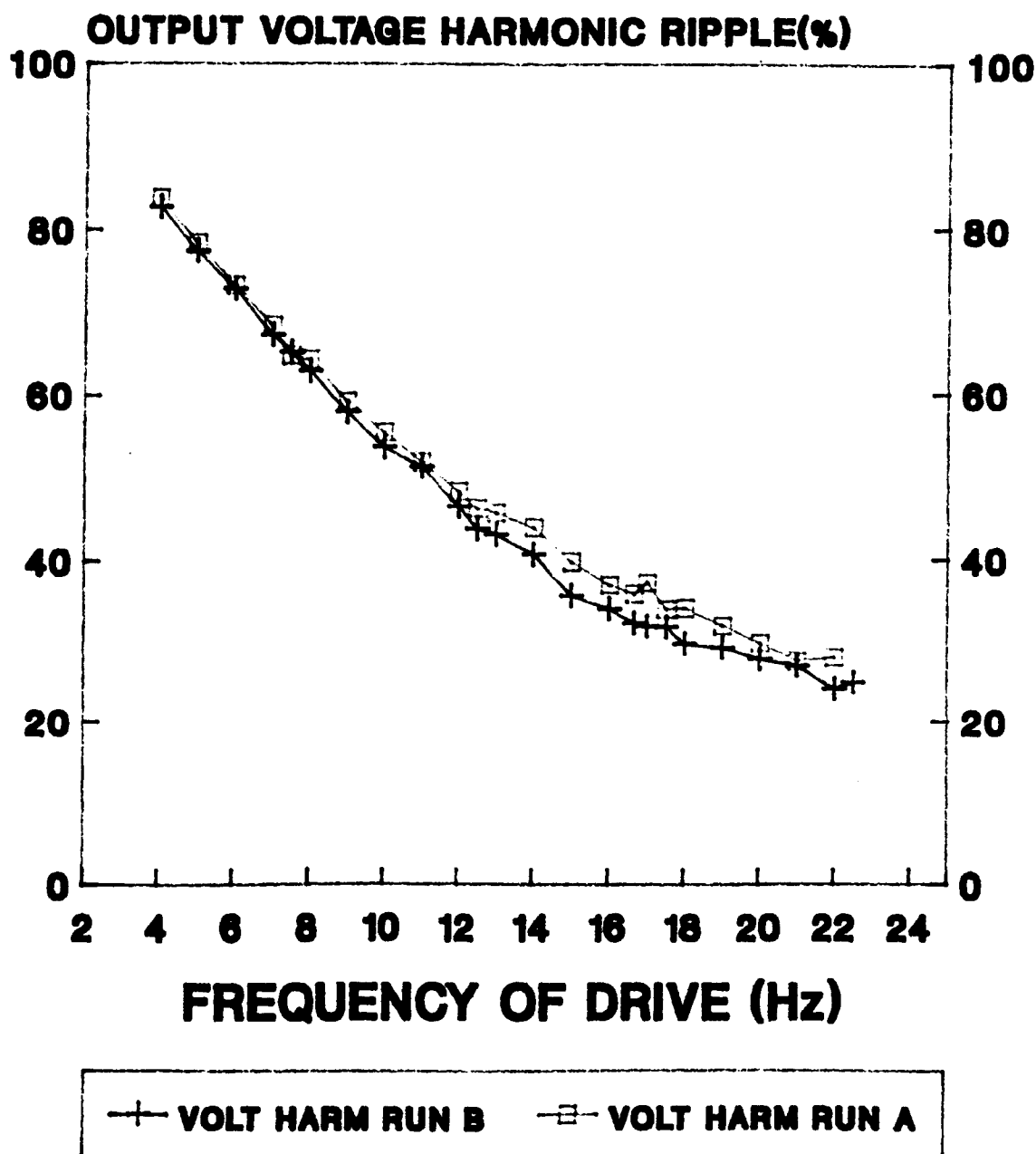


Fig 6.5a Input Harmonic Ripple (%)  
Output Harmonic Ripple (%)

# TEST 5

## INTERBRIDGE



**Fig 6.5b Output Voltage Harmonic Ripple**

# TEST 5

## INTERBRIDGE

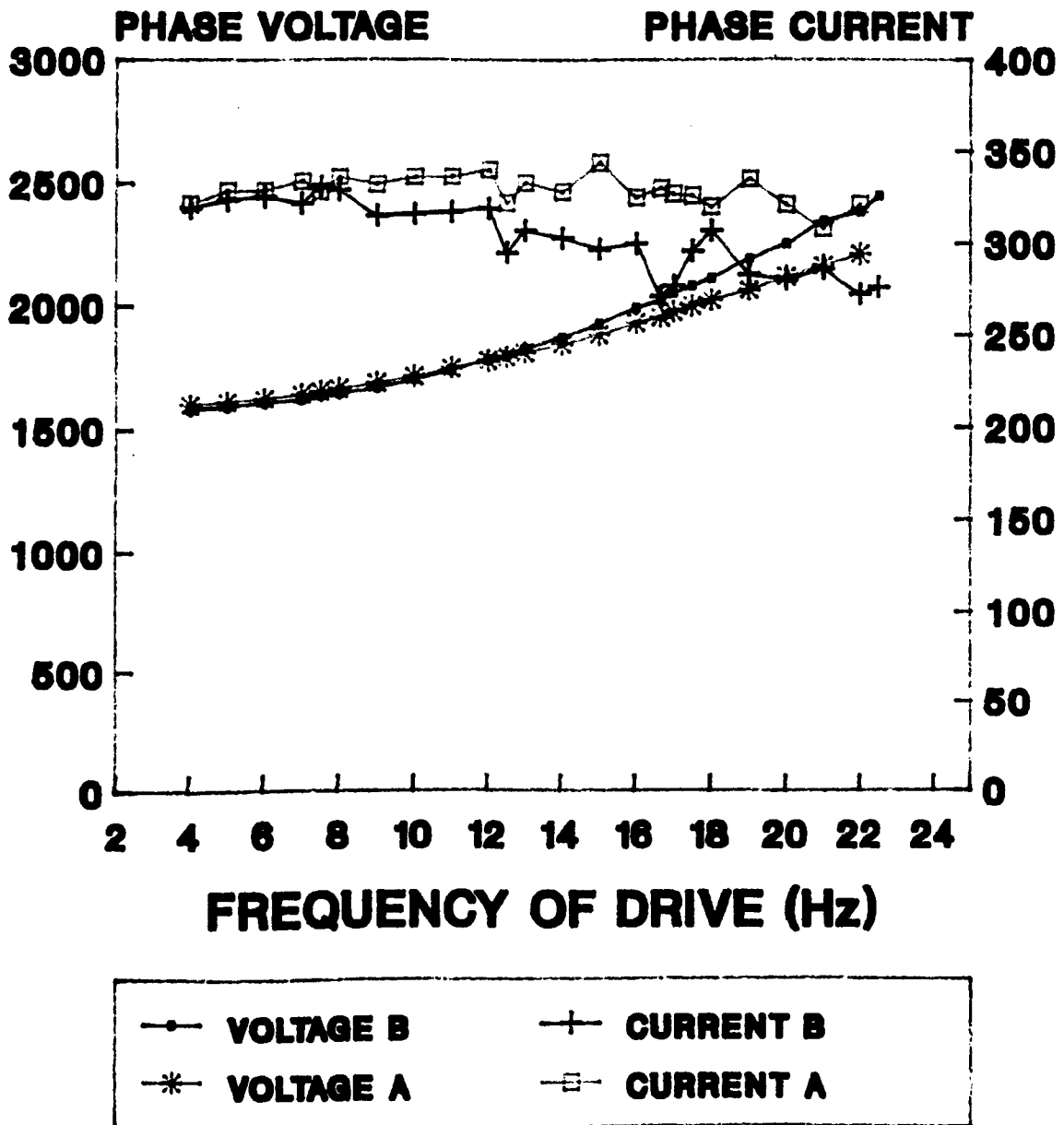


**Fig 6.5a Output Phase Voltage**  
**Output Phase Current**

#### 6.4.2 Test 6: The effects of overlap

The purpose of the test was to assess the effects of including overlap, to achieve this it was necessary to divide the supply and decoupling reactances into two components  $L_s(ov)$  and  $L_d(ov)$  reactance which is used to calculate overlap in the simulation, and  $L_s(r)$  and  $L_d(r)$  the reactance which effects supply voltage regulation this parameter only has effect when the computer simulator is not in overlap.

##### Test conditions:

The computer simulation was operated over the range of drive frequency 4-22 Hz with the following system parameters:

Run A	Run B	Run C
$L_s(ov) 0 \%$	$L_s(ov) 0 \%$	$L_s(ov) 2.5 \%$
$L_s(r) 0 \%$	$L_s(r) 2.5 \%$	$L_s(r) 2.5 \%$
$L_d(ov) 0 \%$	$L_d(ov) 0 \%$	$L_d(ov) 5 \%$
$L_d(r) 0 \%$	$L_d(r) 5 \%$	$L_d(r) 5 \%$
I/B 0.00 mS	I/B 0.00 mS	I/B 0.00 mS
No Overlap	No Overlap	Overlap
dq motor	dq Motor	dq motor
(I/B - interbridge )		

$L_s(ov)$  This is the value of supply inductance used in the program for the sections dealing with overlap.

$L_s(r)$  This is the value of supply inductance used in the



program for the sections dealing with the regulation of the supply system when the program is not in overlap.

Ld(ov) This is the value of decoupling inductance used in the program for the sections dealing with the overlap.

Ld(r) This is the value of decoupling inductance used in the program for the sections dealing with the regulation of the supply system when the program is not in overlap.

**Test results:**

The following system operational characteristics were plotted against the drive frequency :-

Fig 6.6a Input current harmonic ripple (%)

Input voltage harmonic ripple (%)

Fig 6.6b Input voltage regulation

Fig 6.6c Output phase voltage (V)

Output phase current (A)

Fig 6.6d Output voltage harmonic ripple (%)

Fig 6.6e Output current harmonic ripple (%)

# TEST 6 OVERLAP

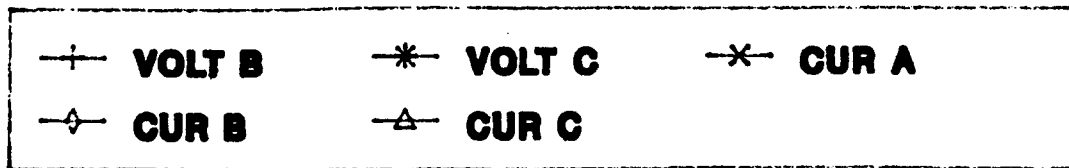
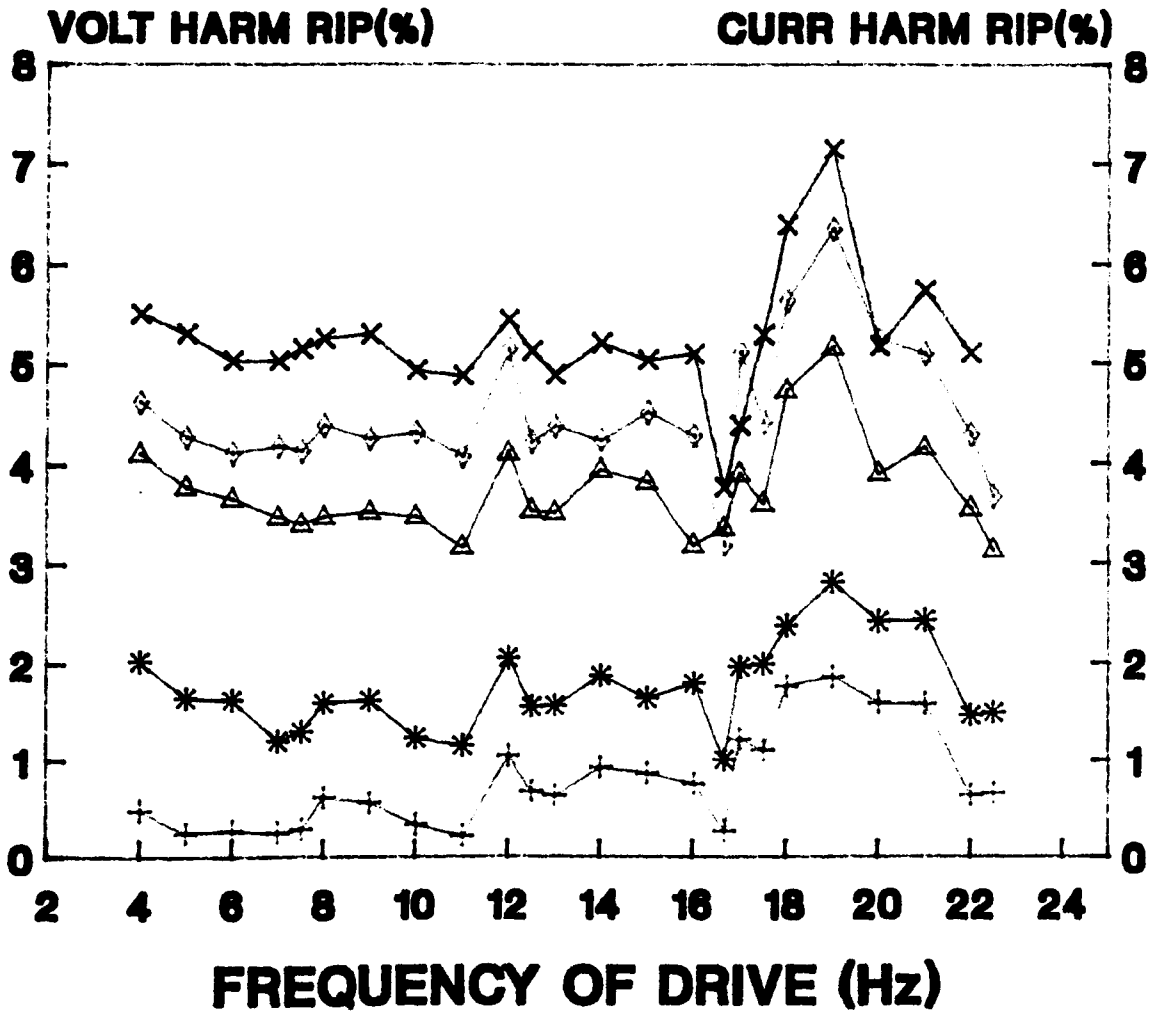


**Fig 6.6a Input Voltage Harmonic Ripple  
Input Current Harmonic Ripple**

# TEST 6 OVERLAP

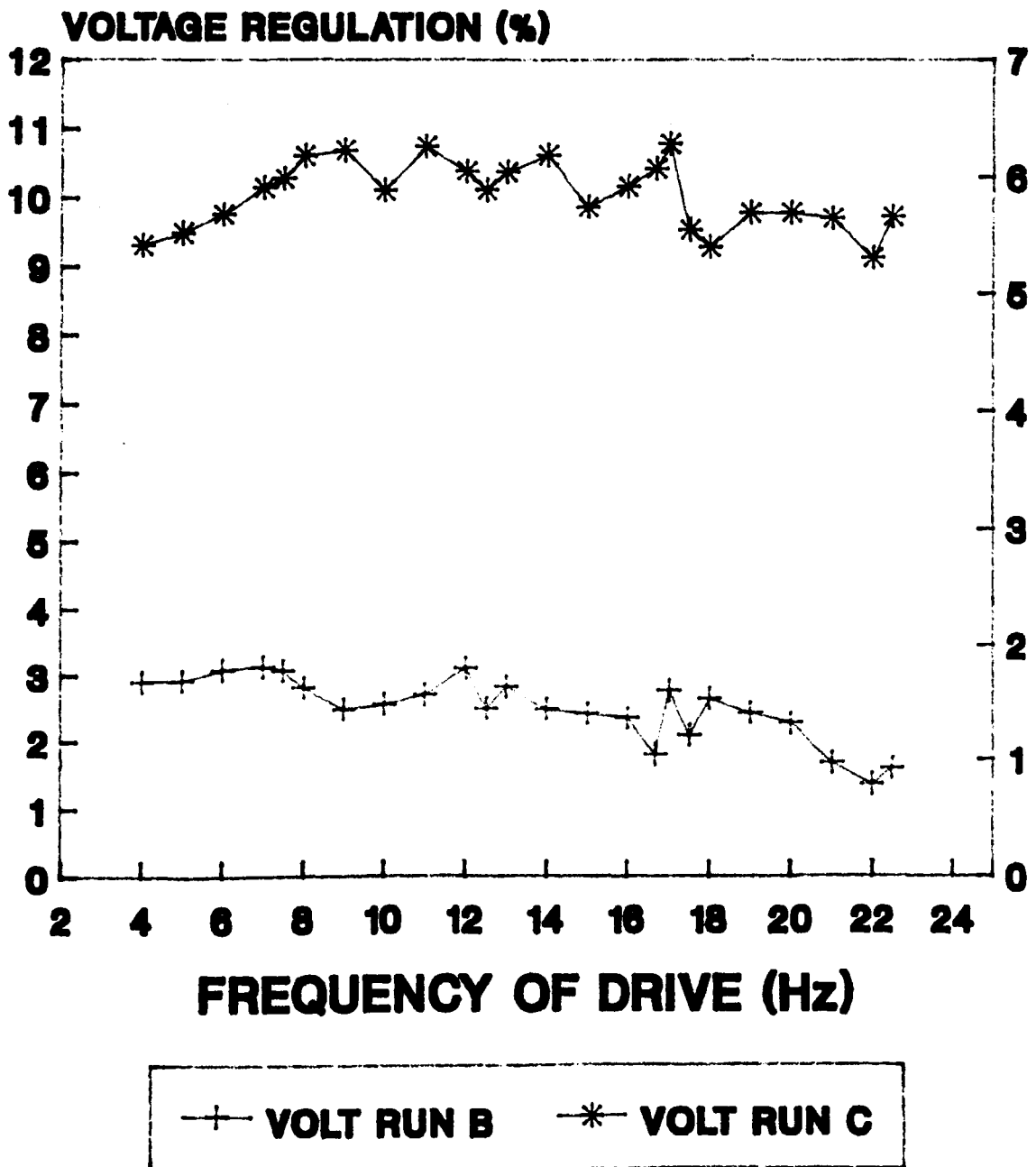


**Fig 6.6b Input Voltage Regulation**

# TEST 6 OVERLAP

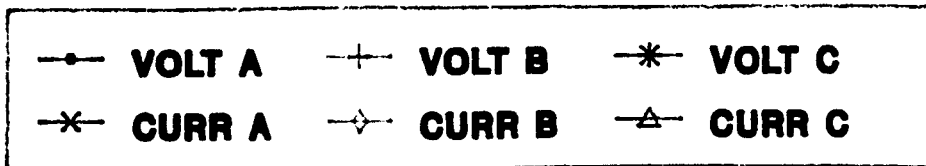
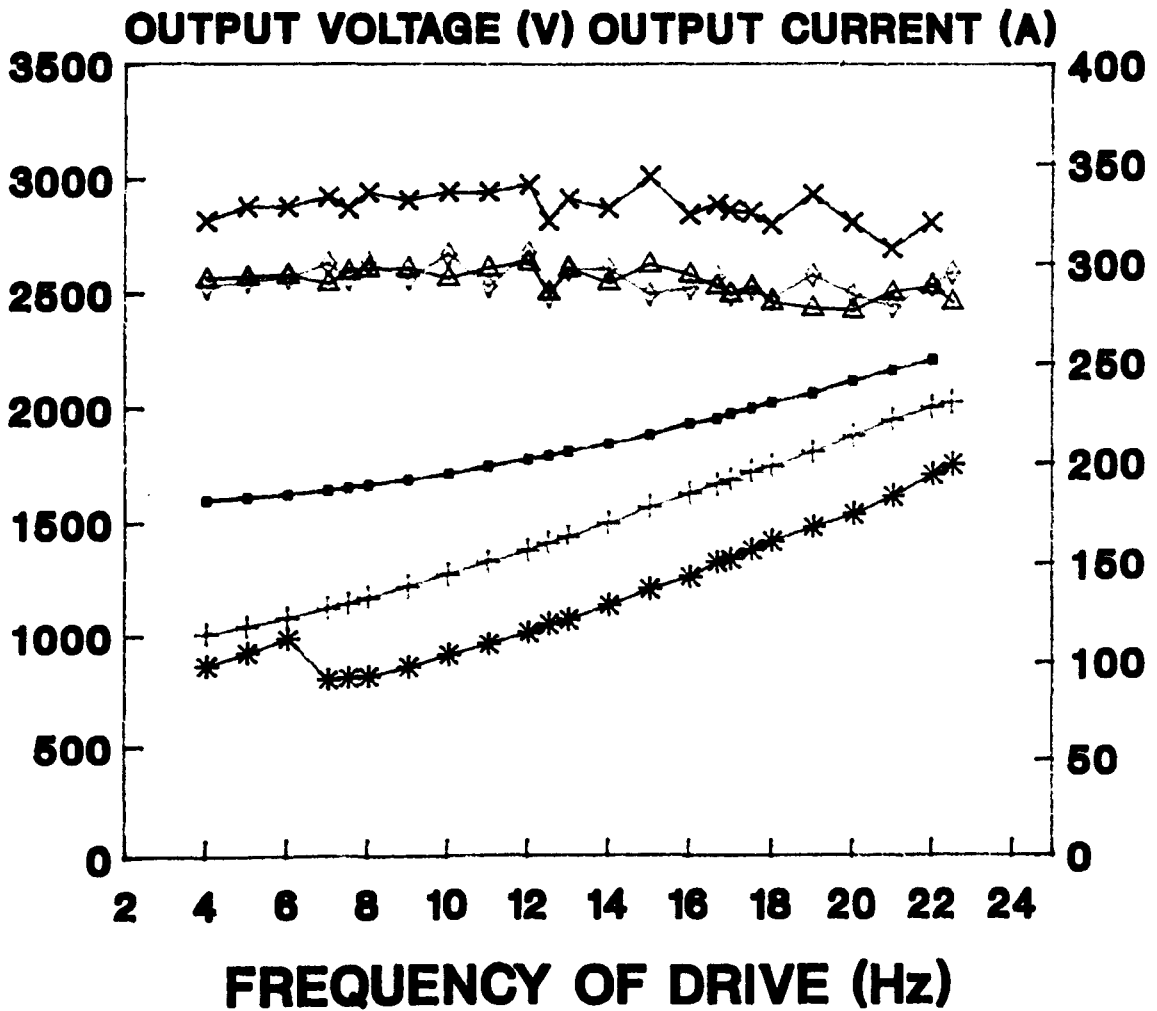


**Fig 6.6c Output Phase Voltage  
Output Phase Current**

# TEST 6 OVERLAP

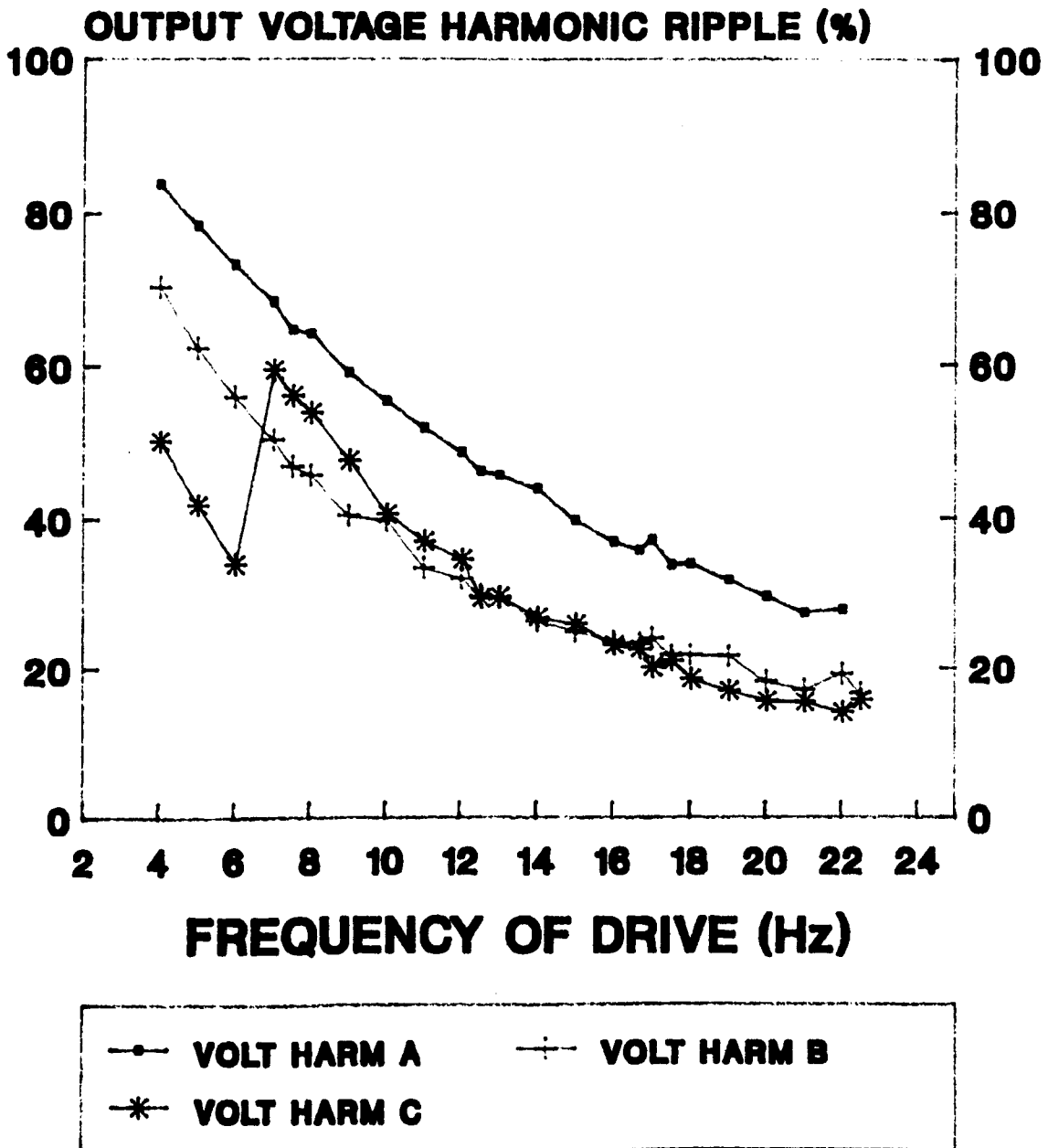
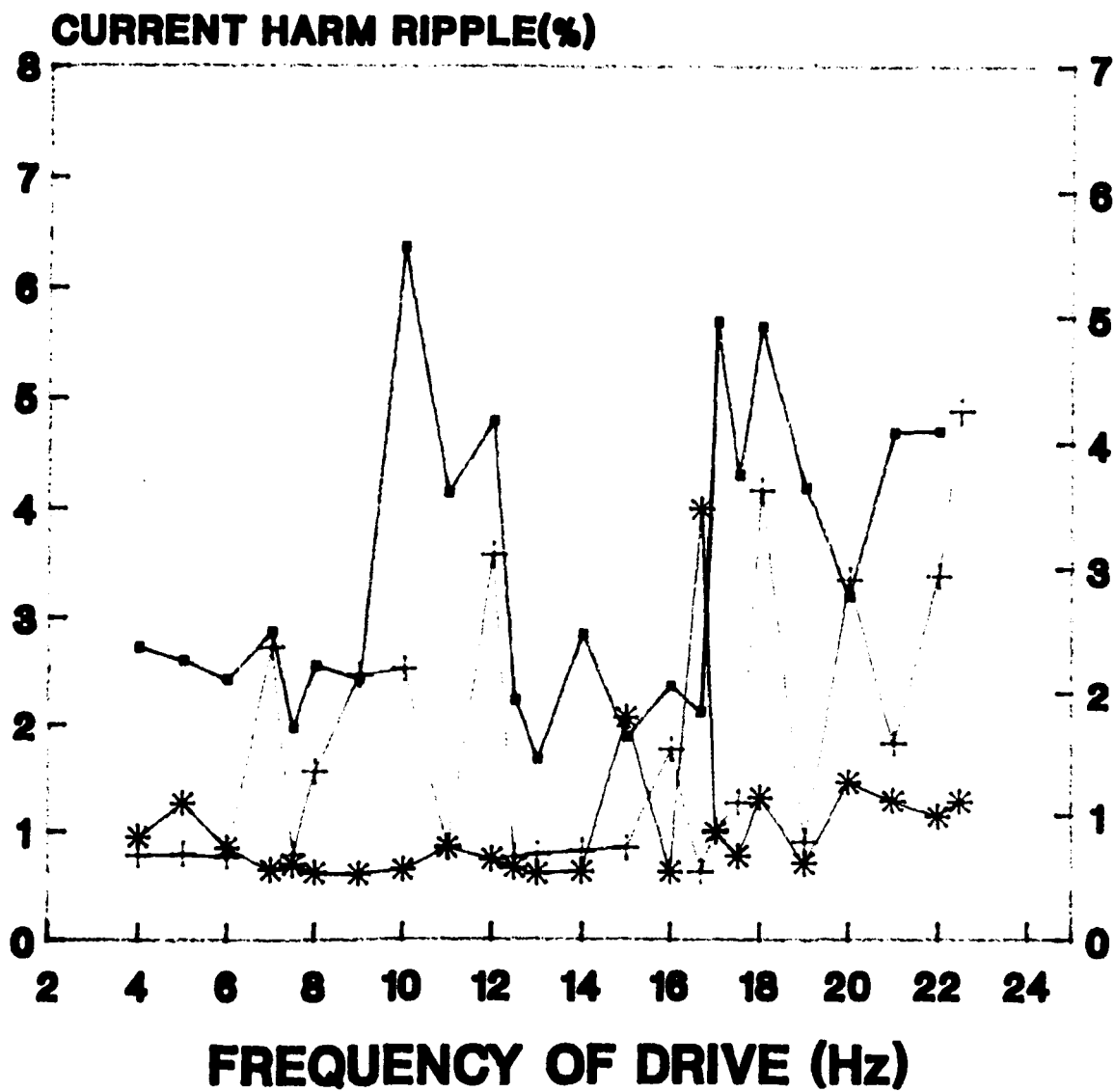


**Fig 6.6d Output Voltage Harmonic Ripple**

# TEST 6 OVERLAP



—●— CURR A.    -+- CURR B.    -\* CURR C.

**Fig 6.6e Output Current Harmonic Ripple**

#### 6.4.3 Test 7 The effects of the supply reactance

The purpose of the test was to assess the effects of including a 10% supply reactance on the performance of the cyclo-converter and the power supply system, in particular the supply voltage harmonics and the load regulation.

##### Test conditions:

The computer simulation was operated over the range of drive frequency 4-22 Hz with the following system characteristics

Run A	Run B
Supply reactance 0%	Supply reactance 2.5 %
Decoupling reactance 0 %	Decoupling reactance 0 %
Interbridge delay 0.00 mS	Interbridge delay 0.00mS
Overlap	Overlap
dq axis motor model	dq axis motor model

##### Test results:

The following system operational characteristics were plotted against the drive frequency :-

Fig 6.7a Input current harmonic ripple (%)

Input voltage harmonic ripple (%)

Fig 6.7b Output voltage harmonic ripple (%)

Fig 6.7c Output phase voltage (V)

Output phase current (A)

# TEST 7

## SUPPLY REACTANCE(INC O/V)

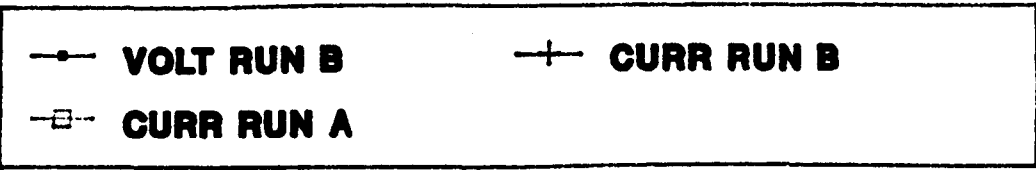
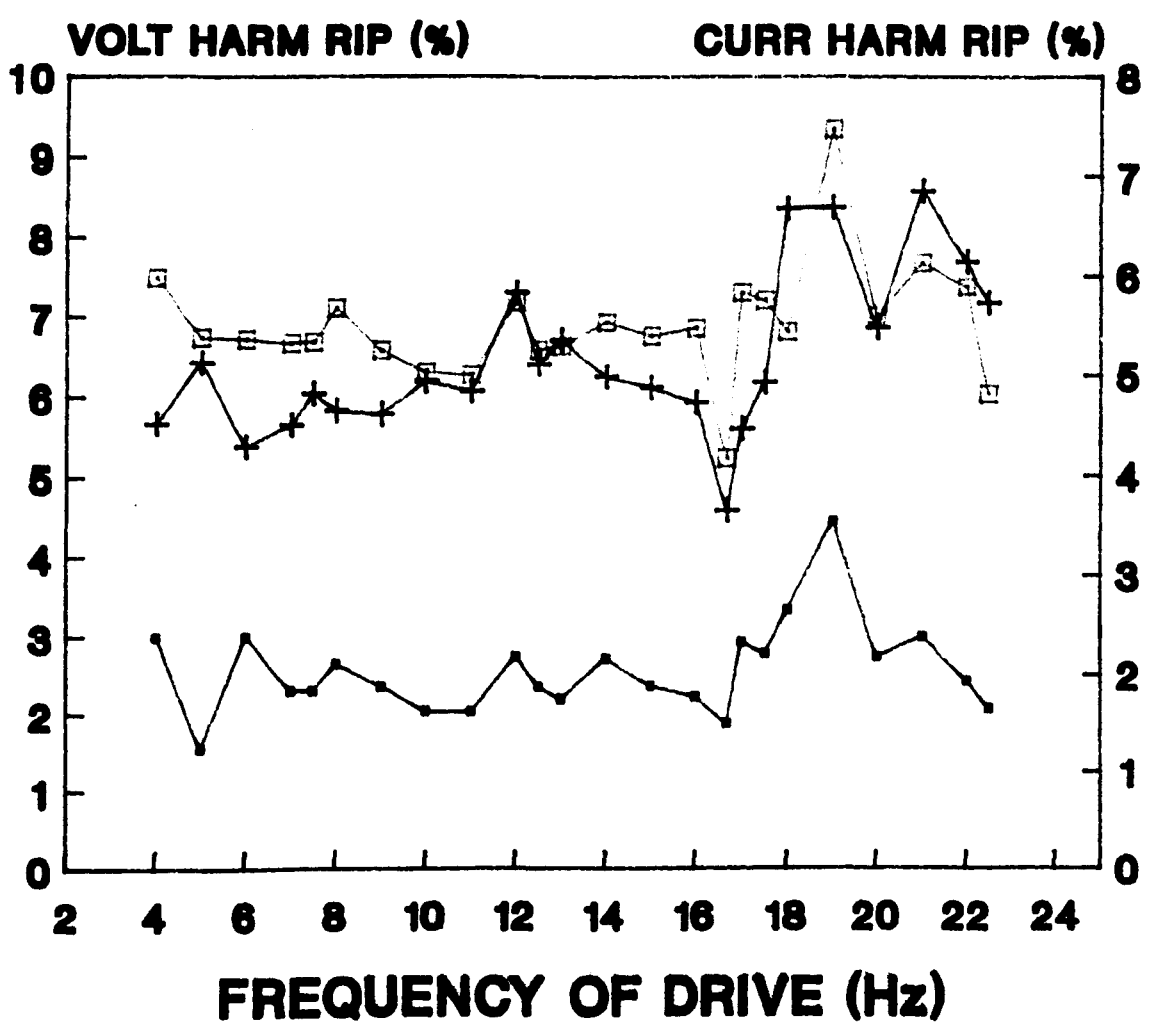
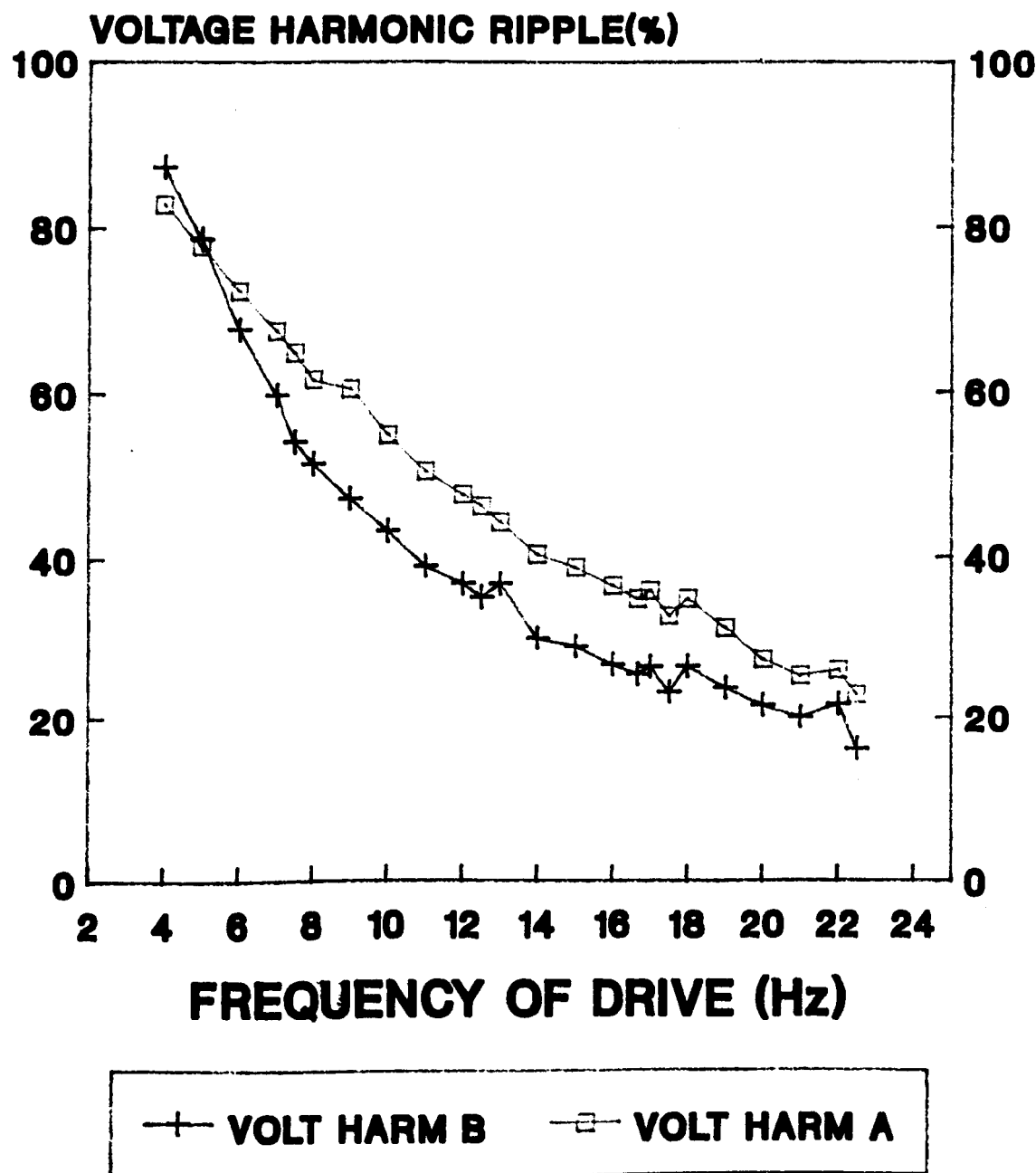


Fig 6.7a Input Voltage Harmonic Ripple  
Input Current Harmonic Ripple



# TEST 7

## SUPPLY REACTANCE(INC O/V)



**Fig 6.7b Output Voltage Harmonic Ripple**

# TEST 7

## SUPPLY REACTANCE(INC O/V)

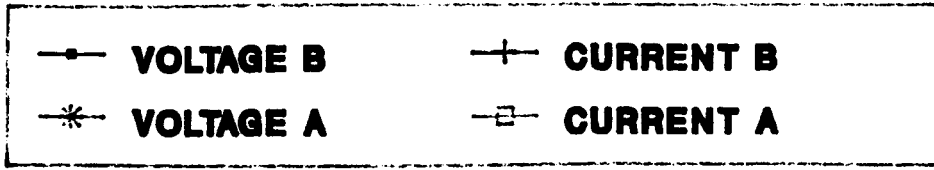
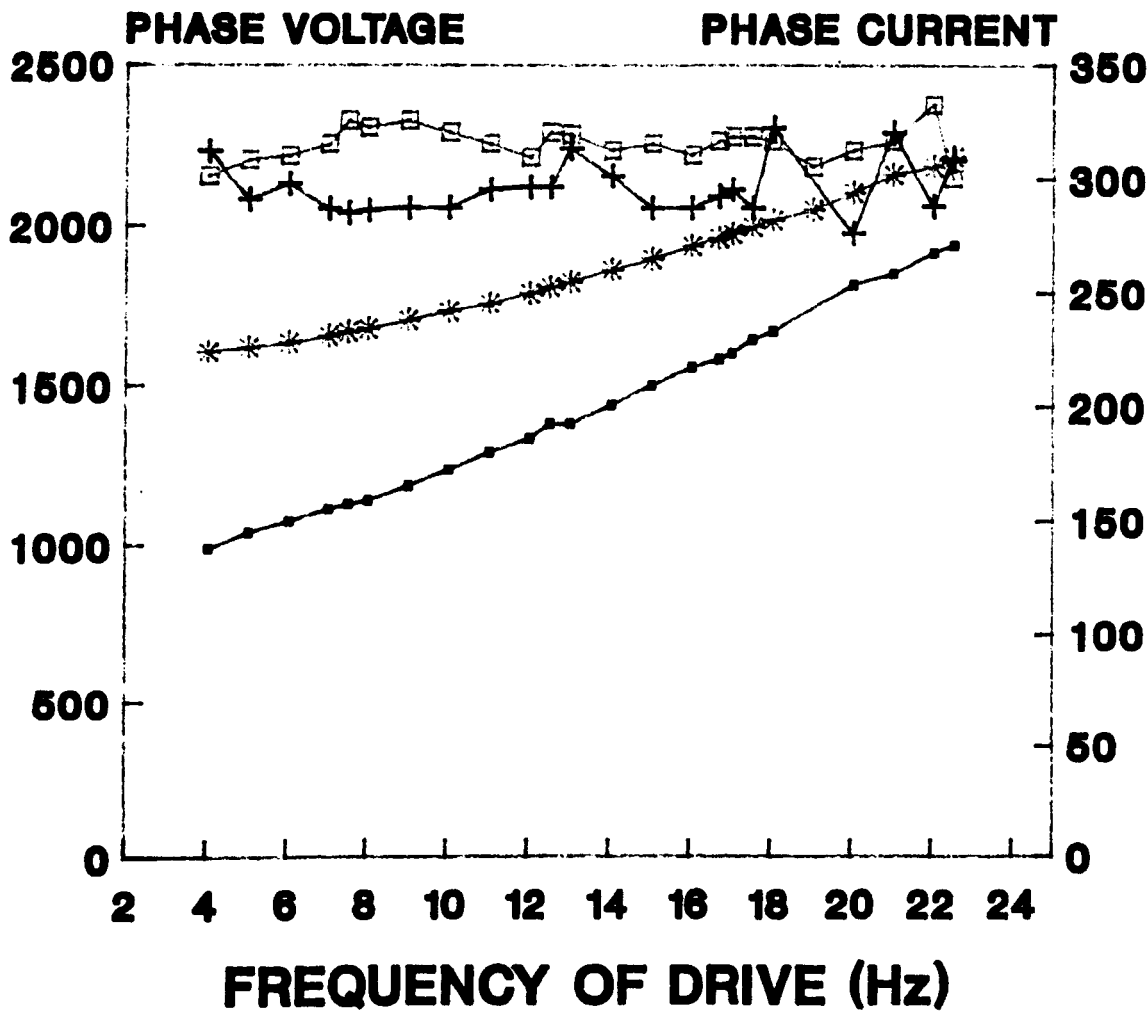


**Fig 6.7c Output Phase Voltage**  
**Output Phase Current**

#### 6.4.4 Test 8 The effects of the decoupling reactance

The purpose of the test was to assess the effects of including a decoupling reactance, to see its effects on the supply voltage harmonics. The decoupling reactance is used to filter out the effects of the line current on the supply reactance therefore, to observe the behaviour of the decoupling reactance it is necessary to have include a supply reactance.

##### Test conditions:

The computer simulation was operated over the range of drive frequency 4-22 Hz with the following system characteristics

Run A	Run B
Supply reactance 2.5 %	Supply reactance 2.5%
Decoupling reactance 0 %	Decoupling reactance 5 %
Interbridge delay 0.00 mS	Interbridge delay 0.00mS
Overlap	Overlap
dq axis motor model	dq axis motor model

##### Test results:

The following system operational characteristics were plotted against the drive frequency :-

Fig 6.8a Input current harmonic ripple(%)

Input voltage harmonic ripple(%)

Fig 6.8b Output voltage harmonic ripple(%)

Fig 6.8c Output phase voltage (V)

Output phase current (A)

# TEST 8

## DECOUPLING REACTOR

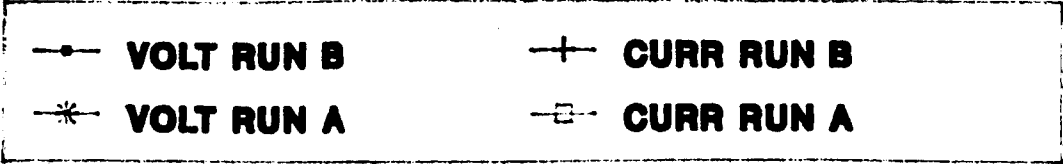
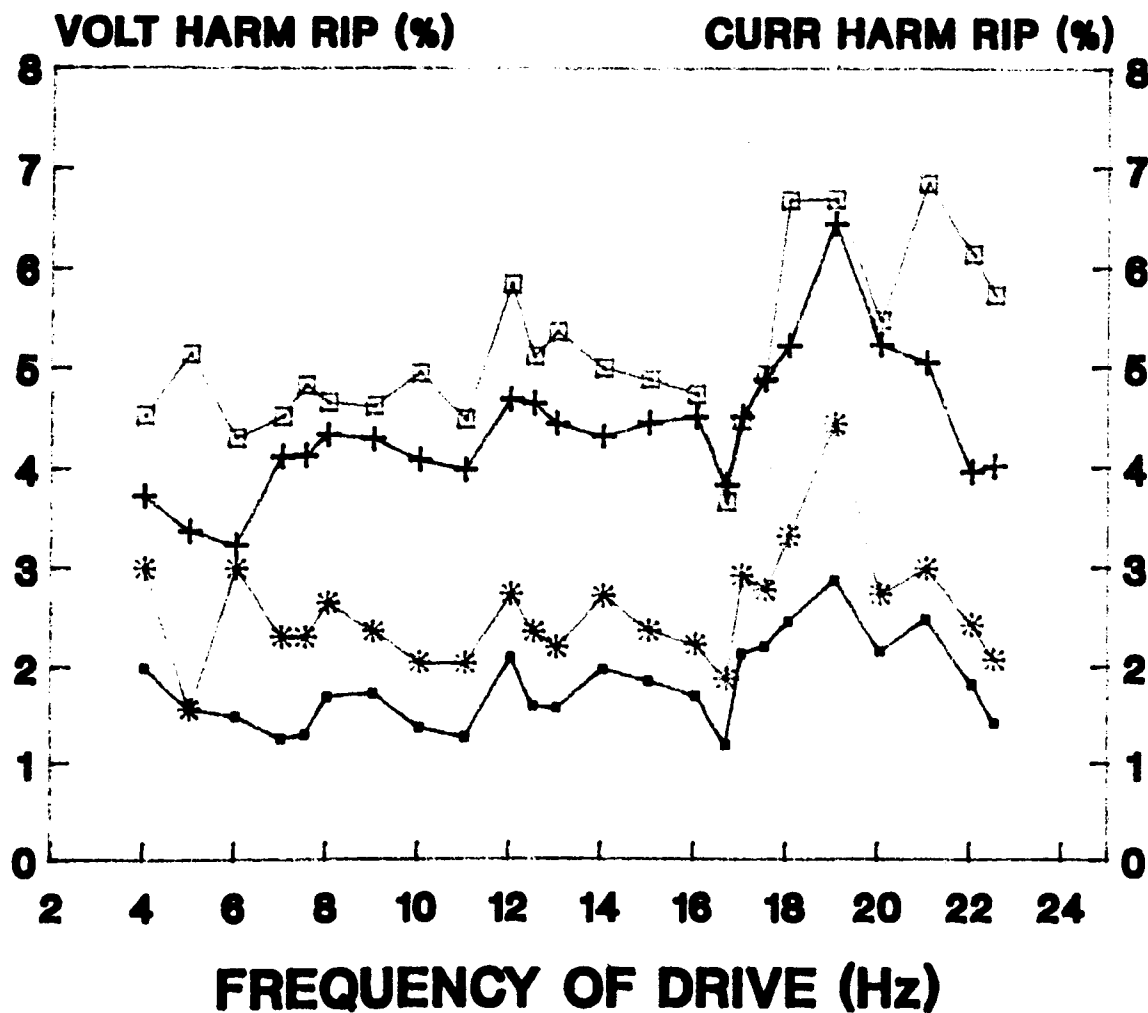
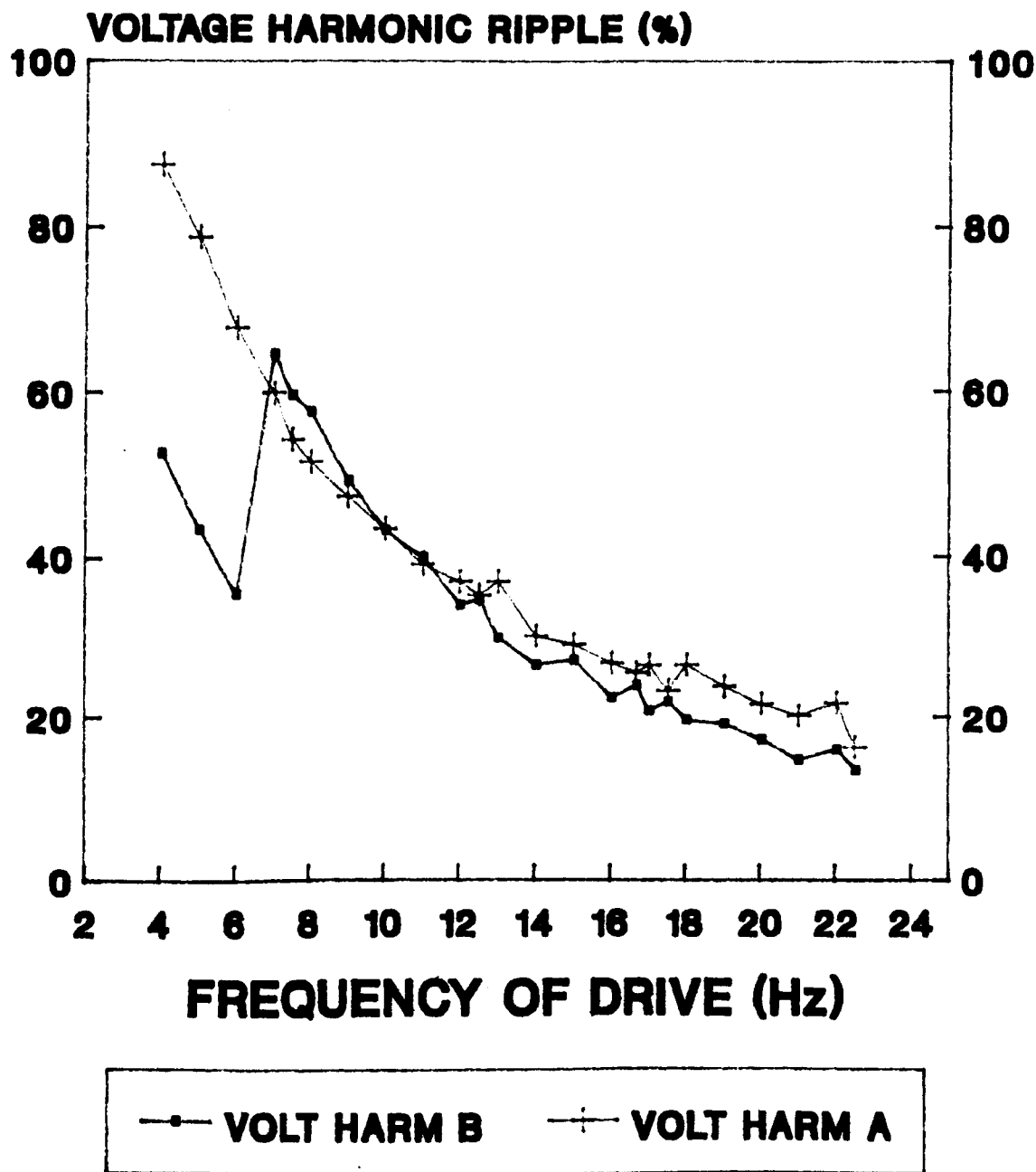


Fig 6.8a Input Voltage harmonic Ripple  
Input Current Harmonic Ripple

# TEST 8

## DECOUPLING REACTOR



**Fig 6.8b Voltage Harmonic Ripple**

# TEST 8

## DECOUPLING REACTANCE

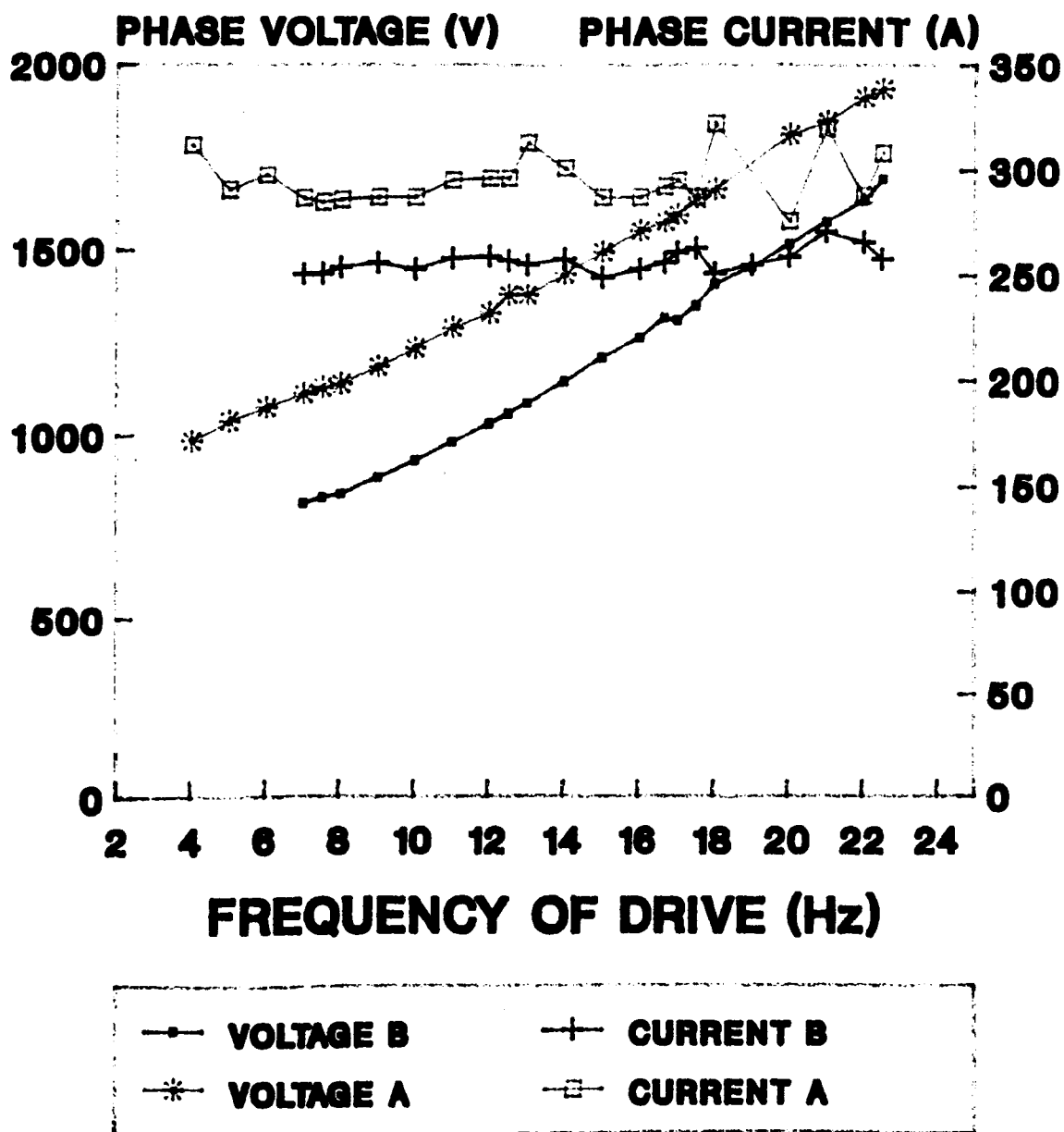


**Fig 6.8o Output Phase Voltage (V)**  
**Output Phase Current (A)**

## 6.5 The modelling of complete systems

Definition of the models used in the testing:-

(a) Model 1 Simplified converter model/dq axis motor

motor

Supply reactance 0 %

Decoupling reactance 0 %

Interbridge delay 0.00 mS

No overlap(reactance 0.0%)

dq axis model motor

(b) Model 2 Simplified converter model /Thevenin

motor

Supply reactance 0 %

Decoupling reactance 0 %

Interbridge delay 0.00 mS

No overlap(reactance 0.0%)

Thevenin model motor

(c) Model 3 Simplified converter model including

Supply reactance/dq axis motor

Supply reactance 2.5 %

Decoupling reactance 0 %

Interbridge delay 0.00 mS

No overlap

dq axis model motor

(d) Model 4 Low reactance Supply

Supply reactance 1 %

Decoupling reactance 2 %

Interbridge delay 0.003 ms

Overlap

dq axis model motor

(e) Model 5 High Reactance Supply

Supply reactance 2.5 %

Decoupling reactance 5.0 %

Interbridge delay 0.003 ms

Overlap

dq axis model motor



**6.5.1 Test 9 Comparison of the Pelly's analytical model and  
the computer model with a sinewave output**

The purpose of test was to compare Pelly's mathematical model with the computer simulation under the same conditions as used by Pelly.

Test conditions:

**Test A**

Computational analysis of the work carried out by Pelly to establish the level of input and output current distortion factor for the cyclo-converter assuming :-

- (1) zero source impedance
- (2) drive frequency is a pure sinewave
- (3) no interbridge delay
- (4) no overlap

The computer simulation was operated over the range of drive frequency 4-22 Hz with the following system characteristics to assess the differences between these two models.

**Run B**

Supply reactance 0 %

Decoupling reactance 0 %

Interbridge delay 0.00 mS

No overlap

Sine wave current output simulated for load

**Test results:**

The following system operational characteristics were plotted against the drive frequency :-

Fig 6.9a Input current harmonic ripple (%)

Fig 6.9b Output voltage harmonic ripple (%)

Output load power factor

# TEST 9

## SINE, PELLY

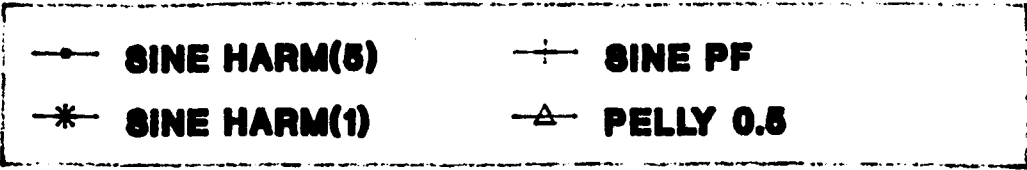
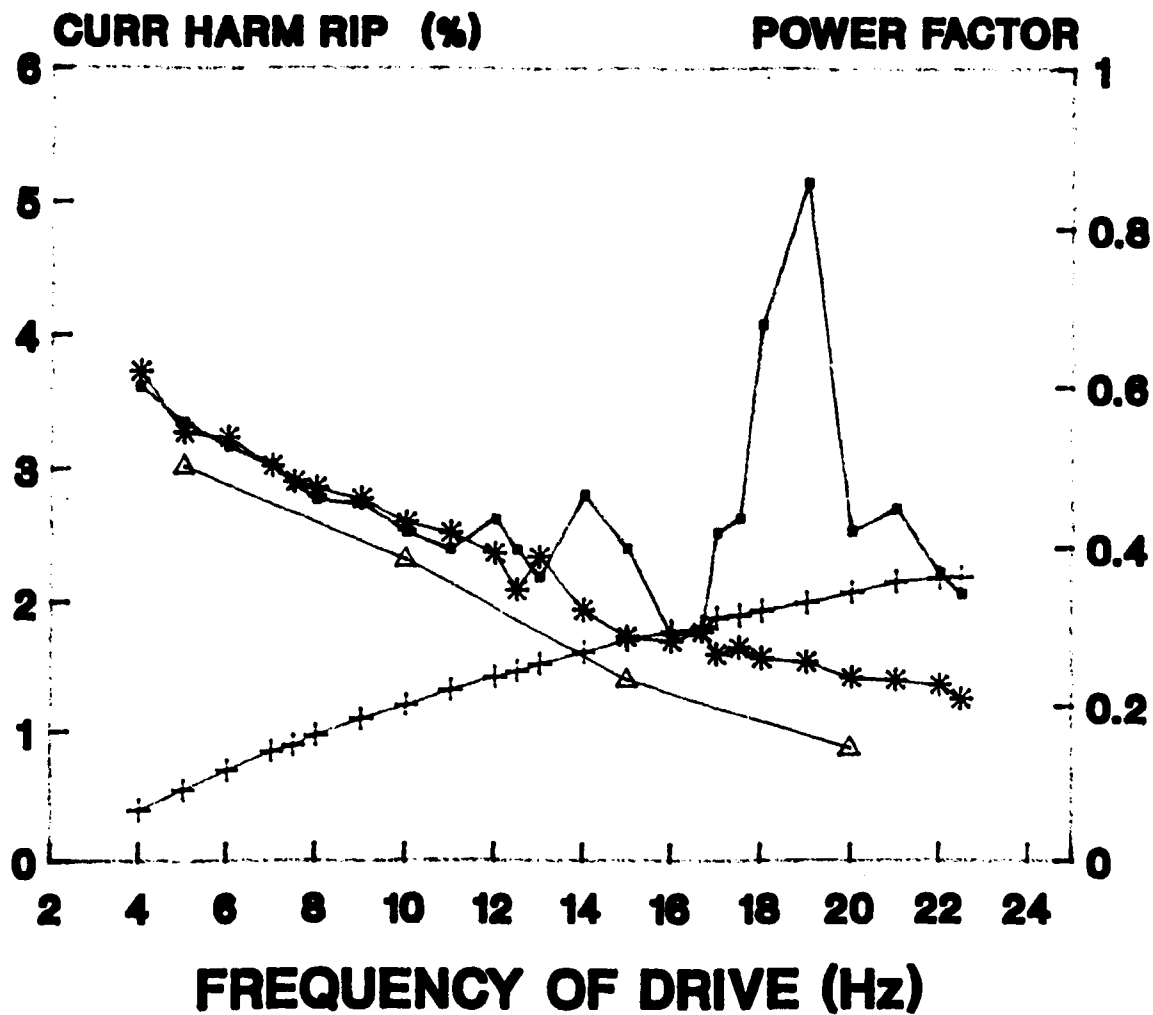
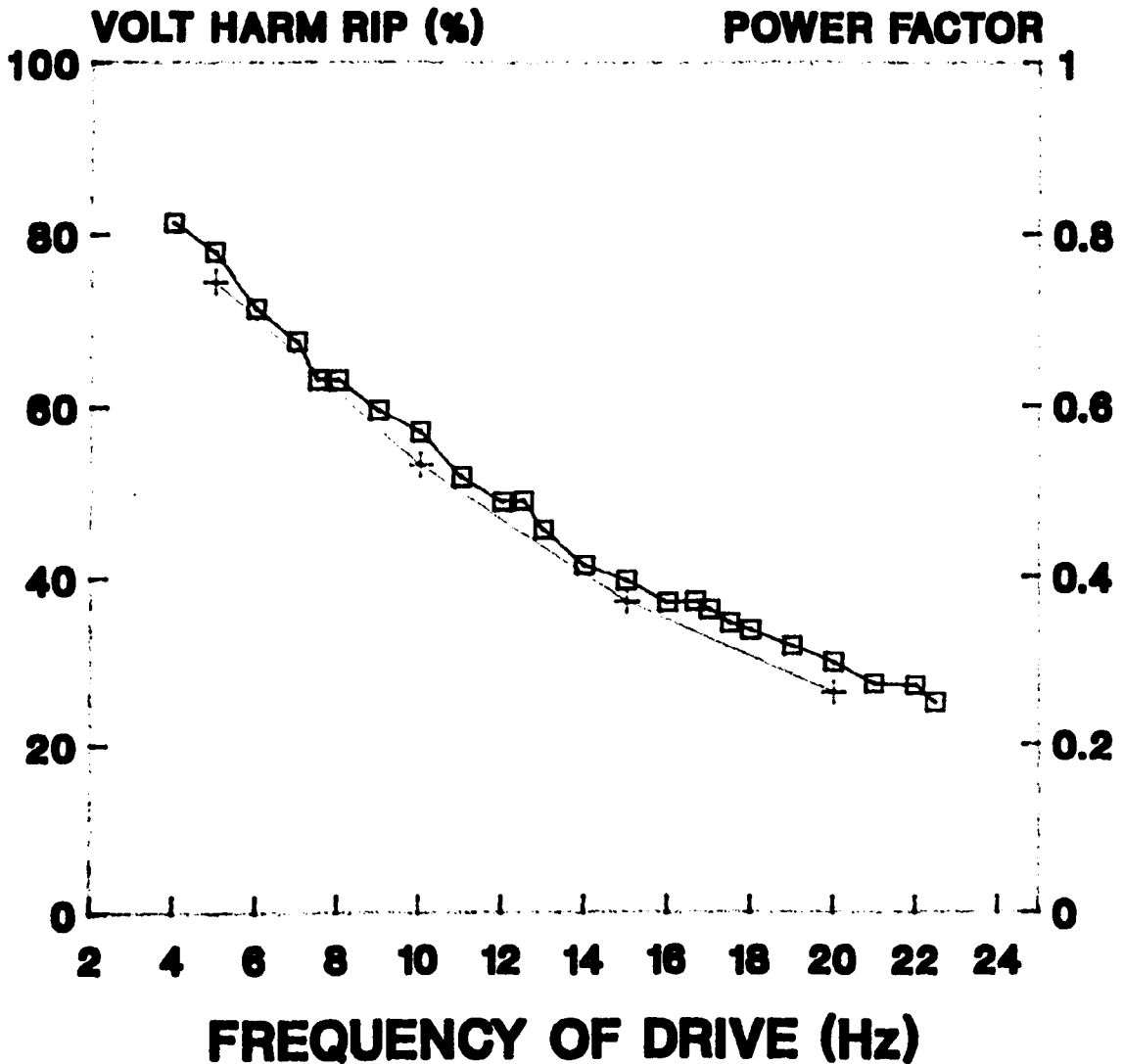


Fig 6.9a Input Current Harm Ripple (%)  
Output load Power Factor

# TEST 9

## PELly SINE



—+— PELLY 0.5    —□— SINE    SINE PF

Fig 6.9b Voltage Harmonic Ripple  
Output Load Power Factor

**6.5.2 Test 10 Comparison of the Pelly's analytical model  
and the simplified converter and dq axis model 1**

The purpose of the test was to compare Pelly's mathematical model including a sinewave load, with the computer simulation of a simplified real model of a cyclo-converter and synchronous machine.

**Test conditions:**

**Test A**

Computational analysis of the work carried out by Pelly to establish the level of input and output current distortion factor for the cyclo-converter assuming.

- (1) zero source impedance
- (2) drive frequency is a pure sinewave
- (3) no interbridge delay
- (4) no overlap

The computer simulation was operated over the range of drive frequency 4-22 Hz with the following system characteristics to assess the differences between these two models.

**Run B**

Supply reactance 0 %

Decoupling reactance 0 %

Interbridge delay 0.00 mS

No overlap

dq axis motor model

Test results:

The following system operational characteristics were plotted against the drive frequency :-

Fig 6.10a Input current harmonic ripple (%)

Fig 6.10b Output voltage harmonic ripple (%)

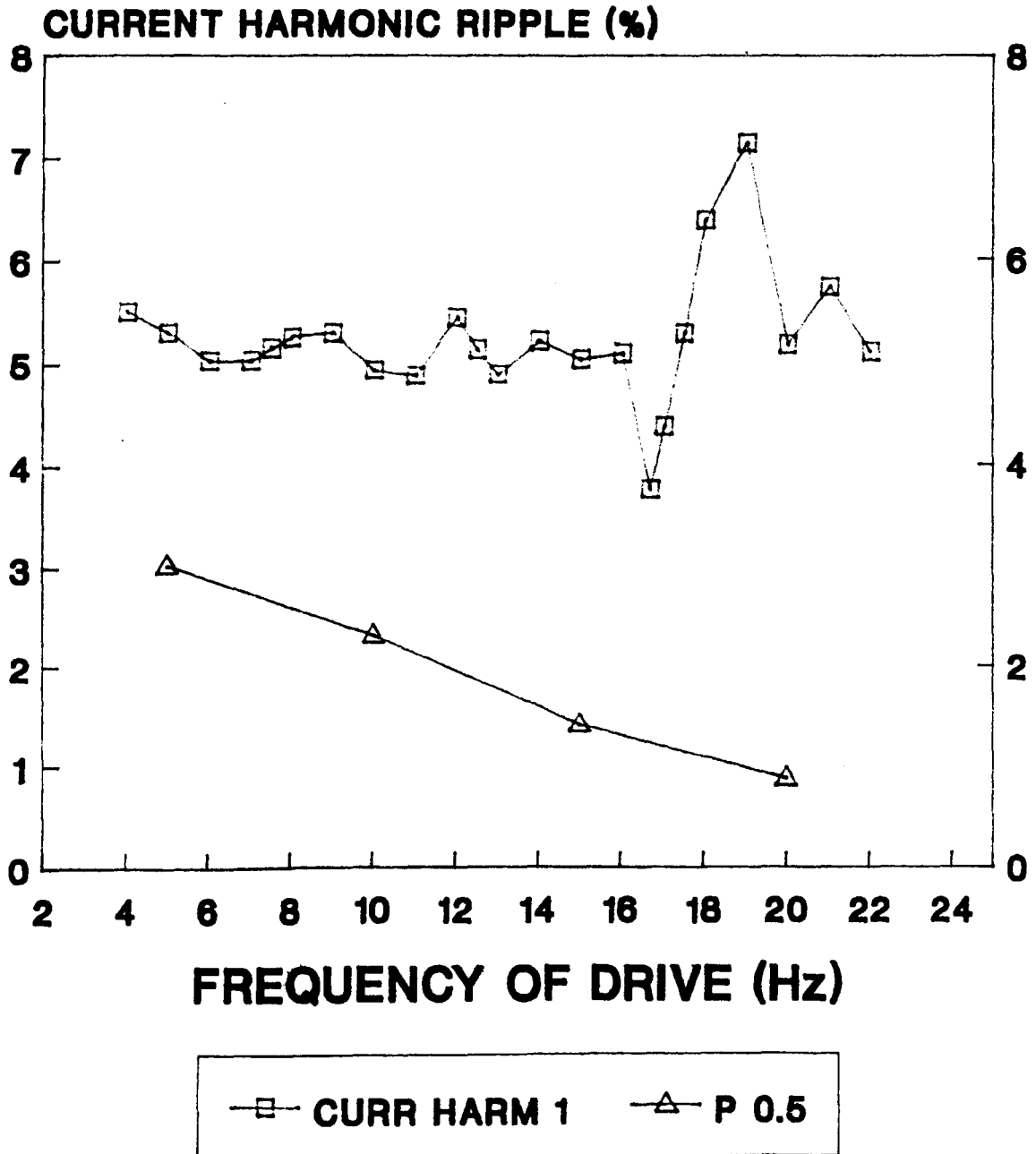
Output load power factor

Fig 6.10c Output phase voltage (V)

Output phase current (A)

# TEST 10

## MODELS 1, PELLY



**Fig 6.10a Input Current Harmonic Ripple**

# TEST 10

## MODEL 1, PELLY

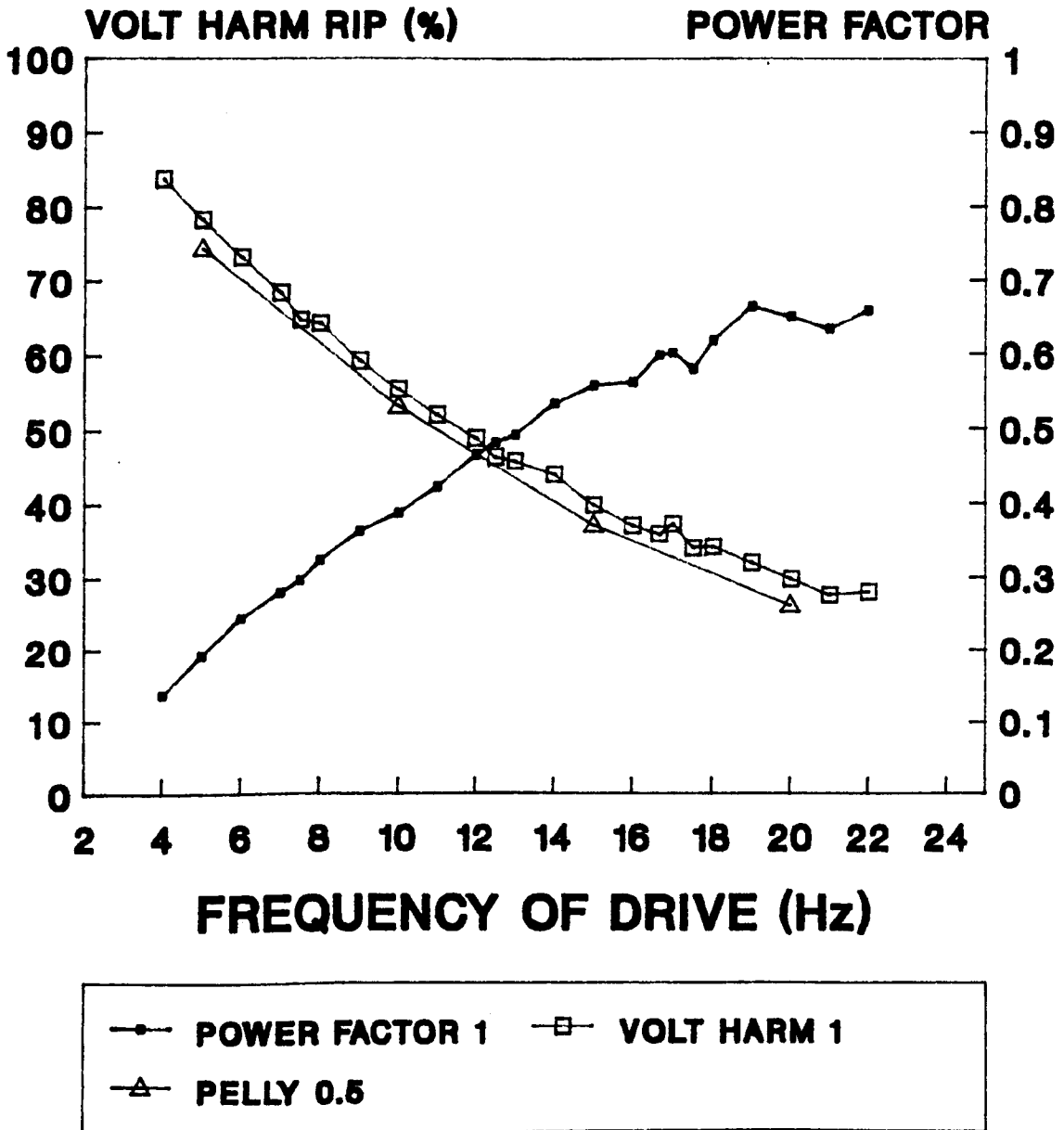


**Fig 6.10b Output Voltage Harmonic Ripple**  
**Output Load Power Factor**



# TEST 10

## MODEL 1, PELLY

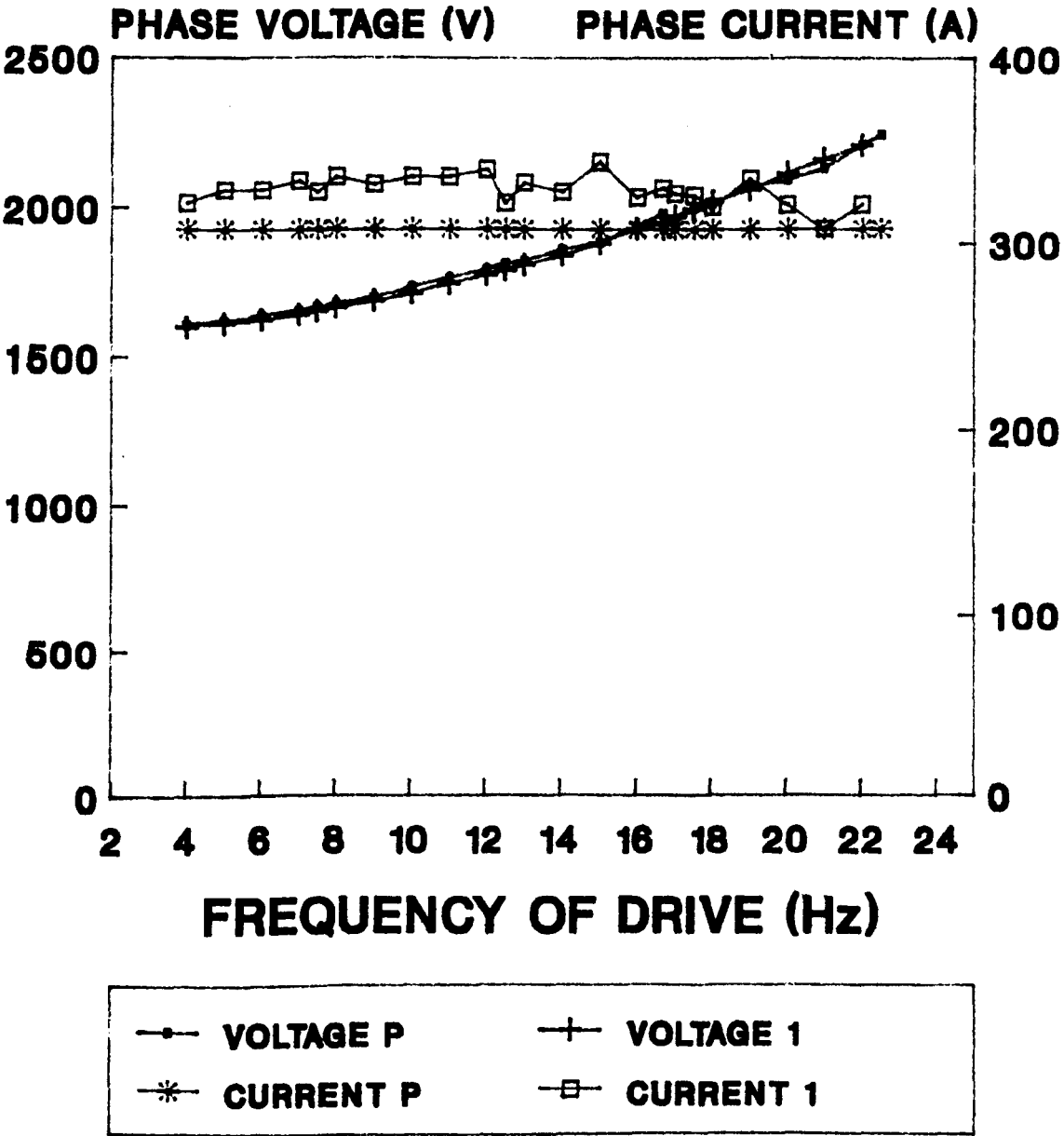


Fig 6.10c Output Phase Voltage  
Output Phase Current

### 6.5.3 Test 11 Comparison of the simplified model 1 ,and model 5

The purpose of the test was to assess the difference in the system performance between models 1 and 5 the most simplified and most complex model involving a cyclo-converter and synchronous machine.

#### Test conditions:

The computer simulation was operated over the range of drive frequency 4-22 Hz with the following system characteristics.

Model 1	Model 5
Supply reactance 0%	Supply reactance 2.5 %
Decoupling reactance 0 %	Decoupling reactance 5 %
Interbridge delay 0.00 mS	Interbridge delay 0.003mS
No overlap	Overlap
dq axis motor model	dq axis motor model

#### Results of test:

The following system operational characteristics were plotted against the drive frequency :-

Fig 6.11a Input current harmonic ripple (%)

Input voltage harmonic ripple (%)

Fig 6.11b Input voltage regulation (%)

Fig 6.11c Output voltage harmonic ripple (%)

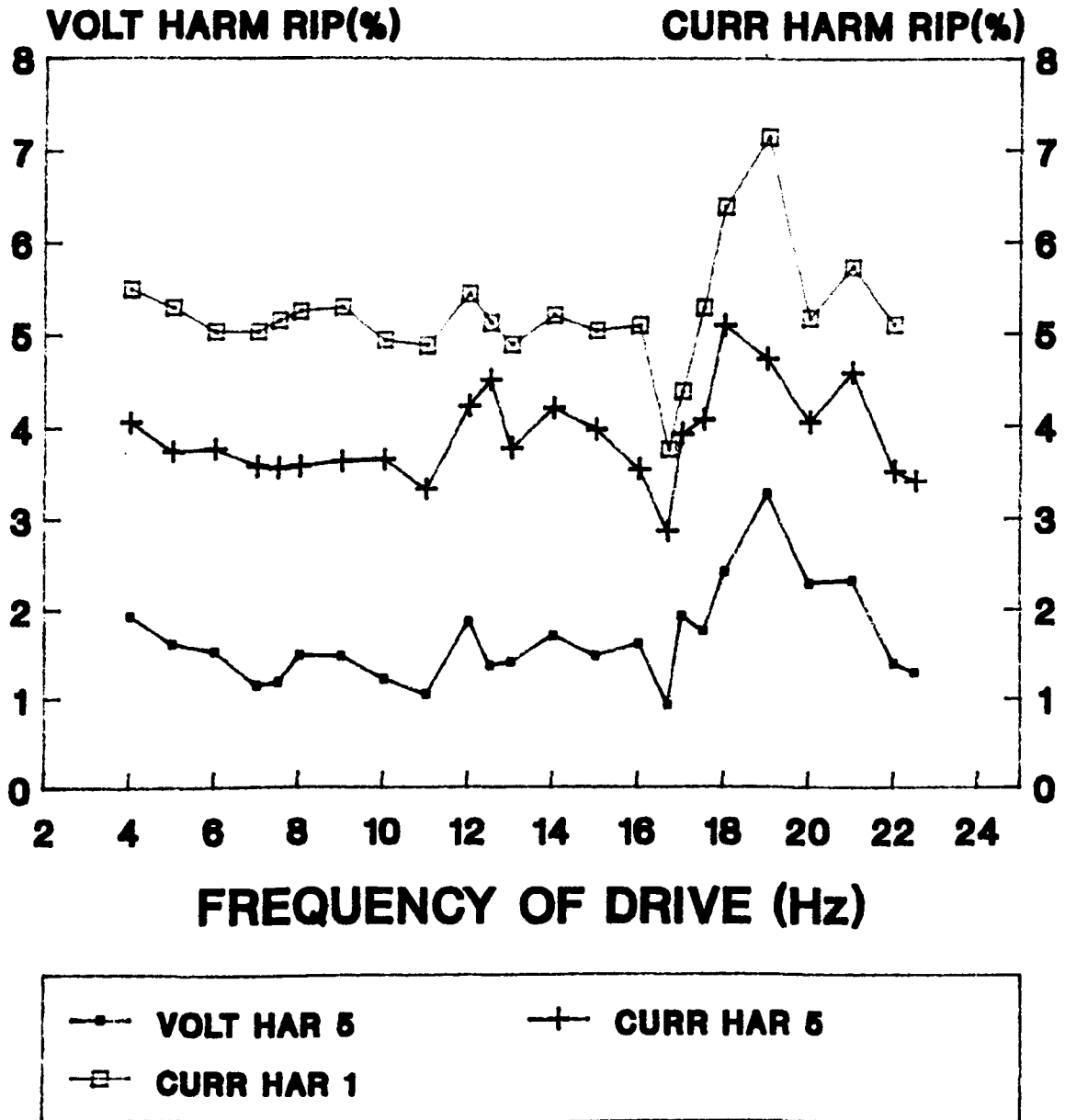
Output current harmonic ripple (%)

Fig 6.11d Output phase voltage (V)

Output phase current (A)

# TEST 11

## MODELS 1,5



**Fig 6.11a Input Voltage Harmonic Ripple**  
**Input Current Harmonic Ripple**

# TEST 11

## MODELS 1,3,4,5

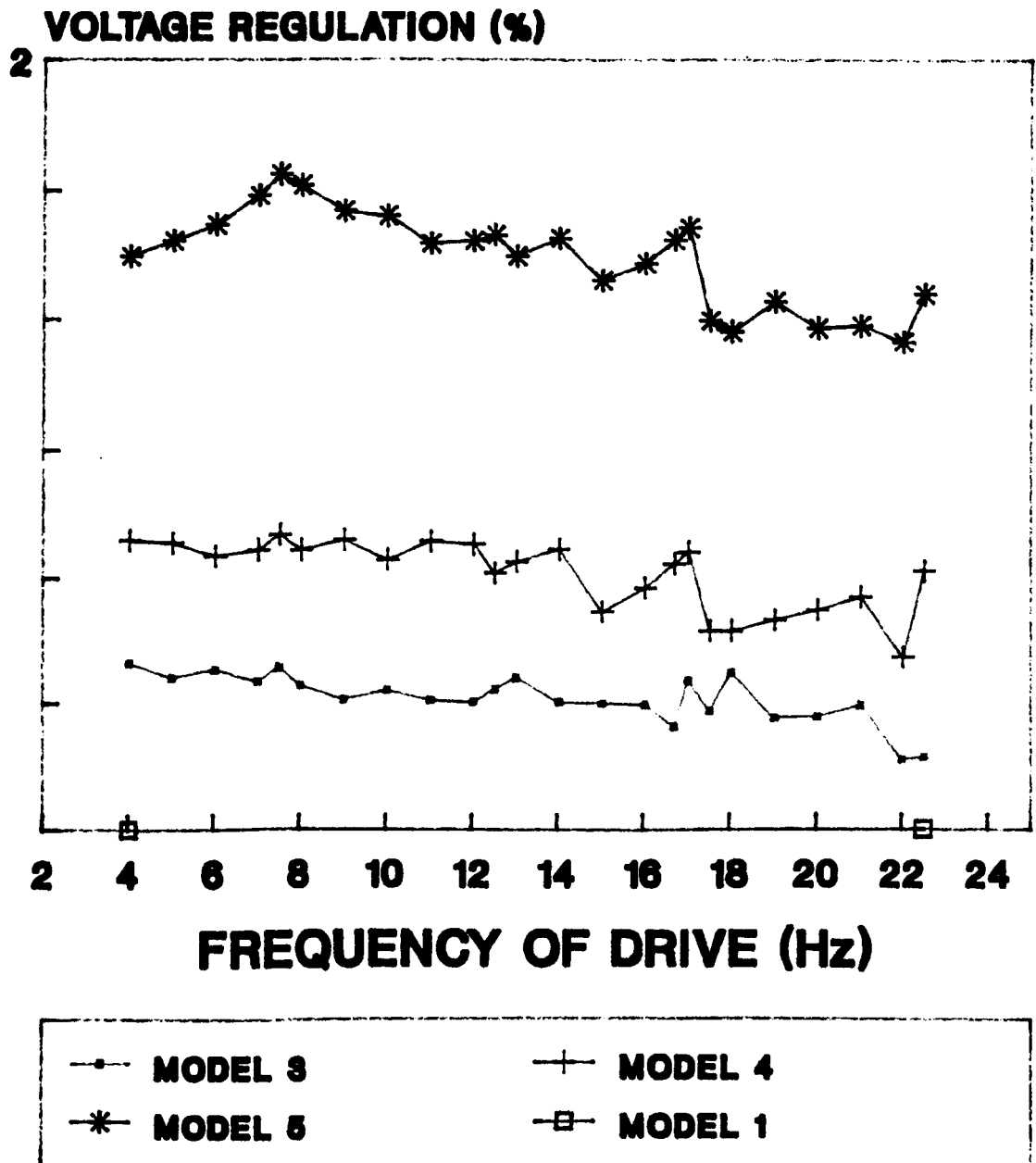


**Fig 6.11b Supply Voltage Regulation**

# TEST 11

## Models 1,5

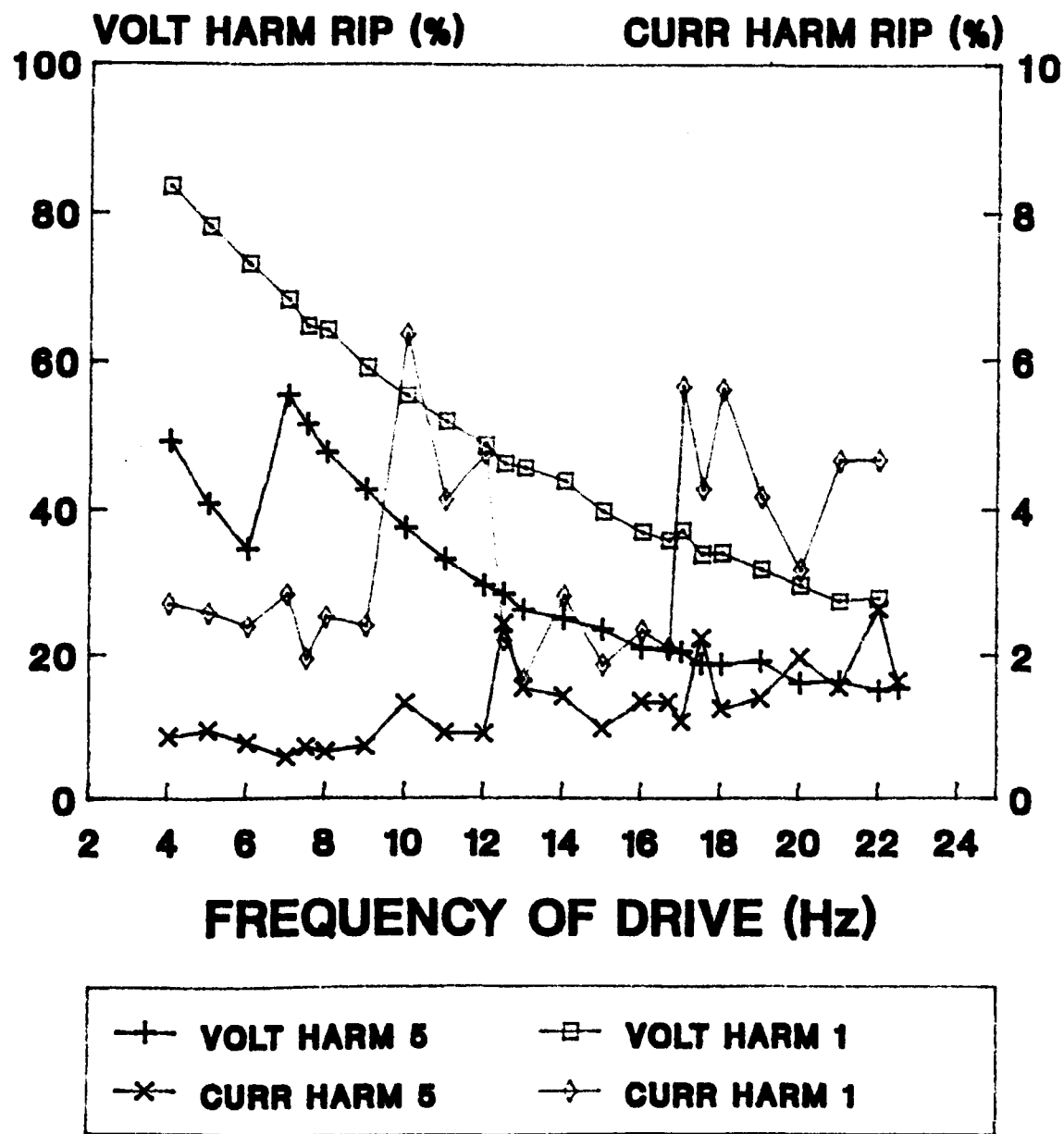


**Fig 6.11c Output Voltage Harmonic Ripple**  
**Output Current Harmonic Ripple**

# TEST 11

## Models 1,5

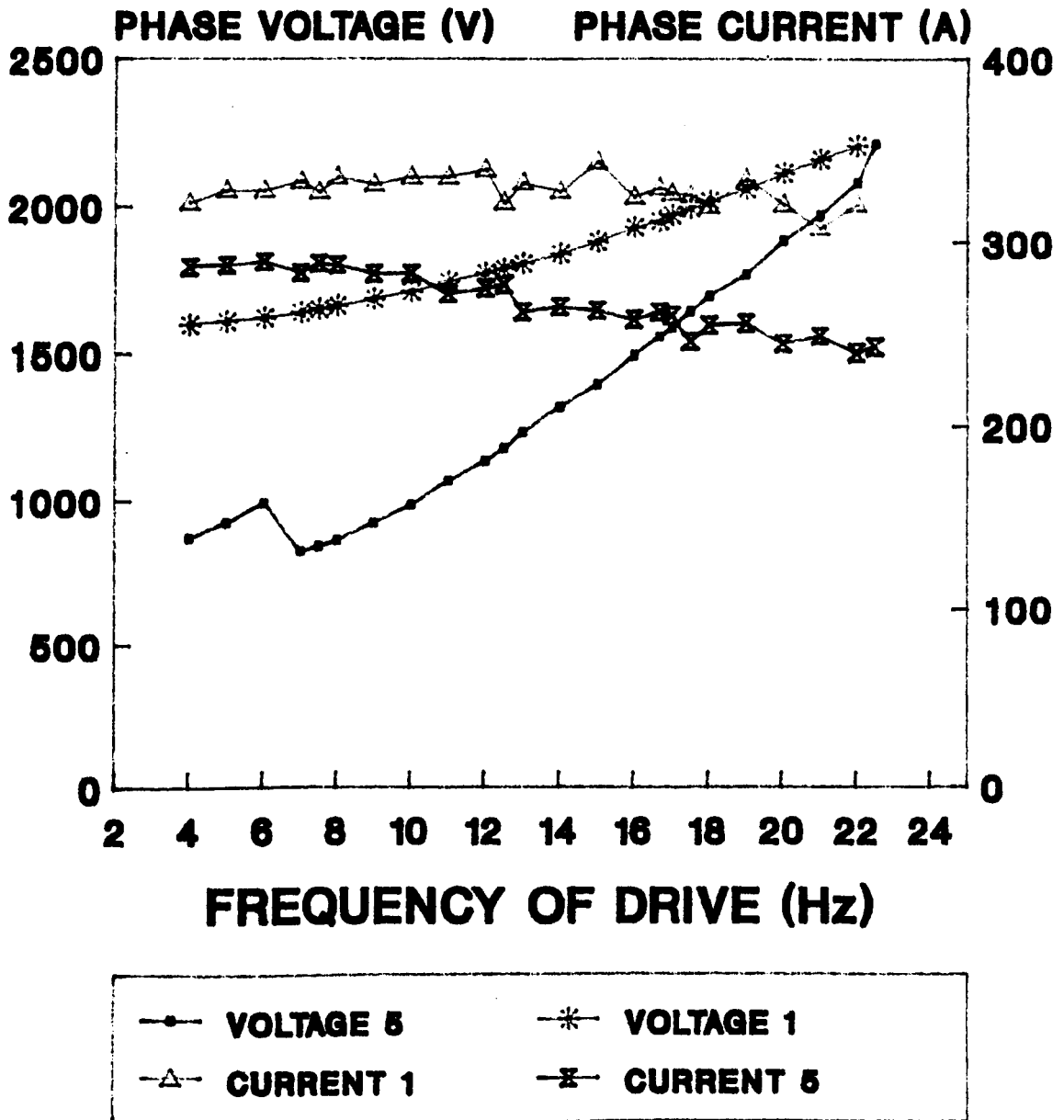


**Fig 6.11d Output Phase Voltage**  
**Output Phase Current**

#### 6.5.4 Test 12 Comparison of the simplified converter and supply reactance model 3 ,and the complex model 5

Purpose of the test:

To assess the difference in the system performance between models 3,5; model 3 is commonly used in simulations however it's weakness in that it only partly models the system characteristics.

Test conditions:

The computer simulation was operated over the range of drive frequency 4-22 Hz with the following system characteristics

Model 3	Model 5
Supply reactance 2.5 %	Supply Reactance 2.5 %
Decoupling Reactance 0 %	Decoupling reactance 5 %
Interbridge Delay 0.00 ms	Interbridge delay 0.003ms
No overlap	Overlap
dq axis motor model	dq axis motor model

Test results:

The following system operational characteristics were plotted against the drive frequency :-

Fig 6.12a Input current harmonic ripple (%)

Input voltage harmonic ripple (%)

Fig 6.12b Output voltage harmonic ripple (%)

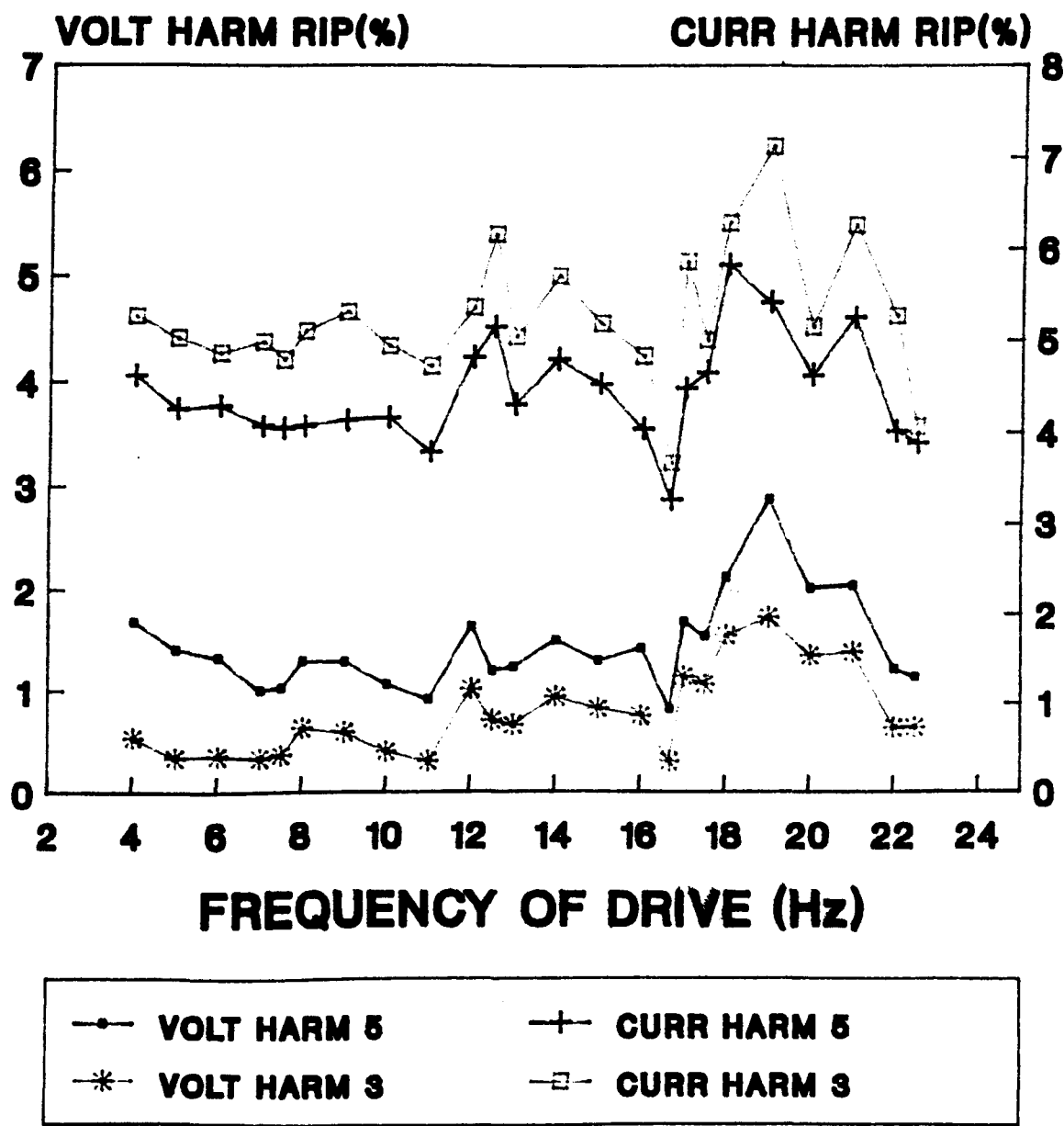
Output current harmonic ripple (%)

Fig 6.12c Output phase voltage (V)

Output phase current (A)

# TEST 12

## MODELS 3,5



**Fig 6.12a Input Voltage Harmonic Ripple**  
**Input Current Harmonic Ripple**



# TEST 12

## MODELS 3,5

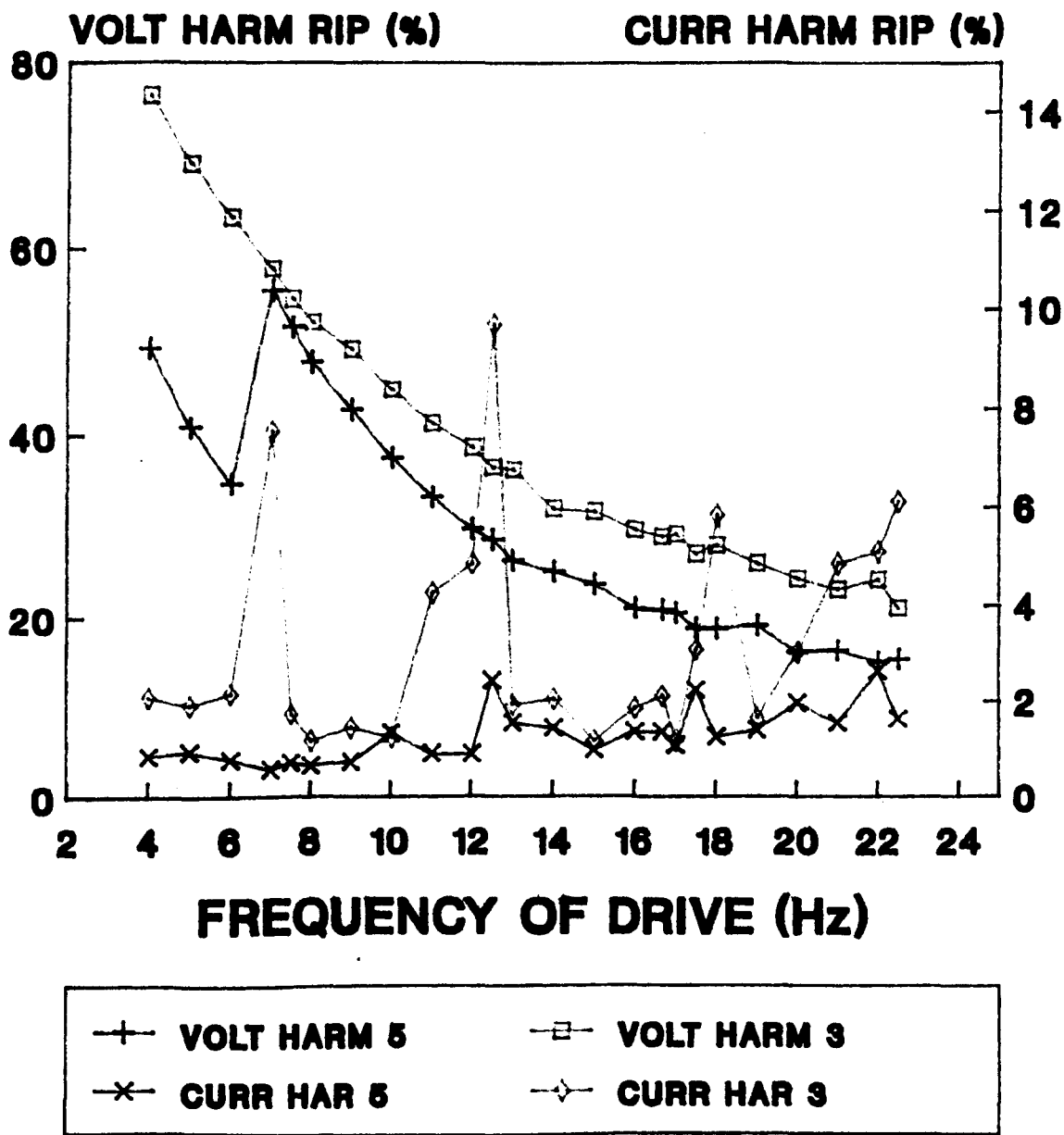


**Fig 6.12b Output Voltage Harmonic Ripple**  
**Output Current Harmonic Ripple**

# TEST 12

## MODELS 3,5

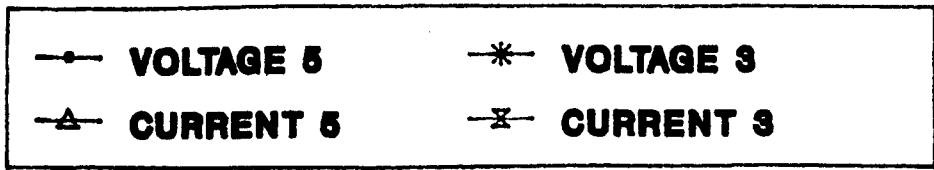
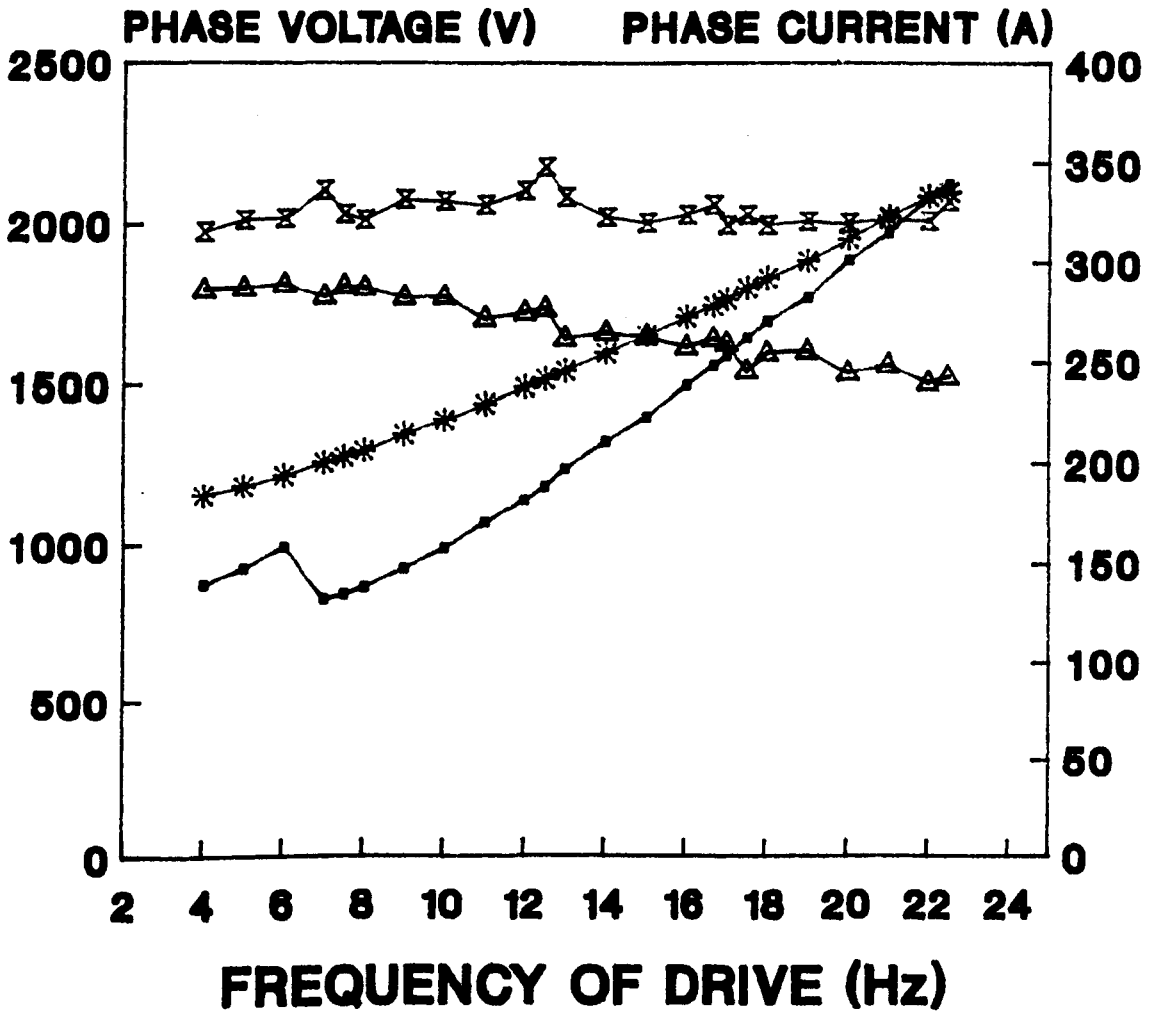


**Fig 6.12c Output Phase Voltage**  
**Output Phase Current**

**6.5.5 Test 13 Comparison of the typical industrial supply  
model 4, and the simplified model 1**

**Purpose of test:**

To assess the performance of complete model for the industrial supply compared to the simplified model and assess whether the complexity of the simulation for the industrial model is worthwhile.

**Conditions of test:**

The computer simulation was operated over the range of drive frequency 4-22 Hz with the following system characteristics to assess the difference between model 4, 5 .

Model 4	Model 5
Supply reactance 1 %	Supply Reactance 2.5 %
Decoupling Reactance 2 %	Decoupling reactance 5.0 %
Interbridge Delay 0.003 mS	Interbridge delay 0.003 mS
Overlap	Overlap
dq axis motor model	dq axis motor model

**Results of test:**

The following system operational characteristics were plotted against the drive frequency :-

Fig 6.13a Input current harmonic ripple (%)

Input voltage harmonic ripple (%)

Fig 6.13b Output voltage harmonic ripple (%)

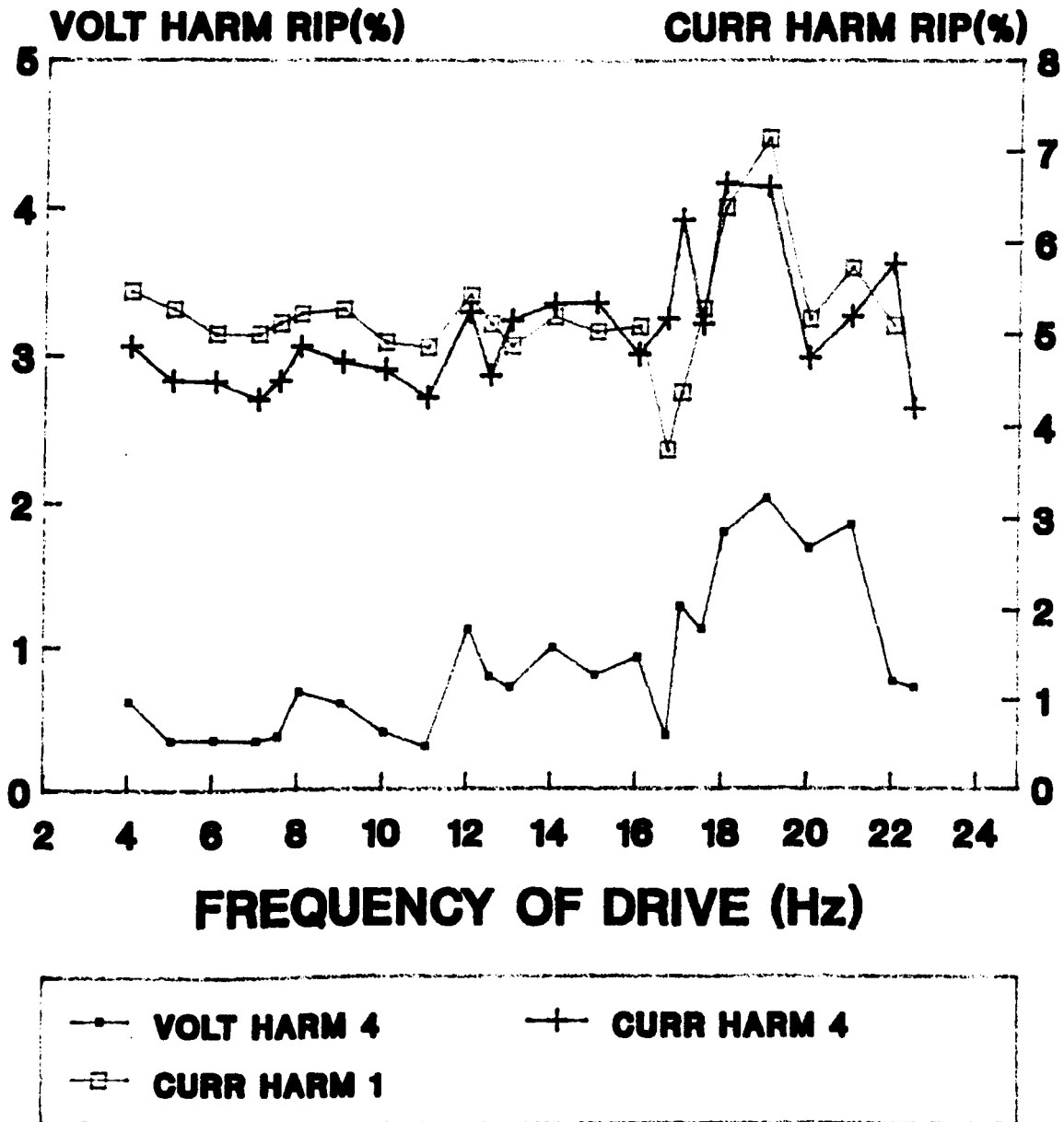
Output current harmonic ripple (%)

Fig 6.13c Output phase voltage (V)

Output phase current (A)

# TEST 13

## MODEL 1,4



**Fig 6.13a Input Voltage Harmonics (%)**  
**Input Current Harmonics (%)**

# TEST 13

## MODEL 1,4

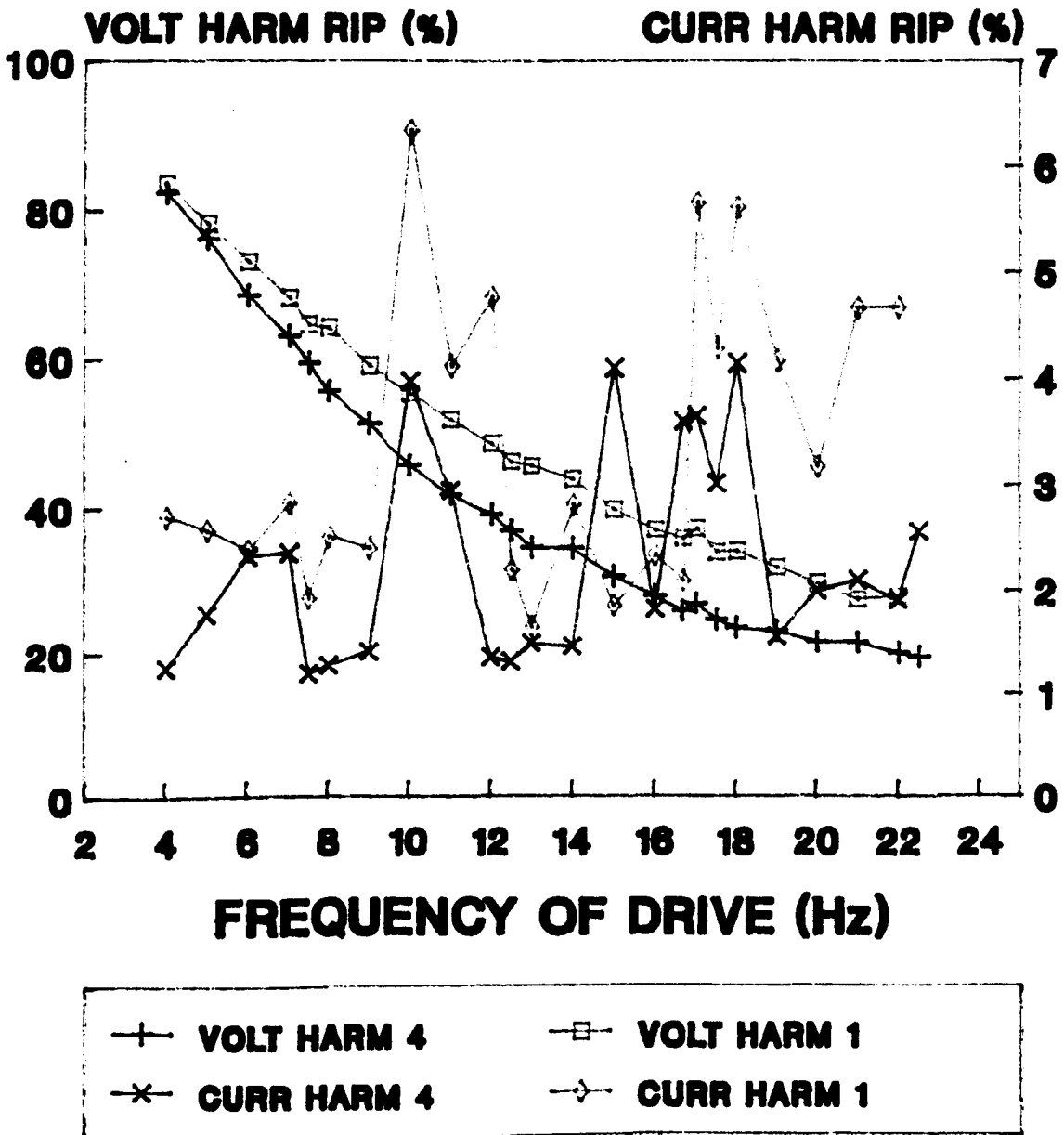


**FIG 6.13b Output Voltage Harmonic Ripple**  
**Output Current Harmonic Ripple**

# TEST 13

## MODEL 1,4

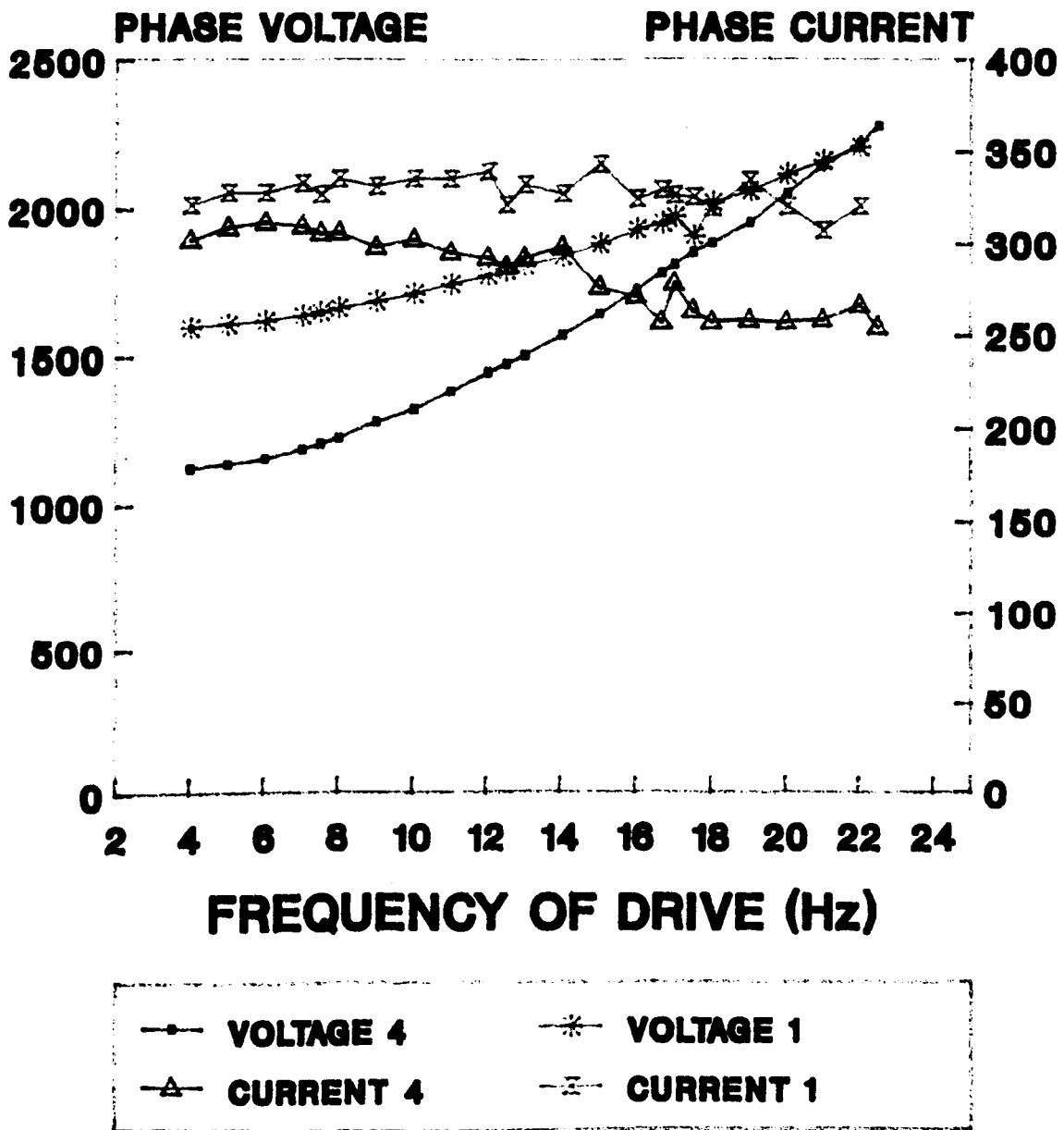


**FIG 6.13c Output Phase Voltage**  
**Output Phase Current**

#### 6.5.6 Test 14 Comparison of the simplified converter and Thevenin motor model

The purpose of the test was to assess the performance of the simplified motor equivalent circuit compared with the dq axis model on the behaviour of the cyclo-converter drive and supply system. To assess whether the added complexity of the dq axis modelling is worthwhile.

##### Test conditions:

The computer simulation was operated over the range of drive frequency 4-22 Hz with the following system characteristics to assess the effects of modelling the motor with the Thevenin motor model and the dq axis motor model, model 1 with the inclusion of interbridge. The purpose of this is to reduce the converter input and output current distortion factors :-

Model 2	Model 1
Supply reactance 0 %	Supply reactance 0 %
Decoupling reactance 0 %	Decoupling reactance 0 %
Interbridge delay 0.00 mS	Interbridge delay 0.00 mS
No overlap	No overlap
Thevenin motor model	dq axis motor model

**Test results:**

The following system operational characteristics were plotted against the drive frequency:

Fig 6.14a Motor efficiency (%)

Fig 6.14b Motor torque ripple factor (PU)

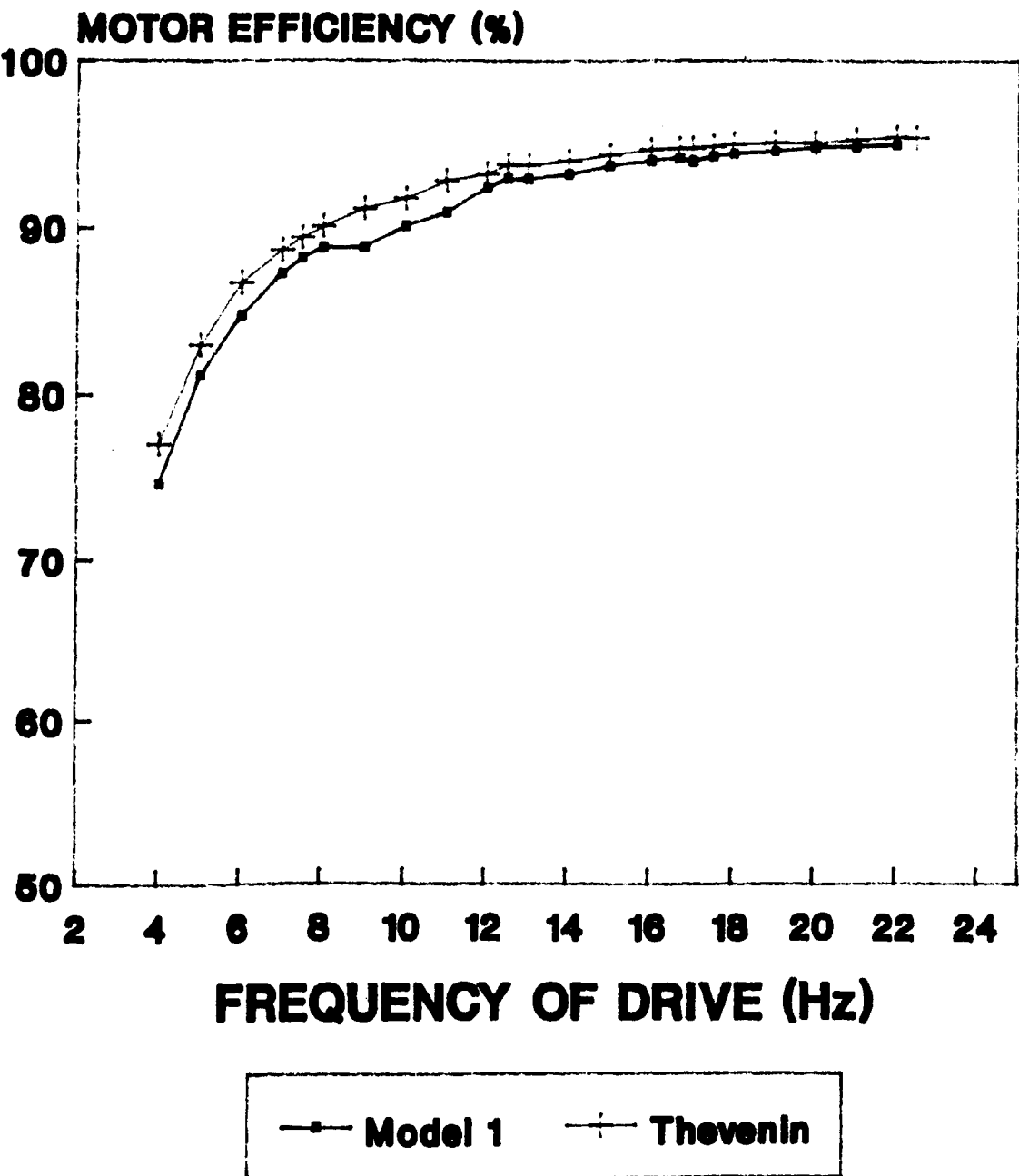
Fig 6.14c Output voltage harmonics (%)

Fig 6.14d Output current harmonics (%)



# TEST 14

## MODEL 1, THEVENIN



**Fig 14a Motor efficiency (%)**

# TEST 14

## MODEL 1, THEVENIN

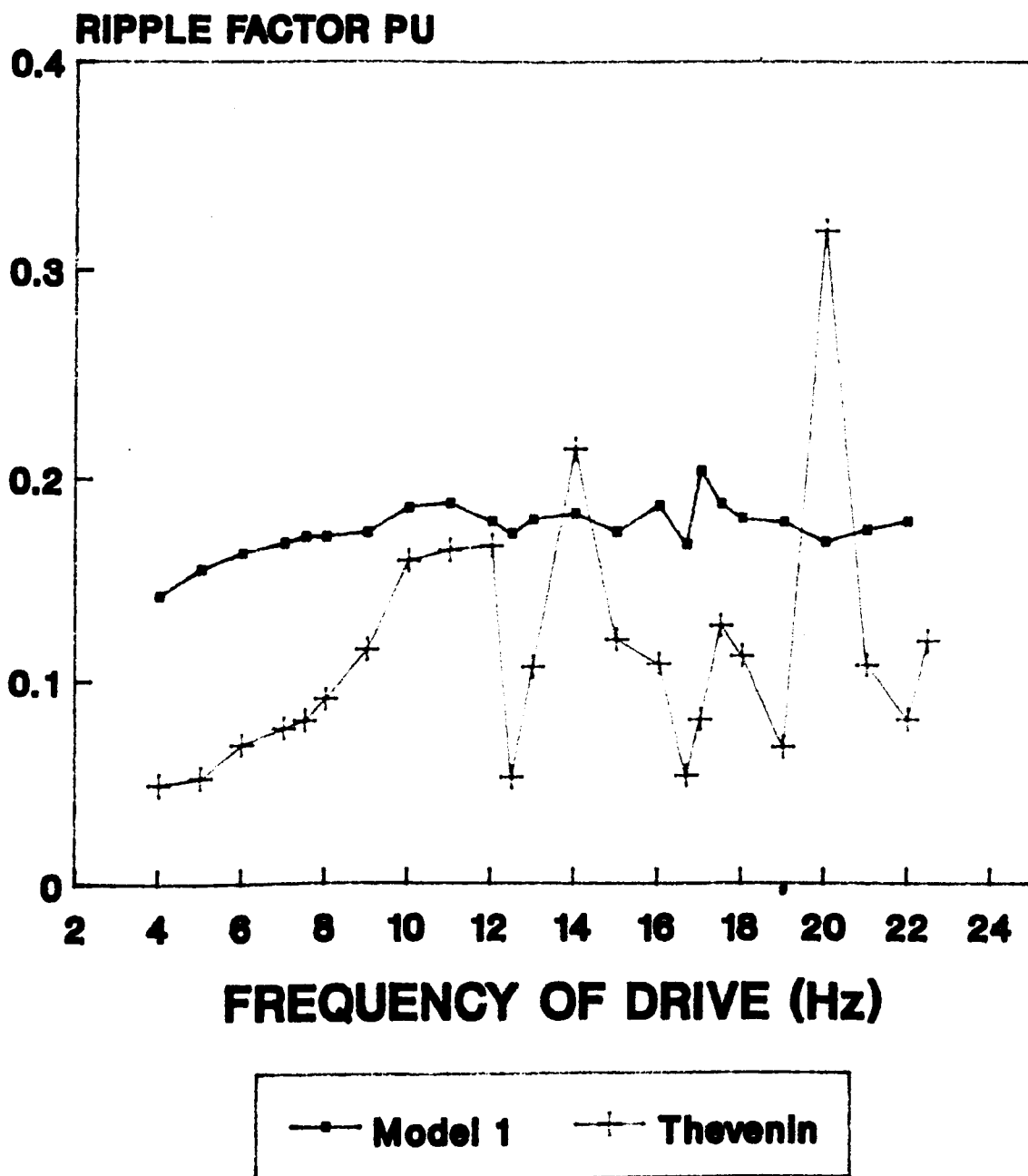


**Fig 6.14b Motor Torque Ripple Factor(PU)**

# TEST 14

## MODEL 1, THEVENIN

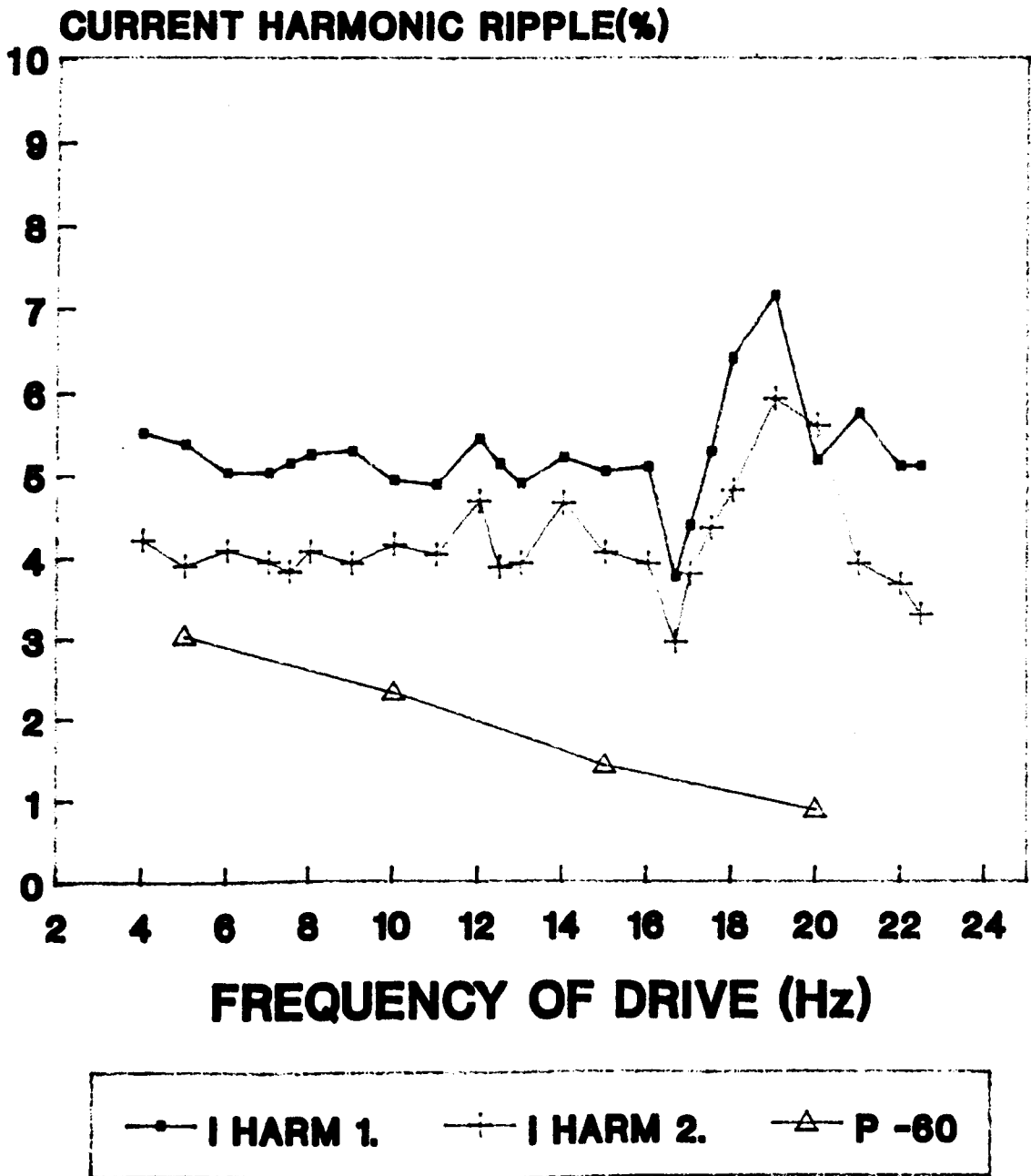
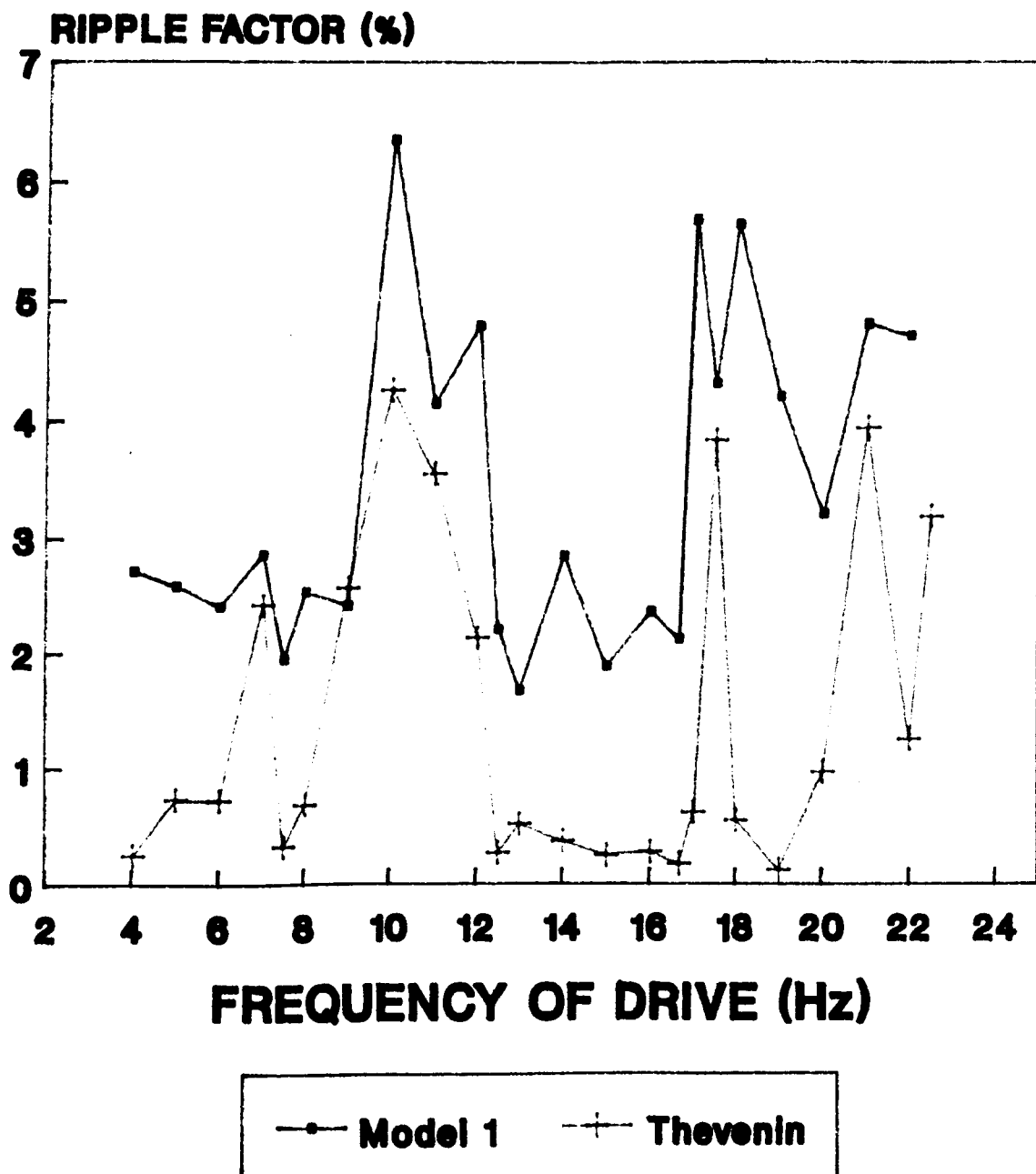


Fig 6.14c Input Current Harmonics (%)

# TEST 14

## MODEL 1, THEVENIN



**Fig 14d Output Current Harmonic**

## Chapter 7

### Effect of system parameters on simulated results

#### 7.1 Introduction

System parameters and converter characteristics are responsible for defining or modifying the characteristic behaviour of the cyclo-converter drive and the power supply system. This section seeks to examine these effects. The parameters and characteristics which will be examined are interbridge delay, commutation overlap, supply reactance and decoupling reactance. In current research these parameters are sometimes ignored or more often than not only one parameter is included in any simulation. The purpose of this section is to establish the effects of each parameter on the computer predicted behaviour of the cyclo-converter input and output characteristics, a summary is provided in table 7.1 .

#### 7.2 Interbridge changover delay Test 5

Interbridge changeover delay provides the necessary period of non conduction to ensure that one output bridge group has turned off, before the second bridge group is turned on. Real systems require this delay to prevent the positive and

Table 7.1 System and Converter Characteristic Variations

System parameters:

Converter and Supply	Load
Interbridge 3ms10 MW	Synchronous Machine
Supply Reactance 2.5%	Rated voltage 1542V at 20 Hz
Decoupling reactance 5%	Rated load 308 A
Drive frequency 4-22 Hz	Rated Frequency 50 Hz

Where percentage is quoted, it relate to a change in the percentage characteristic value, rather than a percentage reduction.

Converter/motor Models	Pelly Test 9	Model 1 Test 10	Interbridge Test 5	Overlap Test 6	Supply Reac. Test 7	Decoupling Reactance. Test 8
<b>Converter Input Characteristics</b>						
Input Voltage	-	Datum	-	+1%(av)	+3%(av)	+2%(av)
Harmonic Content (%)						
Input Current	-4%	Datum	+1%(av)	-1%(av)	-1%(av)	-2%(av)
Harmonic Content (%)						
Supply Regulation (%)	-	Datum	-	+6(%)	-	-
<b>Converter Output Characteristics</b>						
Voltage Regulation(V)	-	Datum	Reduces	250V Average	250 V Average	250V Constant
Current Regulation(A)	-	Datum	Reduces(4-22Hz) By 0 to 50A	Reduces By 5 A	Reduces By 25 A	Reduces By 50 A
Voltage Harmonic Content (%)	-3%(av)	Datum	+3%(av)	+10 to 0% (4-22 Hz)	0 to-10% (4-22Hz)	+5 to-10% (4-22Hz)
Current Harmonic Content (%)	-	Datum	-	-2%	-	-

negative converters from conducting simultaneously and shorting out the supply system, this characteristic is however quite frequently ignored in computer models.

#### 7.2.1 Input current harmonic content: Fig 6.5a

The alternating output voltage waveform is produced by taking discrete portions of the input power supply voltage waveform, the two waveforms are phase related and therefore produces a beating effect.

The converter will produce an output waveform which is principally related to the number of pulses on the supply system, for instance for a 6 pulse bridge converter:

5 Hz output cycle is synthesised from 60 input pulses
10 Hz output cycle is synthesised from 30 input pulses
15 Hz output cycle is synthesised from 20 input pulses
20 Hz output cycle is synthesised from 15 input pulses

The firing instants for the converter are decided by the cosine waveform control system, the actual point of firing is also dependent on the modulation depth which is decided upon at the outset of the simulation run.

At the point of bridge changeover, the control system of the converter may be considering commutation to the next device in the converter. If the control system decides to commutate

to the next device in the bridge, in preference to initiating bridge changeover, this will force the converter to wait for another supply input pulse before interbridge changeover can commence. The output power factor of the cyclo-converter may also effect the instant of interbridge changeover.

The discrepancy in the input current distortion factor compared to Pelly Fig 6.9a, increases as the frequency of the drive increases, this is because the periodic time of the output load waveform becomes nearer to the periodic time of the supply waveform. The delay of an extra pulse on the load side compared to the periodic time of the load drive frequency becomes more significant. At frequencies higher than 10 Hz the error increases making it more essential that this parameter should be included in the simulation.

If a delay is introduced at interbridge, the output current and voltage waveform have an interruption, this is partly responsible for suppressing the distortion to the output and input current waveforms. The inclusion of interbridge delay produces a more precise computer model and system waveforms, and reduces the adverse effect of beating which would otherwise produce misleading distortion factors and poor output and input current waveforms.



### 7.2.2 Output phase voltage: Fig 6.5c

The inclusion of interbridge has two effects on the cyclo output voltage. The synthesised output voltage is suppressed during the interbridge delay, the motor back emf is therefore seen on the motor terminals. The level of converter output voltage during interbridge, is dependant on whether the motor field is over excited or under excited, compared to the run where interbridge delay is excluded. Fig 6.5c shows that with the motor over excited, the motor back emf is responsible for increasing the motor terminal volts.

The output phase voltage 'B' in Fig 6.5c, is dependant on the emf of the motor, and therefore the impressed rms voltage is disguised. The inclusion of interbridge delay is responsible for larger reduction at higher frequencies, this is due to the fact that the fixed time for interbridge is more significant the shorter the periodic time of the drive waveform (ie high frequencies).

The actual interbridge delay may in reality be greater than that specified, since the converter may choose not to commence the firing until the voltage polarity is correct at the commencement of the next half cycle. This has the effect of producing a drop in the output voltage and current waveforms.

### 7.2.3 Output voltage harmonics: Fig 6.5b

It can be observed from Fig 6.5b that the exclusion of interbridge from the model will have the effect of over predicting the harmonic content on the cyclo output voltage. This is due to the interbridge process introducing a portion in the waveform which reduces the harmonic content of a peaky output waveform. It can also be seen from Fig 6.5b that the percentage reduction in output voltage harmonic varies between 1-5%, over the frequency range 4-22 Hz.

### 7.2.4 Output phase current: Fig 6.5c

The reduction in the rms output voltage applied by the cyclo-converter to the motor terminals, due to the inclusion of interbridge, produces a subsequent reduction in the rms output current of the converter.

The interbridge delay of 3 ms has a significant effect on the results of the simulation and is responsible for reducing the voltage impressed on the motor terminals. The level of this reduction by 15%-2% as the frequency reduces from 22-4 Hz. It is not surprising that the current reduces by a larger percentage at higher frequencies.

#### 7.2.5 Output current harmonics: Fig 6.5a

When interbridge delay is omitted, the output harmonic content increases when the periodic time of the drive is a multiple of, or near to, that for the supply frequency (drive frequencies of 10,12.5,15,20 Hz). This is due the beating effect between the drive and supply frequencies, Fig 6.5a shows that for this system the 10 Hz result was particularly critical.

#### 7.3 Overlap within the cyclo-converter Test 6

The inclusion of overlap in the converter model significantly increases the complexity of the model and the run time of the program. There are 6 devices per bridge circuit for a 6 pulse cyclo-converter, this means 12 per phase of the cyclo-converter, and a total of 36 devices for a complete system. When dealing with overlap each device changover has to be identified, the circuit parameters known, and the voltages producing the overlap currents specified. Where more than one converter is to be fed from the same busbars it is often necessary to include decoupling reactors to reduce the harmonics generated back into the supply system.

In a real system the effects of overlap within the converter are inseparable from the effects of regulation of the supply system. However in a computer model it is possible to

separate up these two effects since the supply inductors are responsible for two features which have to be modelled independently:

(a) Run A: this is a simulation where the effects of regulation and overlap are ignored.

(b) Run B: this is a simulation where the effects of line current  $di/dt$  are considered (the  $di/dt$  produced by overlap are suppressed)

(c) Run C: this is a simulation where the effects of line current  $di/dt$  are considered (including those produced by the overlap process within the converter).

#### 7.3.1 Input supply voltage: Fig 6.6b

The effect of the supply and decoupling reactances is two fold. The regulation of the supply network Run B (ignoring overlap), produces a drop in supply voltage of between 2-3%, (compare Run A with Run B). The regulation when overlap is included Run C, increases by a further 6-7%, (compare Run B with Run C).

### 7.3.2 Input voltage harmonics : Fig 6.6a

The supply reactances limit the speed at which commutation is conducted within the converter producing an overlap period. During the commutation process the input phases of the converter are shorted out producing notches in the supply waveform see Fig 6.1m

#### Fig 6.6a compares Run A and Run B

This compares voltage harmonic ripple, and shows that the inclusion of the supply reactances without the effect of overlap increases the supply voltage harmonic content by between 0.25-2.0 % over the drive frequency 4-22 Hz,

#### Fig 6.6a compares Run B and Run C

This compares voltage harmonic ripple, and shows that the harmonic content of the voltage supply waveform is increased by another 1.5%, due to the inclusion of the overlap process.

The Electricity Supply Industry has issued Engineering Recommendations on the limits of various disturbances, these limits have been included in the Appendix E. The recommendation states that the total voltage harmonic distortion should not exceed 4% at 11kV. The effect therefore of supply reactances (including overlap) are very significant in that they produces harmonic content varying from 1- 3% over the drive frequency range 4-22 Hz, with an

average increase in the voltage harmonic content of 1% compared to the run where the  $di/dt$  effect for overlap is ignored.

### 7.3.3 Input current harmonics:

The supply reactances will have a distinct effect on the line current in that the reactances act as low pass filter and therefore reduce the current harmonic distortion. The reactances are also responsible for the overlap process within the converter which introduces a distortion into the supply voltage network and reduces the supply current distortion by defining the rise and fall times of the line current.

Fig 6.6a, 6.6e compares Run A, Run B

Shows that the inclusion of the regulation effect of the supply reactors appears to reduce the harmonic content of the cyclo-converter input current by 1% over the complete drive frequency range.

There is a significant droop in the characteristic at 16.67 Hz and a rise at 12 Hz, this is also reflected in Fig 6.6a and is due to the beating between the input and output frequencies.

Fig 6.6a, 6.6e compares Run B, Run C

Shows that the effect of including overlap into the simulation has the effect of modifying the rise and fall of the line current and reducing the input current distortion by 1% as expected.

#### 7.3.4 Output phase voltage :

Figs 6.6c compares Run A, Run B

The inclusion of the supply and decoupling reactances in the simulation reduces the phase output RMS voltage by approximately 10-30% over the complete range of drive frequency 4-22 Hz. The reduction between the characteristics is related to the frequency of the drive, with the greater regulation being produced at the lower frequencies.

Fig 6.6c compares Run B Run C

The inclusion of overlap within the simulation reduces the output phase voltage by approximately 250 volts over the complete range of drive frequency 4-22 Hz, this is to be expected in that the overlap process is independent of frequency.

Overlap has the effect of reducing the voltage to the converter load, the amount of voltage lost is related to the magnitude of the supply reactances and the instantaneous magnitude of the output load current being commutated by the converter.

The voltage lost due to overlap is produced by the current rising and falling in each of the converter devices. As the drive frequency falls the voltage to frequency control reduces the converter output voltage. The voltage lost due to overlap becomes more significant since the loss of voltage for each overlap is independent of drive frequency.

The regulation of the supply system, reduces the ratio of the voltage to frequency, particularly at low frequencies. This can be observed in the Fig 6.6c Run C where it has been necessary to introduce voltage boost.

#### 7.3.5 Output voltage Harmonics

It can be seen from the Fig 6.6d that the harmonic content obtained with Runs A,B and C are related to frequency, as predicted by Pelly's theoretical analysis.

The characteristic behaviour of the supply reactances is to reduce the overall level of the harmonic content since they behave as low pass filters to the supply current.



Fig 6.6d compares Run A Run B

Shows that the inclusion of the supply reactance (ignoring the effect of overlap) has the effect of reducing the harmonic content of the cyclo-converter output waveform by 20% over the drive frequency 4-22 Hz. This characteristic can be observed in Fig 6.4L, 6.4k , which shows that the output load current shape is superimposed on the cyclo output voltage waveform, this is due to regulation effect of the supply network.

Fig 6.6d compares Run B Run C

Shows that the output voltage harmonic content is affected by the overlap process and is dependant upon the drive frequency. The Fig 6.4m shows the effects of overlap on the cyclo output voltage waveform, the commutation period is clearly visible. The effect of overlap on the converter output voltage harmonics is to increase the level of distortion, this is particularly noticeable below 12 Hz.

As the frequency reduces the voltage drop in the stator resistance becomes more significant in relation to the applied voltage. The motor phase current will therefore reduce in magnitude, both the motor phase and supply line current will become richer in harmonic content particularly at those frequencies which are present in the cyclo-converter output voltage spectrum.

If this characteristic feature is to be avoided and the flux level in the motor remain constant, it is necessary to include voltage boost at low drive frequencies.

#### 7.3.6 Output phase current:

Fig 6.6c compares Run A Run B

Shows that by including the supply and decoupling reactances (ignoring overlap ) has the effect of reducing the converter output voltage by 20-35% over the range of the drive frequency 4-22 Hz, this in turn reduces the converter output current by 10% .

Fig 6.6c compares Run B Run C

The effect of overlap, is to reduce the output voltage and hence producing a further reduction in the level of output current of 2% .

#### 7.4 Supply system reactance (including regulation and overlap) Test 7

Supply system reactance is usually considered to be balanced across the three phases of a supply system and includes the reactance of the alternator and any reactance due to cables in the supply system. The supply reactances have the same regulatory effect as the decoupling reactor, the only difference is that the regulation on each supply line is due to the total line currents from all three converters. These

reactances will be responsible for the reduction in output voltage from the cyclo converter during normal operation as well as during overlap.

#### 7.4.1 Input supply voltage harmonics: Fig 6.7a

The effect of overlap due to the supply reactances is to produce both regulation and commutation notches in the supply waveform, without the inclusion of decoupling reactances the harmonic content is high.

The harmonic content of the supply voltage waveform varies from 2-4% over the drive frequency range 4-22 Hz, (see G5/3 levels Appendix E ). This is high and would be unsuitable in most supply distribution networks due to the level of interference which would be produced for other users connected to the same system.

#### 7.4.2 Input supply current harmonics: Fig 6.7a

Shows that the introduction of a supply reactance has the effect of reducing the harmonic content of the supply currents by 1%. This is not surprising since the introduction of the supply reactance has the effect of acting as a filter reducing the harmonic content of cyclo-converter input and output currents.

#### 7.4.3 Output phase voltage: Fig 6.7c

Shows the regulation of the output of the cyclo-converter with and without the supply reactances. The inclusion of the supply reactance causes an overall regulation of the cyclo-converter output voltage of 10-30% , over the drive frequency range of 4-22 Hz..

#### 7.4.4 Output voltage harmonics :Fig 6.7b

Shows that the supply reactances also effect the converter output by acting as an input filter and reducing the harmonic content of the input current waveform. This has the effect of reducing the distortion of the cyclo output voltage waveform, making it more sinusoidal. The inclusion of the supply reactance has the effect of reducing the harmonic content of cyclo output voltage by 0-10% over the drive frequency of 4-22 Hz. It should be observed that the modification to the harmonic content is not constant and that at frequencies less than 5 Hz the harmonic content actually increases . This is due to the inclusion of overlap and has been explained in section 7.3.

#### 7.5 Decoupling reactance (including overlap) Test 8

The decoupling reactance is necessary in many power cyclo-converter arrangements to reduce the interference which may occur between cyclo-converter groups connected to the same high voltage system.

The supply reactance produces the overlap process within the converter. These notches will increase the harmonic content of the converter output voltage and supply line waveforms. It is able to significantly reduce the commutation notch produced by the converter and the supply reactance, this is can be seen in Fig 6.4n.

#### 7.5.1 Supply voltage harmonics: Fig 6.8a

Shows that by using a decoupling reactor with a supply reactance of the harmonic content of the supply voltage can be reduced from 3 to 1.5% .

#### 7.5.2 Output phase voltage: Fig 6.8c

Shows that the decoupling reactors are responsible for a reduction of 250 volts in the output phase voltage as the cyclo-converter drive frequency varies from 4-22 Hz ,

#### 7.5.3 Output voltage harmonics: Fig 6.8b

Shows that the decoupling reactance is responsible for reducing the harmonic content of the cyclo-converter output voltage by up to 5% as the drive frequency varies from 9-22 Hz .

It should be observed that the modification to the harmonic content is not constant and that at frequencies less than 9 Hz the harmonic content actually increases . This is due to the inclusion of overlap and has been explained in section 7.3.

## Chapter 8

### The computational analysis of various system models

#### 8.1 The system models to be used

##### 8.1.1 Introduction

Two approaches are commonly used to simplify the computer modelling of cyclo-converters, the converter and supply system are simplified as in models 1,2,3, or the motor equivalent circuit is simplified as in model 2.

This analysis seeks to compare the simplified converter and supply system with a more detailed modelling of the converter and the power supply network as in models 4,5; the simplified motor used in model 2 will be compared with the dq axis motor used in models 1,3,4,5.

It is intended to show that where the complex modelling of the converter and the motor are used, more accurate prediction on the behaviour and performance of the power supply system and drive may be obtained. Simplified models and Pelly's mathematical analysis have limited application since they do not provide a comprehensive or accurate analysis of the characteristics of a real system. A summary of the results is provided in Table 8.1

Table 8.1 Characteristic Variations for Models 1 to 5

**System parameters**

**Converter/Supply**

Interbridge delay 3ms  
Supply reactance 2.5%  
Decoupling reactance 5%  
Drive Frequency 4-22 Hz

**Load**

Synchronous machine  
Rated Voltage 1542 V at 20 Hz  
Rated Current 308 A  
Rated Frequency 50 Hz

Where percentage is quoted, it relates to a change in the percentage characteristic value, rather than a percentage reduction.

Converter /motor models	Pelly	Model 1	Model 2	Model 3	Model 4	Model 5
<b>Converter Input Characteristics</b>						
Input Voltage	-	Datum	-	+1%(av)	+1%(av)	+2%(av)
Harmonic Content (%)						
Input Current	-4%(av)	Datum	-1%(av)	-1.0%(av)	-0.5%(av)	-2%(av)
Harmonic Content (%)						
Supply Regulation (%)	-	Datum	-	+2%(av)	+4%(av)	+10%(av)
<b>Converter Output Characteristics</b>						
Voltage Regulation (V)	-	Datum	-	Reduces	Reduces	Reduces
Current Regulation (A)	-	Datum		-60A(av)	-40A(av)	-70A(av)
Voltage	-3%(av)	Datum	-3%	-5%(av)	-10%(av)	-15%(av)
Harmonic Content (%)						
Current	-	Datum	-	-1%(av)	-1%(av)	-2(%)
Harmonic Content (%)						
<b>Motor Characteristics</b>						
Output Torque Ripple Factor (%)	-	Datum	-10 % (of rated torque)	-	-	-
Motor Efficiency (%)	-	Datum	+3%	-	-	-



### 8.1.2 The base model

The base model has been identified so that the characteristic differences between models can be identified. Model 1 has been chosen as the base model since it is a simplified model and possibly one which is most commonly used. It's main deficiency is that the more complex system characteristics and converter characteristics are not taken into consideration. This may well simplify the computer source code and reduce the computing time, however it is liable to give inaccurate information regarding the characteristic performance and behaviour of the complete system.

### 8.1.3 The systems models to be examined

(a) Model 1 Simplified converter model/dq axis motor

Base Model

Supply reactance 0 %

Decoupling reactance 0 %

Interbridge delay 0.00 ms

No overlap

dq axis model motor

(b) Model 2 Simplified converter model /Thevenin motor

Supply reactance 0 %

Decoupling reactance 0 %

Interbridge delay 0.00 mS

No overlap

Thevenin model motor

(c) Model 3 Simplified converter model including

Supply reactance/dq axis motor

Supply reactance 2.5%

Decoupling reactance 0 %

Interbridge delay 0.00 mS

No overlap

dq axis model motor

(d) Model 4 Typical Industrial Supply

Supply reactance 1 %

Decoupling reactance 2 %

Interbridge delay 0.003 mS

Overlap

dq axis model motor

(e) Model 5 High Reactance Supply

Supply Reactance 2.5 %

Decoupling reactance 5 %

Interbridge delay 0.003 mS

Overlap

dq axis model motor

## 8.2 Test 9 Comparison of Pelly's model with sinewave output current produced computationally

This test was designed to model Pelly's mathematical analysis. The computer model was specified with an output load current waveform of a pure sinewave at a displacement factor of 0.5 Lag with respect to the reference sinewave. This enabled a direct comparison to be made between the two models. It was also possible to assess the error that exists between Pelly's analytical model and the computational model. The results for this can be seen in Fig 6.9a, 6.9b, there is a high degree of correlation between the two sets of results.

### 8.2.1 Input current harmonics Fig 6.9a

The error between the input current harmonic ripple is within 1%, this is with the analysis over one cycle of the supply frequency (Sine Harm(1)), this compares well with the results obtained by Pelly. To obtain a more representative result the analysis should be taken over a number of cycles of the supply waveform. In this case the author chose 5 cycles as shown in Fig 6.9b (Sine Harm(5)). This indicates that Pelly's results may be in error, since it is not able to predict the beating between the supply and drive frequency, this occurs at frequencies which are near to multiples of the supply frequency 5, 10, 12.5, 15, 20 Hz.

### 8.2.2 Output voltage harmonics Fig 6.9b

This shows that there is considerable similarity in the results obtained the error varying between 2-4% of the harmonic ripple. The error obtained is within reasonable limits and is due to the design of the simulation and the analysis of the system waveforms. Pelly's analysis is based the assumption of constant power factor and the analysis is limited to specific harmonics. The computer simulation predicts that the output power factor will vary from 0.1-0.4 Lag over the drive frequency due to the behaviour of the converter. The harmonic analysis of the drive frequency is up to 1000 Hz or 100 times the drive frequency whichever is the greatest.

### 8.3 Test 10 Comparison of Pelly's analytical model and the simplified converter and dq axis model 1

A marine drive was the second model used for the study, this comprised a 6.6 kV 10 MW synchronous motor supplied from a 6 pulse 'circulating free mode' cyclo-converter. The motor used represented a synchronous machine in dq form with damper windings. Comparison of this system with the analytical model produced by Pelly enabled the assessment of how far Pelly's analytical model is from a system model which is analysed computationally.

The results for this are displayed in Fig's 6.10a 6.10b, 6.10c.

#### 8.3.1 Input current harmonics Fig 6.10a

This shows that the inclusion of a more complex model significantly effects this characteristic producing an error over Pelly's analytical method of 3-5% . If a source impedance is included in the simulation the input line current would be responsible for significant voltage distortion. The difference between the two sets of results is initially due to the increase in the levels of harmonics associated with the synchronous motor and damper windings, this is clearly visible in the load current waveforms Figs 6.4a, 6.4c.

#### 8.3.2 Output voltage harmonics Fig 6.10b

This shows an error of 2-4% of Harmonic Ripple between the two tests over the drive frequency range. Since there is no supply reactance this is the same result as for Fig 6.9a Test 9

#### 8.3.3 Output phase voltage Fig 6.10c

This compares the results of Model 1 with those obtained by the author in his simulation of Pelly's analytical work Test 9, and shows that as expected the converter output voltage is identical.

#### 8.3.4 Output phase Current Fig 6.10c

This shows the current used in Pelly's analysis remaining constant, however in model 1 the current varies slightly due to the effects of beating between the supply and converter output frequencies. The average value of the output current for model 1 is slightly in excess of the full load current of 308 A, this is determined by the load angle set in the computer model for the synchronous machine.

The difference in the two models may also be observed from the waveforms seen in Fig's 6.4a, 6.4c; this shows the input and output voltage and current waveforms for the cyclo converter with the two models. The output waveforms for the cyclo-converter show clearly the significant difference between the ideal sinusoidal current waveform Fig 6.4a and the pulsed current waveform produced computationally Fig 6.4c. The waveforms of the input current also clearly show the pulsed nature of the load current.

It should be noticed that the power factor of Model 1 varies from 0.1 - 0.7 over the drive frequency. The motor equivalent circuit has been modelled so that the motor is operating under near unity power factor for the fundamental drive frequency, the reduction from unity is due to the harmonic content in both the converter output voltage and current waveforms. Pelly's work the converter output power factor remains constant over the drive frequency range,

therefore where the load power factor varies, due to the operation of the converter his results need to analysed across characteristics.

#### 8.4 Test 11 Comparison of results for simple and complex modelling of the supply system, models 1, 5:

The results obtained in this tests will indicate how large a variation can be expected in the performance of the converter and supply network. Model 1 is the simplest converter supply arrangement using the dq motor model and Model 5 is the most complex converter supply arrangement using the dq motor model.

The results indicate the error that will be introduced if complex modelling of the converter and supply is not used. The following results have been obtained from Model 5, with a supply having a supply reactance of 2.5% and a decoupling reactance of 5% .

The effect of complete modelling on system behaviour can be observed on the characteristic waveforms for models 1,5; the input supply current, supply voltage, cyclo output voltage and current waveforms Figs 6.4c, 6.4k.

#### 8.4.1 Input voltage harmonics: Fig 6.11a

Model 1 having no supply or decoupling reactance produces no harmonics on the supply voltage network.

The input voltage for model 5 is modified by the inclusion of the supply reactances, this has the effect of producing overlap within the converter and regulation of the supply voltage. Both characteristics are responsible therefore for the production of harmonics on the supply voltage waveform.

The supply waveform shows a large amount of distortion, with an average percentage of harmonics of 2% over the drive frequency 4-22 Hz.

#### 8.4.2 Input current harmonics: Fig 6.11a

It is can be seen that the variation of the harmonic content in the line current for both models is related as Pelly predicted to the converter operation. The reduction in the line current harmonics for the model 5 is related to the introduction of the converter parameters interbridge delay and overlap, this is explained in section 7.2 and 7.3.

The variation in the input voltage harmonics are related to the harmonics of the input line current, this can be seen by the similarity in the variation of the two characteristics



over the drive frequency range 4-22 Hz. The input current harmonics are responsible for producing the voltage distortion due the reactance of the supply.

#### 8.4.3 Output phase voltage: Fig 6.11d

Included in Model 5 are four characteristics which effect the regulation of the output voltage of the cyclo-converter. The following results have been obtained in section 7, for the frequency range of 4-22 Hz :

- (a) The inclusion of interbridge will reduce the output voltage, the percentage reduction is difficult to determine due to the back emf of the machine,
- (b) The inclusion of the supply and decoupling reactances (without overlap) will reduce the output voltage by 15-35%
- (c) The inclusion of overlap will reduce the output voltage by a further 10-20%

The effect of these parameters individually cannot be superimposed to find the overall reduction in the rms output voltage variation. It is not surprising that the reduction in output rms voltage between models 1 and 5, is 0-50% as the drive frequency varies from 4-22 Hz. The RMS output voltage appears to fall at a constant rate from 22- 7 Hz,

below 7 Hz the output voltage falls and the output voltage distortion increases this is due to overlap (see section 7.3), with Model 5 it is necessary to include voltage boost to keep the phase current constant over the drive frequency.

#### 8.4.4 Output voltage harmonics: Fig 6.11c

The harmonic content falls characteristically from 7-22 Hz, below 7 Hz however this characteristic changes rapidly and the harmonic content of the output voltage for Model 5 increases compared to Model 1. This effect is due to overlap and the subsequent loss in supply voltage, below 7 Hz it is necessary to employ voltage boost, (see section 7.3).

#### 8.4.5 Output phase current: Fig 6.11d

The cyclo-converter output rms current is related to the converter output voltage the drive frequency and the load characteristic. Model 1 sees very little reduction in current over the drive frequency 4-22 Hz. The voltage waveform is controlled by the cosine firing control system, with the voltage to frequency control ensuring that the motor flux and hence motor current remains constant. Model 5 has to take into consideration the regulation of the converter output voltage due to supply reactance and overlap. This has the effect of significantly reducing the rms output current of the converter by 10-20% over the

frequency range 4-22 Hz. The phase current does not reduce as much as the phase voltage due to the harmonic content in the converter output voltage.

It is possible to overcome the reduction of converter output current at low frequencies, this is called voltage boost in practical control systems. This has the effect of increasingly the voltage applied to the motor terminals at low frequencies. The control system will compensate for the increased loss in voltage across the motor stator resistance and overlap process, bringing the converter output current back up to the level required to provide a constant machine flux and torque.

The output current for model 5 does vary over the drive frequency range. This is due to the effects of interbridge delay being more pronounced at higher frequencies. The effect is disguised on the output phase voltage due to the back emf of the machine during the interbridge delay.

#### 8.4.6 Output current harmonics: Fig 6.11c

The percentage of harmonics in the output current waveform is significantly reduced for model 5 compared to model 1. This is not surprising as the harmonic content in the cyclo output voltage has also fallen due to the inclusion of the supply decoupling reactance and interbridge delay within

the converter model. It should be noted that the high level of output harmonics in model 1 is partly responsible for the increase in the distortion to the input current waveform.

**8.5 Test 12 Comparison of results for the complex model 5, and model 3 (models the supply reactance only no overlap)**

This model is commonly used since it models the power supply system including a supply reactance. Model 3 ignores the decoupling reactance commonly required to reduce the interference of the converter into the supply system.

**8.5.1 Input voltage harmonics: Fig 6.12a**

The inclusion of the supply reactance without the decoupling reactance or overlap have the effect of significantly decreasing the harmonics on the supply system, this figure shows that this may be as much as 1% reduction over the model 5.

The exclusion of the decoupling reactance will increase the current harmonic ripple. However the reduction in the voltage harmonic ripple is due to the fact that there are no commutation notches in the supply voltage waveform of model 3, this can be seen in Fig 6.4g 6.4k

#### 8.5.2 Input current harmonics: Fig 6.12a

The two characteristics vary over the range of the drive frequency range 4-22 Hz, producing an average increase of 1% for model 3 compared to model 5. This is to be expected due to the increase in the output voltage and current harmonic content.

#### 8.5.3 Output voltage harmonics: Fig 6.12b

The output voltage harmonic content does follow Pelly's predicted shape, with the modifications which have been discussed in section 7 due the inclusion of the decoupling reactance and overlap for model 5. The effect of the increased level of the commutation notch for model 5 is to modify the characteristic so that below 7 Hz the harmonic content increases significantly due to the overlap effect at low frequencies. Below 7 Hz model 5 has an average reduction of 10% in the harmonic content compared to Model 3.

#### 8.5.4 Output current harmonics: Fig 6.12b

The level of output harmonic content was shown in section 7 to reduce with the inclusion of decoupling reactance, and the overlap process. Model 3 does not included the converter decoupling reactances and overlap and therefore produces a higher level of output and input current harmonic content.

## **8.6 Test 13 Comparison of results for the base model 1 and**

### **Industrial model 4:**

The comparison of the industrial model 4, with the base model 1, is significant in that it shows the variation of results which can be expected with what is a typical industrial application. This model represents the commonest application which can be found in the industrial sector, and therefore requires close examination.

#### **8.6.1 Input voltage harmonics: Fig 6.13a**

The difference in the harmonic content produced by these two models is noticeable. This is due to the fact that the supply, decoupling reactance and overlap have been omitted in model 1. This produces an increase in the harmonic content of 1% over the drive frequency range 4-11 Hz. The input and output current harmonics of model 4 are a major factor on the modulation and level of the voltage harmonics produced with this model.

#### **8.6.2 Input current harmonics: Fig 6.13a**

The Model 4 produced a slightly lower level of current harmonics. Fig 6.13b shows that the level of harmonic content of the input current is related to that of the output current. The reduction is due to the inclusion of the supply reactances and overlap as predicted in Test 7 (overlap).

#### **8.6.3 Output phase voltage: Fig 6.13c**

The cyclo rms output voltage impressed on the motor terminals is reduced. The effects of interbridge in Test 5 indicate that the voltage applied to the load is not determinable due to the back emf of the motor, it is probably responsible for 5-10% of the regulation. The regulation due to the supply reactance is greater than expected, since the supply current comprises the superposition of the currents to each of the 3 individual converters.

#### **8.6.4 Output voltage harmonics: Fig 6.13b**

Fig 6.13b shows that the simplified model 1 over predicts the level of output voltage harmonic ripple, compared to model 4 by 10%.

### **8.7 Test 14 Comparison of the simple Thevenin model 2, and the complex dq axis model 1 for the synchronous motor:**

#### **8.7.1 Motor load angle and its behaviour**

The curves produced were calculated for the condition of constant torque output from the motor as the speed of the output shaft was varied. The inclusion of the damper winding in the dq axis motor modifies the effective impedance between the back emf and the reference voltage. It was necessary to adjust the load angle for the Thevenin model so that the torque delivered from the motor agreed with that

predicted by the base model for the motor. This indicates that there is a different transfer function for each model which will reflect in the control system applied to the drive. This may be hidden in a real system since the motor load would automatically define the correct load angle.

#### 8.7.2 Motor torque ripple and its behaviour Fig 6.14b

The pulsation of the supply voltage produce a characteristic ripple in the torque developed by the motor stator current. The determination of the magnitude of this torque is important for the design of the drive system. The transient torques can be calculated by the model, the information presented here is purely for the steady state case.

Appendix D Fig.6.4d shows the current spectrum for the drive motor when operating from a 5 Hz converter supply. It is quite clear that the principle harmonics are the 300, 600 and 900 Hz components that would be expected from a 6 pulse, rectified supply.

Fig.6.14b shows the torque ripple factor as a function of frequency for the motor delivering full load torque. Results are provided for both simulation showing that the highest torque ripple is predicted by the dq axis motor model. The damper windings have the effect of increasing the harmonic content in the motor stator windings which in turn



are responsible for the increase in the output ripple torque. The simple model therefore will under predict the level of torque ripple which would be expected in a real system.

It can be seen that there is a considerable amount of variation in the magnitude of the torque ripple at the higher converter frequencies. This is in part a computational problem associated both with adjustments to the reference voltage in the model to ensure that it maintains a constant rated torque output, and beating between the sample period for Fourier Analysis and the supply and converter periods.

In all cases the motor torque ripple is rather low being below 10% of rated torque.

#### 8.7.3 Motor efficiency and its behaviour Fig 6.14a

The efficiency of the synchronous motor improves as the speed of rotation increases with the machine operating under constant torque conditions with virtually constant loss.

The efficiency of the full and simple model of the machine follows the expected pattern with very little difference between the two curves, the full model predicting slightly lower efficiencies. The reason for this is quite simply the extra loss in the damper winding.

The efficiency of the machine employed in the model is quite poor and reflects the fact that it is in essence a 50Hz design. Higher efficiencies would be achieved with a specially designed machines as would be employed normally for such a drive system.

#### 8.7.4 Cyclo-converter waveforms: Appendix D Figs 6.4c, 6.4e

The characteristic waveforms which have been obtained for the cyclo-converter, show that the difference in the motor equivalent circuit does make a significant effect on the input and output current waveforms. This shows that the dq axis motor produces a greater level of harmonic content than the Thevenin motor.

Both models show a significant increase in the level of input harmonics in the current waveform, compared to the mathematical analysis produced by Pelly.

## Chapter 9

### Discussion of results

#### 9.1 Introduction:

The behaviour of system parameters and various model have been examined in this thesis. The accuracy obtained depends on the detail that has been introduced into the computer simulation. All of the results obtained show the characteristic behaviour as predicted by Pelly, the inclusion system parameters does significantly modify the results he obtained.

#### 9.2 Interbridge delay:

The behaviour of the cyclo-converter during the changeover from the positive to the negative bridge is called inter-bridge changeover delay. This commonly requires a period of delay to allow the thyristors to turn off adequately. The effect of not including this parameter is to simplify the shape of the input and output waveforms of the cyclo-converter. The percentage error depends on the drive frequency since the period of interbridge is nominally fixed at a minimum period of 3ms, whereas the periodic time of the output voltage and current is related to the drive frequency. When the drive frequency increases the error is the greatest (frequencies  $>10$  Hz), whereas for low drive

frequencies (  $< 10$  Hz ) the effect becomes less significant. The actual period may in reality be greater than that specified, since the converter will not commence firing until the voltage polarity is correct for the next half cycle. The inclusion of interbridge delay produces a reduction in the level of harmonic distortion to both the input and output current waveforms.

Interbridge is responsible for the reduction of the rms output voltage of the converter 'applied to the motor terminals', this in turn produces a reduction of the converter output current and the input line current.

If interbridge is to be included in the simulation, it is important to realise that the converter control system in a real system, would compensate for the loss in voltage applied to the motor terminals. This would ensure that the converter operates at the specified stator current. To include this feature in a computer simulation, it would be necessary to include a current control loop. This would ensure that the voltage to frequency ratio is kept at a constant value, and provide constant motor flux and torque.

### 9.3 Commutation overlap:

Many computer simulations seek to include the supply reactance within the simulation, it is well established that this reactance is not only responsible for the regulation of the supply voltages but also for the production of commutation notches in the supply waveform. The mathematical modelling of these two conditions is not the same and has to be dealt with separately.

The overlap commutation process has been shown to be responsible for a characteristic feature of its own. It is responsible for the reduction of the output converter rms voltage at all frequencies, however at low frequency it produces an increase in the harmonic content of the converter output voltage. If the overlap commutation process is not included then the harmonic content of the supply waveform will be significantly reduced compared to that seen in practice.

If the source reactance is low then ignoring overlap is less significant. If the source reactance is high the overlap angle is of the order of  $30^\circ$ , then with 18 devices in a three phase cyclo-converter, the converter will be in a commutation process for most of the time. It is vital that the overlap process is included where the converter simulation models high reactance supplies.

Some simulation choose to increase the number of iterations while the converter is in overlap to reduce the overall computation time. This complication to the source code is not necessary when modelling high reactance supplies since one of the three phases of the converter will be in overlap for the majority of the time. This is not the case when the supply reactance is low, in which case this technique would assist in reducing computer run times.

In a real system the converter current control loop would compensate for the increased loss in voltage due to overlap as the frequency of the drive falls, and therefore ensure that the converter operates at the specified stator current. To include this feature in a computer simulation, it would be necessary to include a comparable current control mechanism. This would ensure that the voltage to frequency ratio is kept at a constant value, and provide constant motor flux and torque.

#### 9.4 Supply reactances:

The inclusion of the supply reactance into the computer simulation is necessary if the regulation of the power supply system and overlap are to be modelled. The effect of the supply reactance has been shown to reduce the converter

output voltage and harmonic content over the frequency range. This is not unexpected since the reactance behaves fundamentally as a filter.

**High reactance supplies:**

If the supply reactance is omitted the prediction of converter output voltage will be significantly higher than expected.

It is normal to include a decoupling reactance to reduce harmonic content on the supply voltage. The inclusion of both supply and decoupling reactance will predict the correct level of supply regulation and input voltage harmonics.

If the supply reactance is included without a decoupling reactance then there will be an over prediction of the level of supply voltage harmonics.

**Low reactance supplies:**

Where there is a low source reactance as in the case of an industrial supply, the results indicate that the effect on the system characteristics is not negligible. There will be errors introduced in the magnitude of the cyclo-converter output voltage and current as well as in the supply voltage

and current waveform. The percentage errors likely to be introduced may be small but sufficient to make the complexity of modelling this characteristics worthwhile.

#### 9.5 Decoupling Reactance:

The modelling of this characteristic is complex since the current flowing in the decoupling reactance has to be analysed for each commutation period of the converter.

The inclusion of the decoupling reactance into the computer simulation is necessary if the regulation of the power supply system and overlap are to be modelled correctly. The effect of the decoupling reactance has been shown to reduce the converter output voltage and harmonic content over the frequency range.

The main purpose of including this reactance is to reduce the harmonic distortion to the supply network as a result of the commutation process in the converter. Ignoring the decoupling reactance, in instances where high reactance supplies are being modelled, will produce large errors to the regulation of the cyclo-converter output voltage and high input and output voltage waveform distortion.



The inclusion of the commutation process without the inclusion of the decoupling reactors, has the effect of increasing the harmonic content of the supply above that which would normally be seen in practice. The decoupling reactor acts as a low pass filter thereby reducing the effect of the commutation notch and providing electrical isolation between each converter.

#### 9.6 Pelly's model

The work of Pelly is well established and has been shown to be of great benefit to design engineers, however it lacks detail when it comes to a practical system. The results Pelly obtained are for a mathematical model, and can only provide an indication of the level of harmonic content which are present in the output voltage and the input current waveforms of a real system. The theory makes unrealistic assumptions about the shape of the load current waveforms, and the supply reactance and is unable to provide any information relating to :-

The output current harmonics, and the subsequent level of torque pulsations produced on the motor windings, mountings and shaft,

The characteristic behaviour of the supply and decoupling reactances on the supply network and the cyclo-converter output waveforms,

The distortion to the supply and cyclo-converter voltage waveforms due to commutation overlap process.

The results only provide the trend in the characteristic behaviour of the cyclo input current and output voltage distortion.

Pelly's mathematical analysis is not able to take into consideration the beating effects that can take place between the drive and supply frequencies, this has been shown to have significant effect upon the input and output current distortion particularly at higher frequencies.

The analysis only provides limited information for an industrial supply, these results being valid only when the drive frequency is low, since the converter output current waveform becomes more sinusoidal. This makes the mathematical solution extremely limited in its application and possibly misleading if taken to the extreme.

### 9.7 Simplified model 1:

The simplified model with a dq axis motor, will predict differences which can be expected between a mathematical model with a pure sinewave output as in Pelly's work. This model will take into consideration the current pulsations produced by the synthesised cyclo-converter output voltage and the motor load.

Model 1 will provide considerably more detail information compared with Pelly's work, particularly in relation to the harmonic content of the converter input and output current waveforms. This model produces current forms which are representative of a real motor load. The harmonic content in the input line current is significantly increased reflecting the increased pulsations as shown in the characteristic waveforms.

If this model is used to analyse a system with interbridge delay or where the source reactance is high, the prediction of the converter output levels of voltage and current would be higher than obtained in reality. It would be necessary to compensate by reducing the load angle of the motor so that the converter output current and voltage are reduced to the level that would be seen if the modelling was more precise.

This will now produce the correct magnitude of load current to the converter, however the motor power factor and converter output voltage will all show significant error.

#### 9.8 The Thevenin model 2:

The differences observed between the performance of the Thevenin and the dq axis models is significant particularly when the performance of the motor is being analysed. It is important to realise that the Thevenin equivalent motor does not take into consideration the losses in the rotor damper bars. Higher efficiencies will be obtained with this model compared the dq axis model. The harmonic content of the converter output current waveform is reduced due to the motor simplification, this inevitably reflects in the supply line currents which produce a lower level of current and voltage waveform distortion.

The results produced are calculated for the condition of constant torque output from the motor as the speed of the output shaft is varied. The inclusion of the damper winding in the dq axis motor and the supply reactances modifies the effective impedance between the back emf and the reference voltage. It was necessary to adjust the load angle in the simulation to obtain the required torque from the motor. This indicates that there is a different transfer function for each model, which will reflect in the control system

applied to the drive. This may be hidden in a real system since the motor load would automatically define the correct load angle.

#### 9.9 Simplified model 3 with supply reactance:

This model represents a system with only a supply reactance, the main error with this model occurs when used in marine application or where the supplies have a relatively high source reactance, which produce high levels of regulation and waveform distortion. The inclusion of the decoupling reactance is not straight forward and significantly increases the complexity of the modelling process, which is why it is frequently omitted.

Model 3 has the effect of significantly reducing the disturbance to the supply line voltage waveform, in that the commutation process and subsequent notches on the supply waveform have been omitted.

The omission of the decoupling reactance will increase the level of harmonic content in the converter input and output current waveforms. Also the regulation of the supply system will be reduced, producing an error in the rms levels of converter output voltage and current, this may be compensated for by increasing the supply reactance.

This model may be used where the supply reactance is low since the poor modelling of the converter and supply during overlap become less significant. It is vital that the decoupling reactor is included when commutation overlap is being modelled with a high reactance, if significant errors are to be avoided with system regulation and the generation of supply and load related harmonics.

#### 9.10 Industrial model 4:

The inclusion of system parameters, supply reactance, decoupling reactance, commutation overlap, and interbridge for the industrial model produced significant effect on the results. The source reactances, overlap and interbridge were all responsible for reducing the converter output voltage and current.

It has to be concluded that when modelling an industrial supply with a low source reactance, the increase in computational time for complex modelling of the supply system and cyclo-converter is worthwhile.

#### 9.11 The high reactance model 5:

The alternator source reactance in the marine application is invariably high due to the fact that the supplies are generated on board ship by a number of alternators connected

in parallel. The high voltage supply is used to provide the ships main drives, sometimes it is necessary to feed the auxiliaries via a motor generator set due to the levels of interference from the main drive.

The results obtained for this computer model show that to obtain sensible results the model must be capable of including a high source reactance. The source reactance was shown to have the greatest effect on the results however the inclusion of all the system parameters, including overlap, and interbridge delay, is vital if a true representation of the system disturbances are to be obtained.

With high reactance supplies the system waveforms are effected by the supply parameters, and also modified by the behaviour of currents and voltages in other parts of the system. The overlap distortion to the supply voltage at low frequencies is partly responsible for the increase in converter output voltage and current distortion.

The greatest error in the prediction of system characteristics will be produced when modelling marine or high reactance supplies, if this model is not used.

## 9.12 Influence of the Cyclo-converter on the Auxiliary

### Supply Waveform:

The supply system to the ships auxiliary circuits is also taken from the output of the main generator. It is therefore subject to interference from the switching action of the cyclo-converter particularly during overlap when the generators sub-transient reactance acts with the line reactors in the converter to form a potential divider between the two shorted phases.

The effect can be seen most clearly in Fig. 6.4m, this shows the computed voltage waveform at the ships primary supply point. The large voltage spikes occur during the overlap periods, and are commonly known as commutation notches.

The level of harmonic disturbance to a ship's supply system can be seen in Fig 6.8a, the graph shows the effect of the decoupling reactances in suppressing the main supply network from the cyclo commutation notches. It has been shown that without decoupling reactances a supply whose reactance is 2.5% will produce 2.5% harmonic ripple, whereas with the inclusion of a decoupling reactor the harmonic distortion is reduced to 1-1.5%.



## Chapter 10

### Conclusions

This work has analysed the effect of supply and converter parameters on the performance of a cyclo-converter, feeding a dq axis synchronous machine including damper windings.

The computer generated results for Wearmouth shown a high degree of correlation with those provided by GEC, and gives confidence in the modelling process. It is difficult to assess the percentage error, since the results provided by GEC are in purely graphical form.

This work has shown that simplifying the analysis of the power system and cyclo-converter drive produces significant errors in the system waveforms. The magnitude of voltage and current levels throughout the system are reduced as these characteristics are included. The levels of voltage and current harmonics are significantly altered by the inclusion of these features. The accuracy of a computer model will depend on how precisely the system parameters have been modelled in the computer program. Omission is liable to introduce significant errors into the results even with a reasonably stiff industrial supply. The results show that a significant level of harmonics are produced by a system which is modelled accurately. When compared with the

Electricity Councils recommendations in G5/3 (Appendix E) it confirms that the level of harmonics produced are significant.

The precise modelling of the motor is vital if the correct level of motor stator current harmonics and converter input current harmonics are to be obtained. Pelly's analytical model and the Thevenin motor model, both significantly under predicted the level of harmonics produced in the supply system. The Thevenin model underpredicts the level of torque pulsation in the motor load, whereas Pelly's results are unable to offer any indication of torque pulsation in motor drives.

The manufacturers and operators of drives require detailed computer predictions prior to manufacture, since excessive levels of torque pulsation may produce damage to machine windings. Whereas excessive levels of input harmonic content may produce interference into the supply network.

Operational data is normally provided for the power system from closed loop conditions, with voltage to frequency control and constant torque control. The models presented in this thesis contains open loop control of the stator current, and include voltage to frequency control, and low frequency voltage boost, which meets in part the above conditions.

The comparison with the Wearmouth tests (with closed loop control), with those simulated (open loop control and including system parameters), show a good degree of correlation. The effect of including system parameters with simulated results (open loop), is that there is no compensation due to the closed loop control system. Excluding system parameters with simulated results (closed loop), will cause the control system to compensate and disguise the errors.

The waveforms in any power system are non repetitive and therefore the results obtained experimentally or computationally, are only typical of what can be expected. The analysis of the power system is therefore a picture of an instant in time which may never be repeated again. To ensure that the results provide a true indication, the fourier analysis of the waveforms should be such that they provide a representative sample of the characteristics being examined, that is they should be over at least one cycle of the load frequency. The difference between the input and output frequencies of the converter will inevitably make the Fourier analysis a problem. In practice therefore, there can be significant error with Fourier analysis. The error in results obtained have been minimised as far as is practically possible.

This thesis has demonstrated that if the model does not accurately include the system parameters and follow the operational control strategy, the predicted results will deviate from those which would be obtained with a real system. The models examined do provide an increasing approximation to those conditions found in a real system.

There are significant areas for further work. The computer modelling could be developed to allow topological modification to be achieved more easily. Modelling the alternator supply would provide more detailed analysis and performance of the supply network, in particular the level of harmonic torque pulsation and the generation of negative phase sequence components in the supply network.

The modelling of the control system has already been partly accomplished with the analysis of the cyclo-converter under constant speed, with voltage to frequency control. However it would not be too difficult to also include a current loop to modify the performance of the converter to obtain computer simulated results for a specified level of current or torque.

## APPENDIX

### Appendix A:

#### A1 The synchronous motor characteristics as used in Tests 10-15.

The motor equivalent circuit is as specified by Say<sup>18</sup> and the notation is in the dq axis generalised machine form. This data has been compiled from a data sheet provided by CESELECT Projects Ltd:

##### A1.1 Rated Motor Characteristics:

Synchronous machine salient pole

Rated motor line voltage	6600 Volts
Rated motor VA (base)	3520 kVA
Rated full load motor line current	308 Amps
Rated motor frequency	50 Hz
Rated angular velocity	214.3 Rev min <sup>-1</sup>
No of pole pairs	14
Rated field voltage (synchronising)	294 Volts
Rated motor torque	149 KN

##### A1.2 Motor parameters

D axis inductances (not saturated)

$L_{ad}$	Mutual inductance
$L$	Leakage inductance
$L_d$	d axis inductance ( $L_{ad} + L$ )
$L_{kd}$	d axis inductance damper winding
$M_{dd}$	Mutual inductance D axis / d axis damper ( $L_{ad} + L$ )
$M_{ddf}$	Mutual inductance d axis damper / field axis ( $L_{ad} + L$ )
$M_{df}$	Mutual inductance d axis / motor field ( $L_{ad}$ )
$L_f$	Field inductance ( $L_f + L_{ad}$ )

$L_{ad}$	= 0.04097 H
$L$	= 0.00725 H
$L_d$	= 0.04846 H
$L_{kd}$	= 0.04578 H
$M_{dd}$	= 0.04097 H
$M_{ddf}$	= 0.04097 H
$M_{df}$	= 0.04097 H
$L_f$	= 0.05519 H

##### Q axis inductances

$L_{aq}$	Mutual inductance
$L_q$	q axis inductance
$M_{qq}$	Mutual inductance Q axis / q axis damper ( $L_{aq}$ )
$L_{kq}$	q axis inductance damper winding ( $L_{kq} + L_{aq}$ )

$L_{aq} = 0.02793 \text{ H}$   
 $L_q = 0.03585 \text{ H}$   
 $M_{qq} = 0.02793 \text{ H}$   
 $L_{kq} = 0.03207 \text{ H}$

#### Resistances

$R_a$  stator resistance ( 75 °C ) = 0.157 ohms  
 $R_d$  d axis damper resistance ( 75 °C ) = 0.680 ohms  
 $R_q$  q axis damper resistance ( 75 °C ) = 0.544 ohms  
 $R_f$  field resistance ( 20 °C ) = 0.637 ohms

Core loss rated voltage 40 kW  
Friction and windage loss 6 kW

#### A2 Per unit notation

$$\text{pu(reactance)} = \frac{\text{rated voltage}}{\text{rated current}} = \frac{3810}{308} = 12.37$$

$$L(\text{henries}) = \frac{X_{pu} \times \text{pu}}{\text{Angular velocity}}$$

**Appendix B**

**Table B1**

Results from Pelly's Mathematical analysis and details of the relationship between the drive frequency and the percentage harmonics of the input current of a 6 pulse cyclo-converter:

**Table B2**

Results from Pelly's Mathematical analysis and details of the relationship between the drive frequency and the percentage harmonics of the output voltage of a 6 pulse cyclo-converter:

**Table B 1** This shows the results of Pelly's mathematical analysis and details the relationship between the distortion factor percentage harmonics of the input current of a 6 pulse cyclo-converter.

Displacement factor  $Q = 1.0$

Frequency	Output Voltage Ratio	Distortion Factor	Percent. Harmonics
20 Hz	0.4	0.9746	2.54%
15 Hz	0.3	0.9707	2.93%
10 Hz	0.2	0.9662	3.38%
5 Hz	0.1	0.9655	3.45%

Displacement factor  $Q = 0.5$  lag

20 Hz	0.4	0.9913	0.87%
15 Hz	0.3	0.98595	1.39%
10 Hz	0.2	0.9768	2.31%
5 Hz	0.1	0.9698	3.02%

Displacement factor  $Q = 0.0$

20 Hz	0.4	0.99386	0.614%
15 Hz	0.3	0.98961	1.04%
10 Hz	0.2	0.98049	1.95%
5 Hz	0.1	0.9706	2.94%

**Table B 2** This shows the results of Pelly's mathematical analysis and details the relationship between the distortion factor, percentage harmonics of a 6 pulse current waveform at the output voltage of the cyclo-converter.

Displacement factor  $Q = 1.0$

Frequency	Output Voltage Ratio	Distortion Factor	Percent. Harmonics
20 Hz	0.4	0.74131	25.87%
15 Hz	0.3	0.63094	36.91%
10 Hz	0.2	0.47272	52.73%
5 Hz	0.1	0.25675	74.33%

Displacement factor  $Q = 0.5$  Lag

20 Hz	0.4	0.7375	26.25%
15 Hz	0.3	0.62859	37.14%
10 Hz	0.2	0.4688	53.11%
5 Hz	0.1	0.25609	74.39%

Displacement factor  $Q = 0.0$

20 Hz	0.4	0.73814	26.18%
15 Hz	0.3	0.62813	37.18%
10 Hz	0.2	0.4684	53.16%
5 Hz	0.1	0.25592	74.4%



## Appendix C

The commutation process within the converter:

### C1 The positive converter:

- a) Commutation process from C1 to A1,  
Calculation of the currents during overlap,  
Fig's 3.2a 3.2b commutation process.
- (b) Commutation from devices B2 to C2 negative output of  
converter:  
See Fig.3.3 for diagramtic representation of  
overlap for equation given.

At the point of commutation the yellow voltage  $V_{ph}(2)$  is more positive than the blue phase voltage  $V_{ph}(3)$ , therefore a current is driven around as shown turning B2 off and bringing C2 on. At the same time the phase supplies are required to provide the current to the other converters as indicated.

Circuit equations:

$$V_{ph}(2) - V_{ph}(3) = (p(I_s(3)) - p(I_{s0}(2))) * L_s + p(I_{ov}(5)) * (L_d + L_s) - p(I_{ov}(6)) * (L_c + L_s) \quad -(6)$$

$$I_{ov}(5) = I_{ph}(1) - I_{ov}(6) \quad -(7)$$

$$V_{ph}(2) - V_{ph}(3) = (p(I_s(3)) - p(I_{s0}(2))) * L_s + p(I_{ov}(6)) * (L_d + L_s) - (p(I_{ph}(1)) - p(I_{ov}(6))) * (L_d + L_s)$$

$$p(I_{ov}(6)) = (V_{ph}(2) - V_{ph}(3) - (p(I_s(2)) - p(I_{s0}(3))) * L_s + p(I_{ph}(1)) * (L_d + L_s)) / (2 * L_d + 2 * L_s)$$

### C2 Negative Converter:

- (a) Commutation from devices C1' to A1' positive output of  
converter:  
See Fig.3.4 for diagramtic representation of  
overlap for equation given.

At the point of commutation the blue phase voltage  $V_{PH}(3)$  is more positive than the red phase voltage  $V_{PH}(1)$ , therefore a current is driven around as shown turning C2' off and bringing A2' on. At the same time the phase supplies are required to provide the current to the other converters as indicated.

Circuit equations:

$$V_{ph}(3) - V_{ph}(1) = (p(I_{s0}(3)) - p(I_s(1))) * L_s + p(I_{ov}(4)) * (L_d + L_s) - p(I_{ov}(6)) * (L_c + L_s) \quad -(8)$$

$$I_{ov}(6) = I_{ph}(1) - I_{ov}(4) \quad -(9)$$

$$V_{ph}(3) - V_{ph}(1) = (p(I_{so}(3)) - p(I_{s}(1))) * L_s + \\ p(I_{ov}(4)) * (L_d + L_s) - (p(I_{ph}(1)) - p(I_{ov}(4))) * (L_d + L_s)$$

$$p(I_{ov}(4)) = (V_{ph}(3) - V_{ph}(1) - (p(I_{so}(3)) - p(I_{s}(1))) * L_s \\ + p(I_{ph}(1)) * (L_d + L_s)) / (2 * L_d + 2 * L_s)$$

(b) Commutation from devices B1' to C1' negative output of converter:

See Fig.3.5 for diagramtic representation of overlap for equation given.

At the point of commutation the blue phase voltage VPH(3) is more positive than the yellow phase voltage VPH(2), therefore a current is driven around as shown turning B1' off and bringing C1' on. At the same time the phase supplies are required to provide the current to the other converters as indicated.

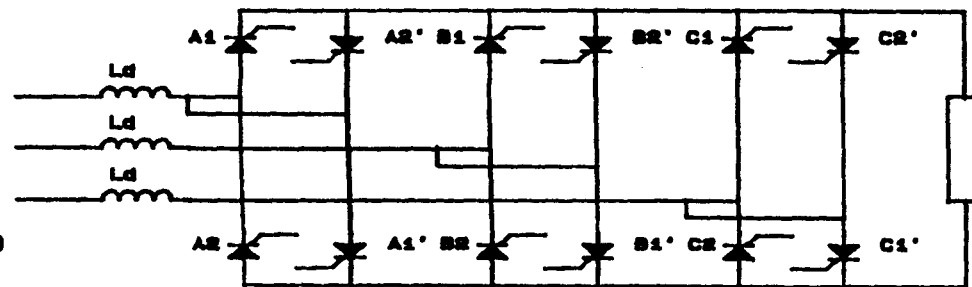
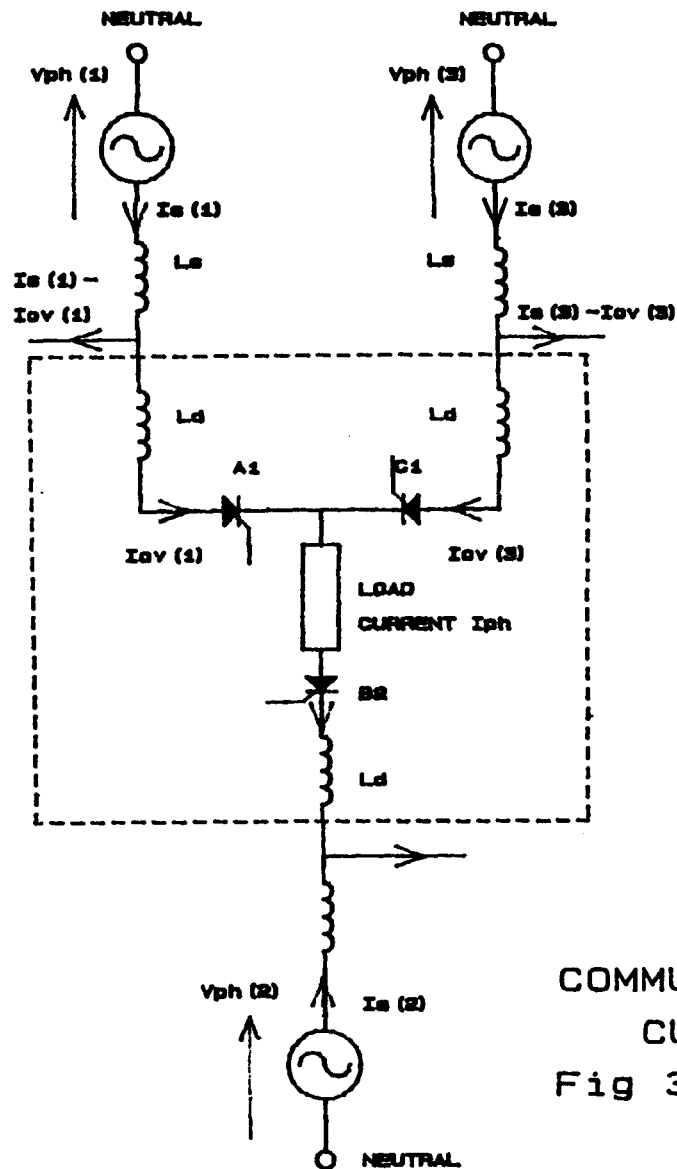
Circuit equations:

$$V_{ph}(3) - V_{ph}(2) = (p(I_{s}(3)) - p(I_{so}(2))) * L_s + \\ p(I_{ov}(3)) * (L_d + L_s) - p(I_{ov}(2)) * (L_c + L_s) \quad -(10)$$

$$I_{ov}(2) = I_{ph}(1) - I_{ov}(3) \quad -(11)$$

$$V_{ph}(3) - V_{ph}(2) = (p(I_{s}(3)) - p(I_{so}(2))) * L_s + \\ p(I_{ov}(3)) * (L_d + L_s) - (p(I_{ph}(1)) - p(I_{ov}(3))) * (L_d + L_s)$$

$$p(I_{ov}(3)) = (V_{ph}(3) - V_{ph}(2) - (p(I_{s}(3)) - p(I_{so}(1))) * L_s \\ + p(I_{ph}(1)) * (L_d + L_s)) / (2 * L_d + 2 * L_s)$$



INVERSE PARALLEL BRIDGE PAIR  
PER CYCLO PHASE

$A1, A2, A3, A4, A5, A6$  POSITIVE BRIDGE

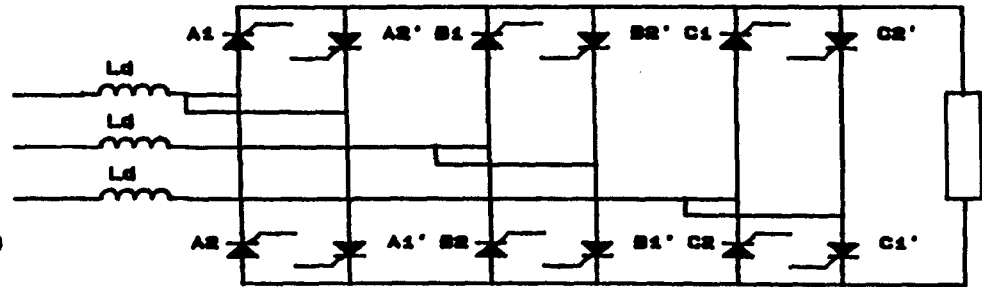
$A1', A2', A3', A4', A5', A6'$  NEGATIVE BRIDGE

$A1$  Commutating on

$C1$  Commutating off

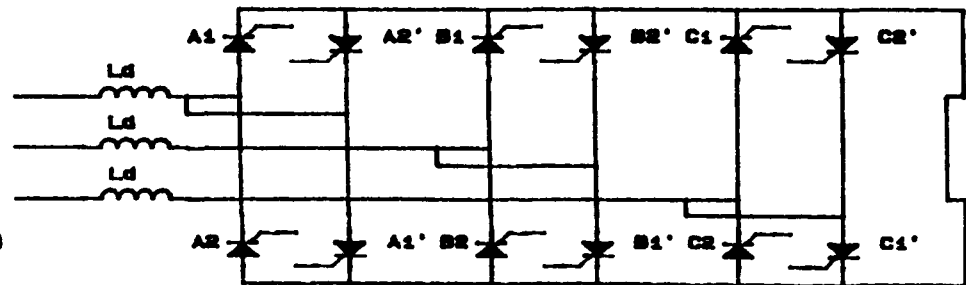
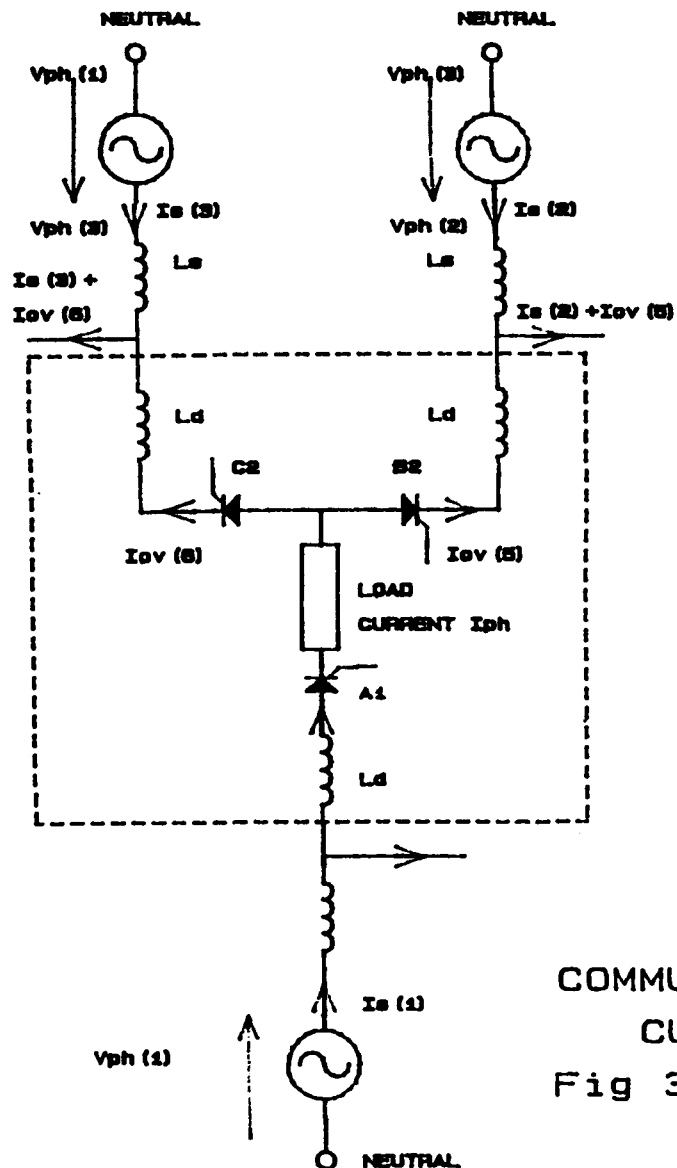
COMMUTATION PROCESS FOR POSITIVE BRIDGE  
CURRENT COMMUTATING FROM  $C1$  TO  $A1$

Fig 3.2a



## C1 Computing off

**Fig 3.2b**



### INVERSE PARALLEL BRIDGE PAIR PER CYCLO PHASE

$A1, A2, A3, A4, A5, A6$  POSITIVE BRIDGE

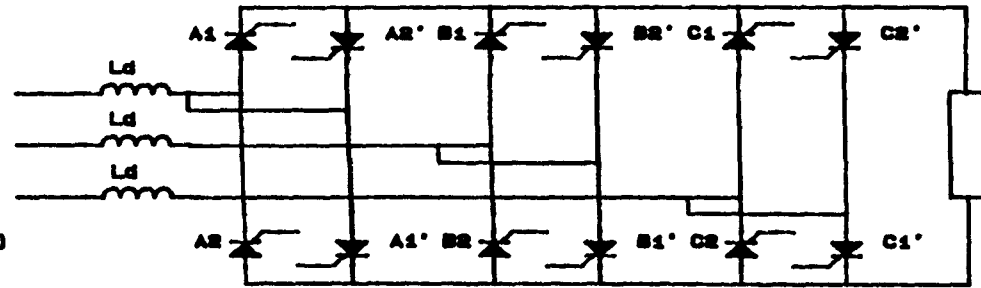
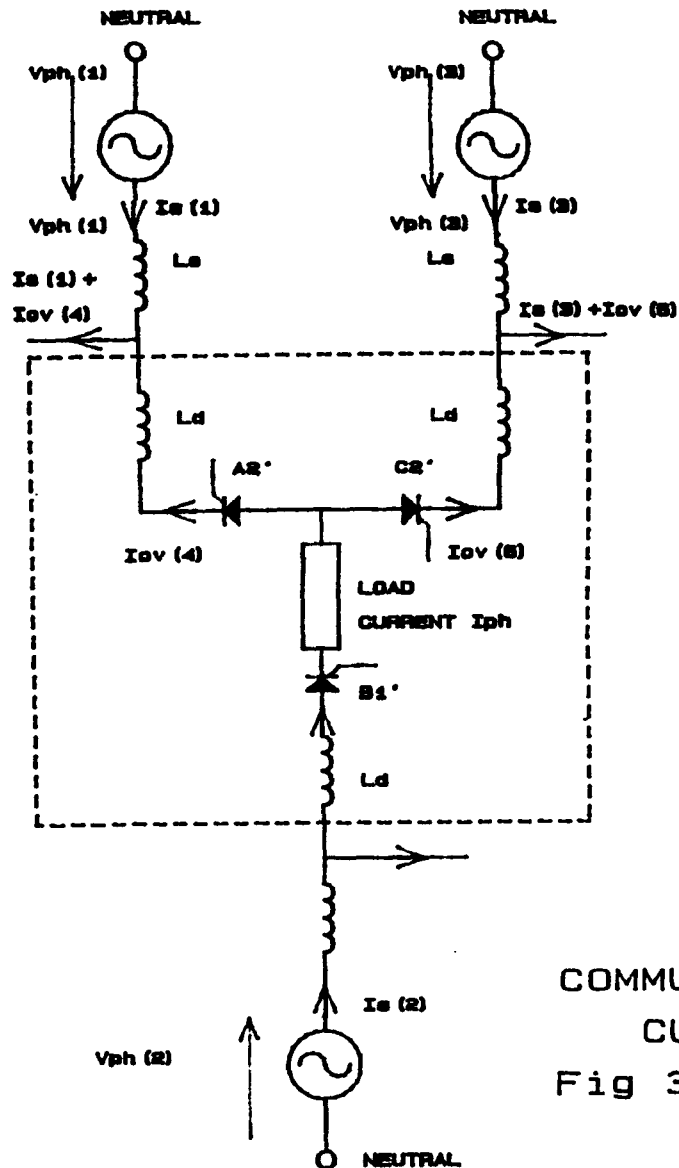
$A1', A2', A3', A4', A5', A6'$  NEGATIVE BRIDGE

$C2$  Commutating on

$B2$  Commutating off

COMMUTATION PROCESS FOR POSITIVE BRIDGE  
CURRENT COMMUTATING FROM  $B2$  TO  $C2$

Fig 3.3



### INVERSE PARALLEL BRIDGE PAIR PER CYCLO PHASE

A1, A2, A3, A4, A5, A6 POSITIVE BRIDGE

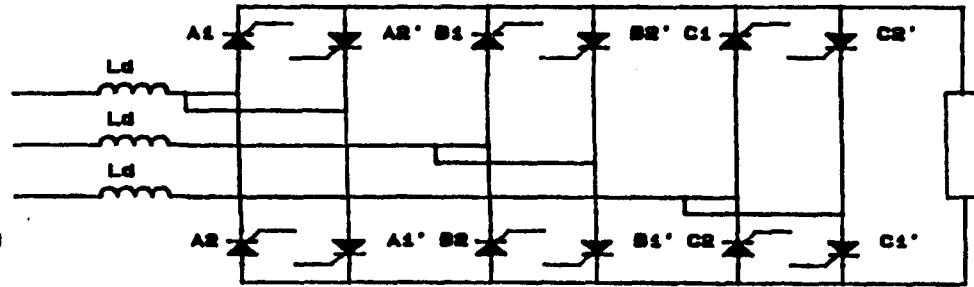
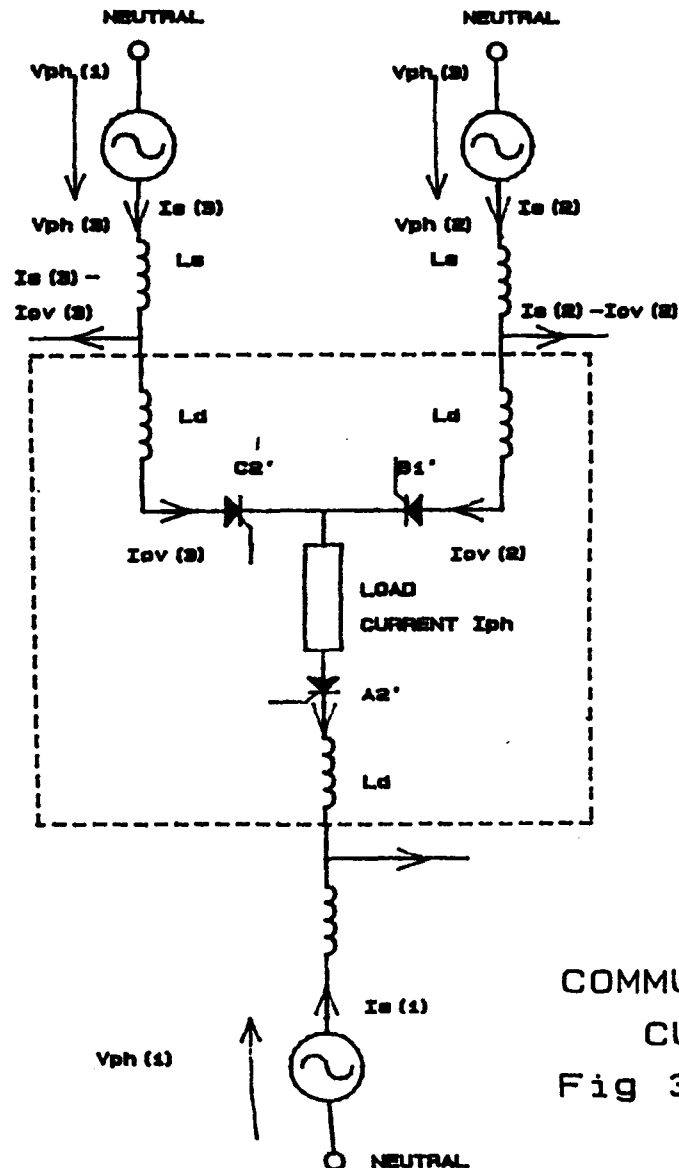
A1', A2', A3', A4', A5', A6' NEGATIVE BRIDGE

A2' Commutating on

C2' Commutating off

COMMUTATION PROCESS FOR NEGATIVE BRIDGE  
CURRENT COMMUTATING FROM C2' TO A2'

Fig 3.4



### INVERSE PARALLEL BRIDGE PAIR PER CYCLO PHASE

$A1, A2, A3, A4, A5, A6$  POSITIVE BRIDGE

$A1', A2', A3', A4', A5', A6'$  NEGATIVE BRIDGE

$C1'$  Commutating on

$B1'$  Commutating off

COMMUTATION PROCESS FOR NEGATIVE BRIDGE  
CURRENT COMMUTATING FROM  $B1'$  TO  $C1'$

Fig 3.5

## **Appendix D**

**Cyclo-converter characteristic waveforms for models 1 to 5:**

**The order of the waveforms and harmonic spectrums on each Figure is as follows:**

### **System waveforms:**

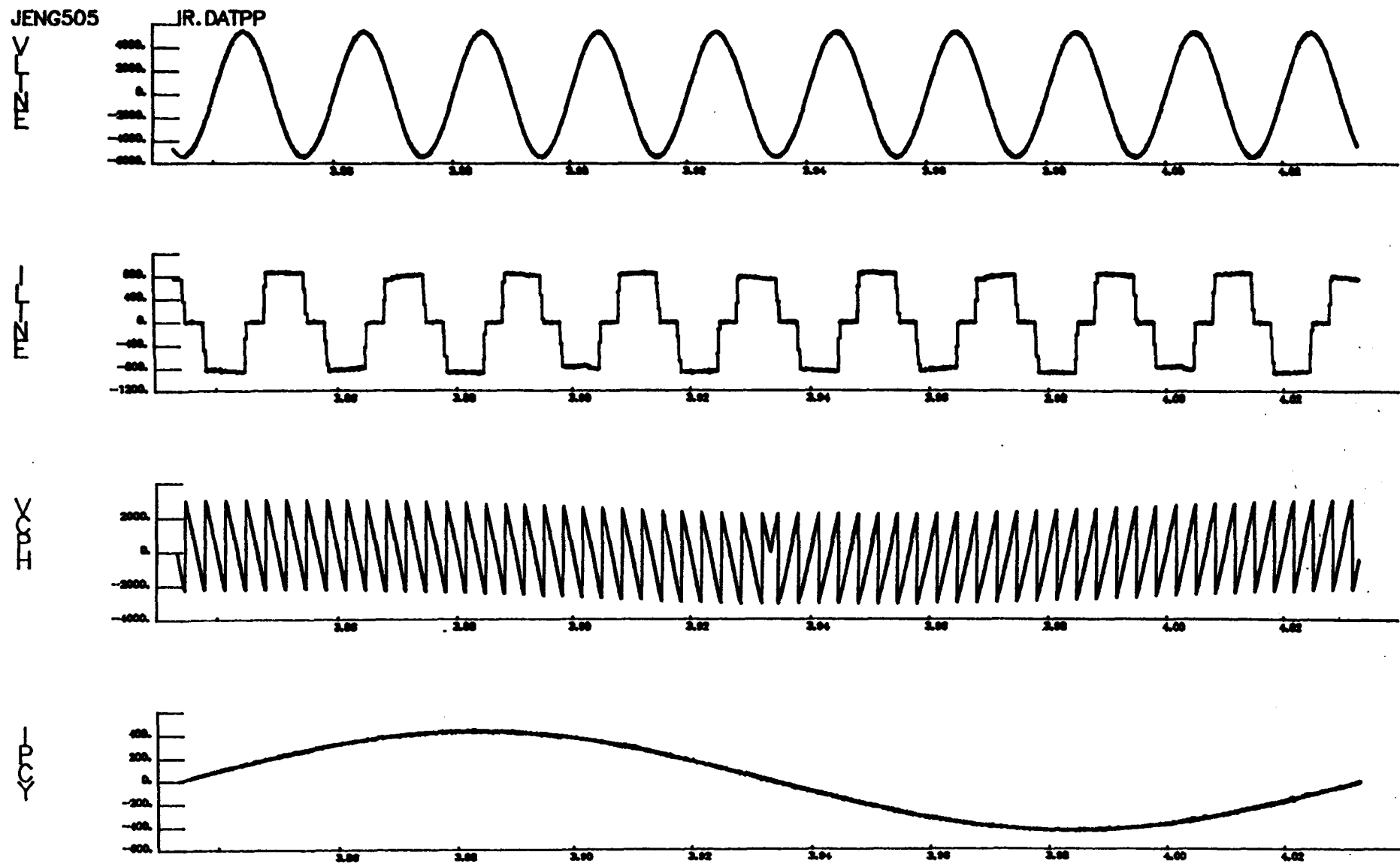
- Cyclo-converter supply voltage
- Cyclo-converter supply current
- Cyclo-converter output phase voltage
- Cyclo-converter output phase current

### **Harmonic spectrums:**

- Cyclo-converter supply voltage
- Cyclo-converter supply current
- Cyclo-converter output phase voltage
- Cyclo-converter output phase current

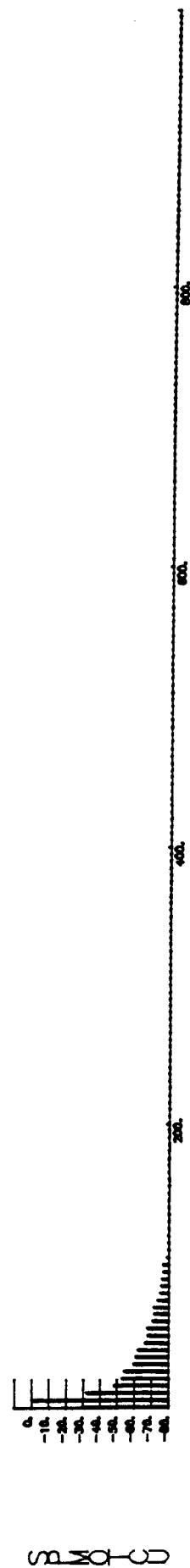
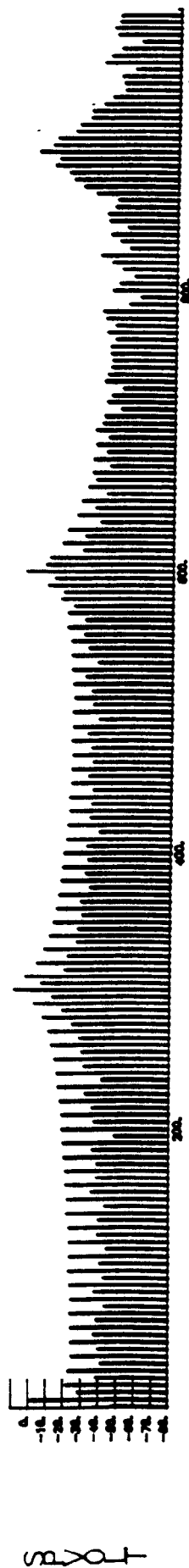
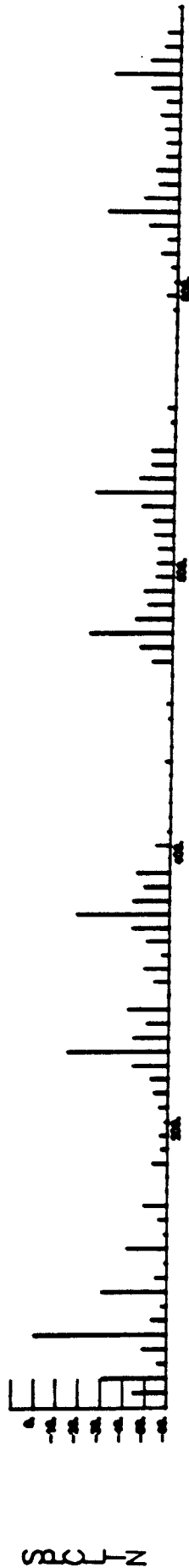
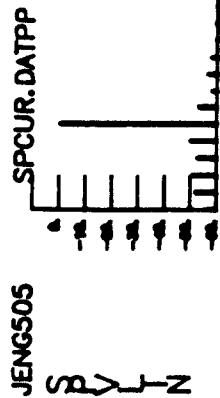
- D1 **Model 1 Sinewave output current:**  
Fig 6.4a voltage and current waveforms,  
Fig 6.4b harmonic analysis of voltage  
and current waveforms.
- D2 **Model 1 Simplified converter model/dq axis motor:**  
Fig 6.4c voltage and current waveforms,  
Fig 6.4d harmonic analysis of voltage  
and current waveforms.
- D3 **Model 2 Simplified converter model/ Thevenin motor:**  
Fig 6.4e voltage and current waveforms,  
Fig 6.4f harmonic analysis of voltage  
and current waveforms.
- D4 **Model 3 Simplified converter model including supply reactance/dq axis motor:**  
Fig 6.4g voltage and current waveforms,  
Fig 6.4h harmonic analysis of voltage  
and current waveforms.
- D5 **Model 4 Typical industrial supply:**  
Fig 6.4i voltage and current waveforms,  
Fig 6.4j harmonic analysis of voltage  
and current waveforms.
- D6 **Model 5 High reactance supply:**  
Fig 6.4k voltage and current waveforms,  
Fig 6.4l harmonic analysis of voltage  
and current waveforms.
- D7 **Fig 6.4m Waveform of typical commutation process**  
**Fig 6.4n Waveform of commutation with and without Decoupling reactor**





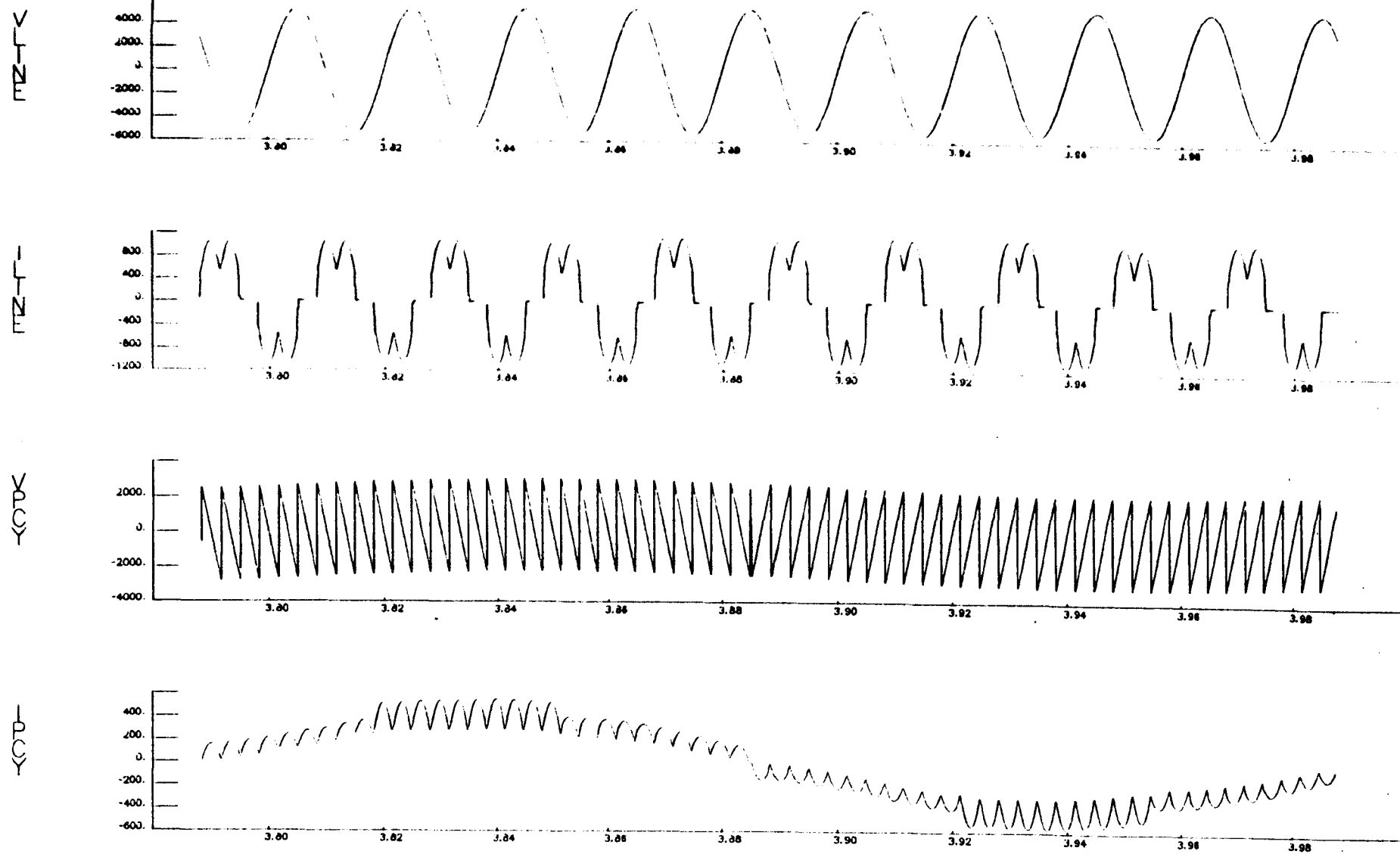
TIME [MODEL SINE]

Fig 6.4a Waveforms of system with Sinewave output current



FREQ [SINEWAVE] Fig 6.4b Harmonics of system with Sinewave output current

JENG505

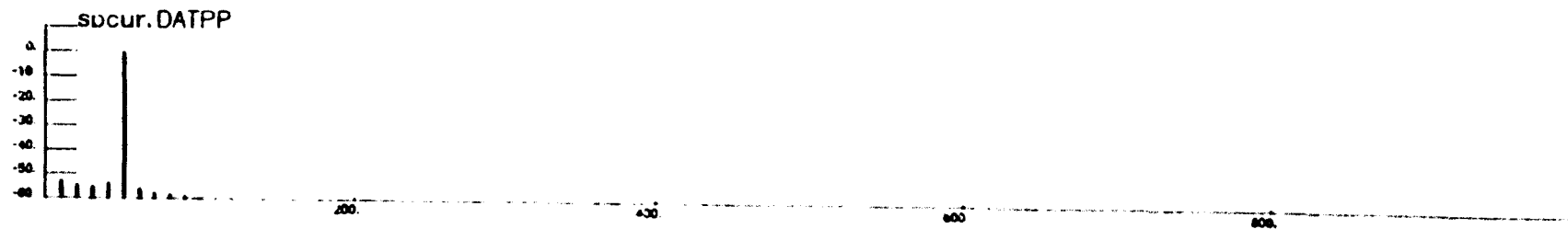


TIME [MODEL 1 5Hz]

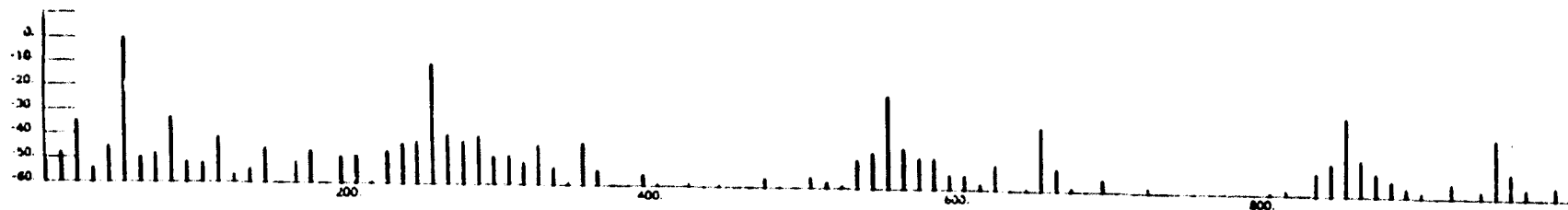
Fig 6.4c Waveforms of system with Model 1

JENG505

Z-T-Z



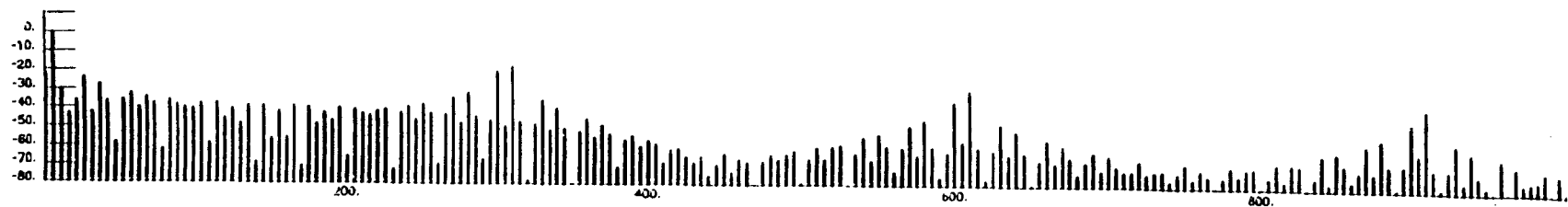
Z-O-Z



Z-X-Z

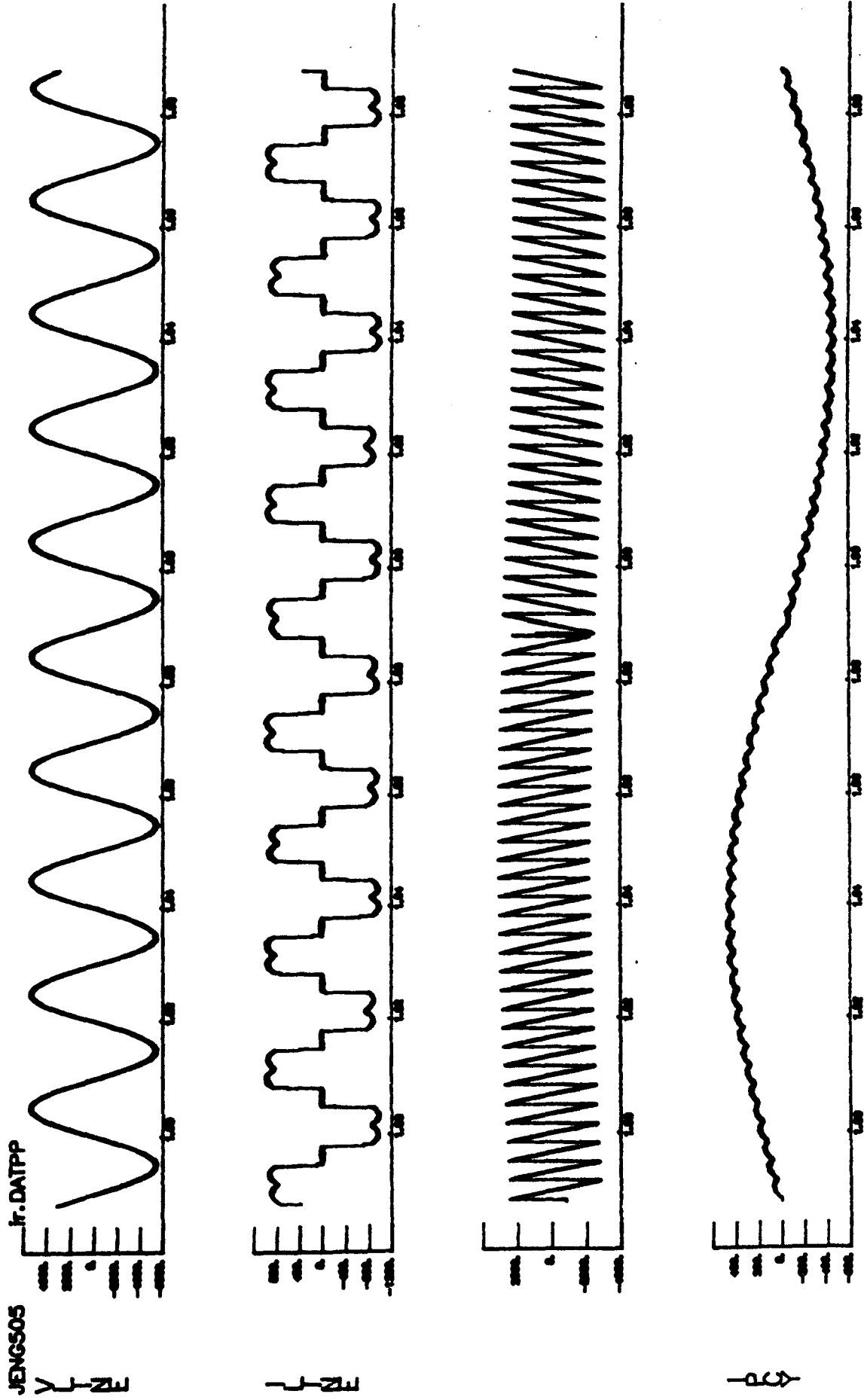


Z-O-O



FREQ [MODEL 1 5Hz]

Fig 6.4d Harmonics of system with Model 1



TIME [MODEL 2 <sup>u</sup> 5 Hz] Fig 6.4e Waveforms of system with Model 2

JENG505

SPY-T-Z

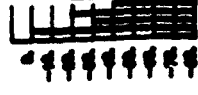
sour.datpp



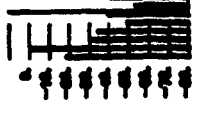
SPY-T-Z



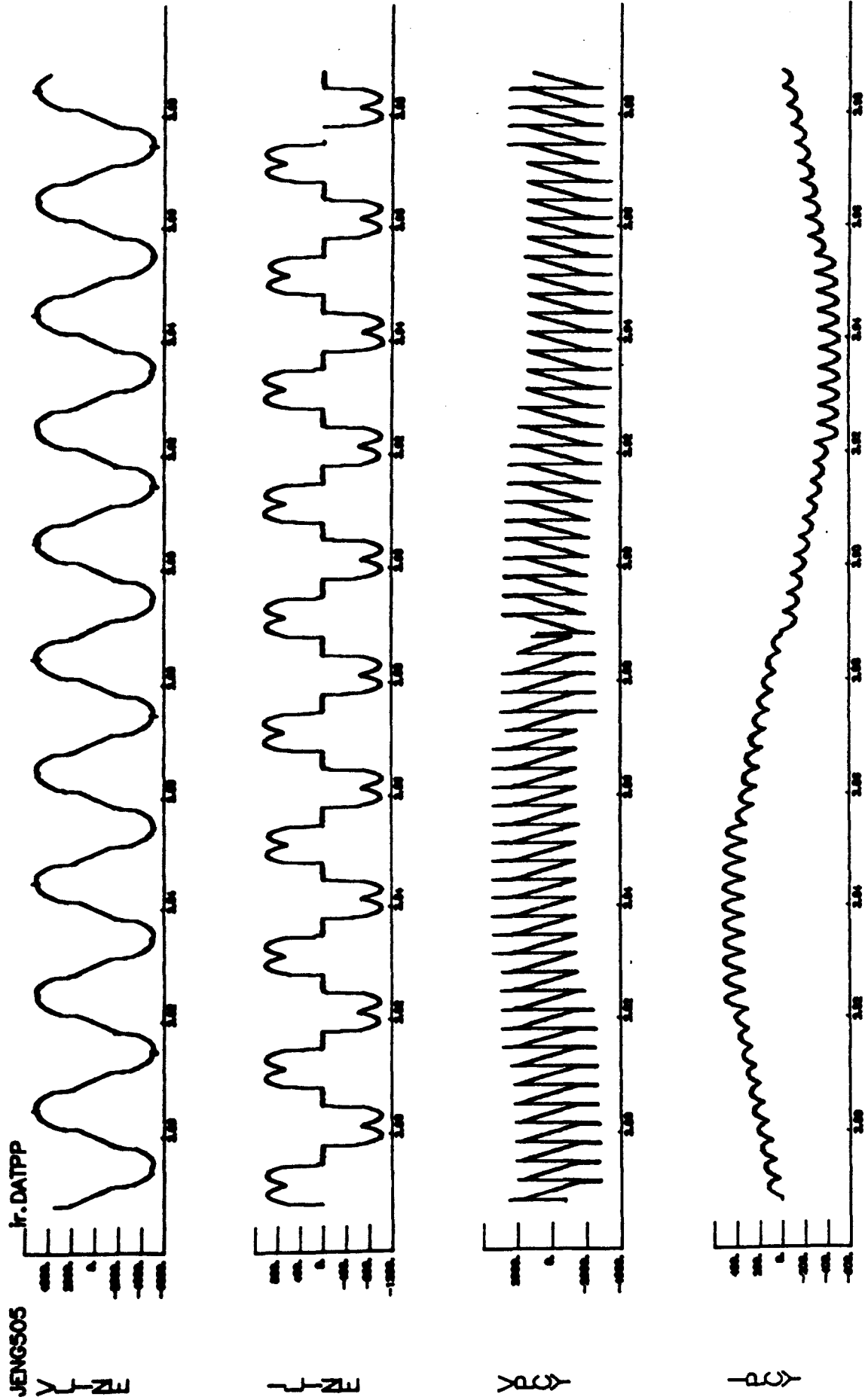
SPY-T



SPY-T



FREQ [MODEL<sup>2</sup> 5Hz] Fig 6.4f Harmonics of system with Model 2



TIME [MODEL 3]  
 Fig 6.4g Waveforms of system with Model 3

JENG505

SECUR.DATPP

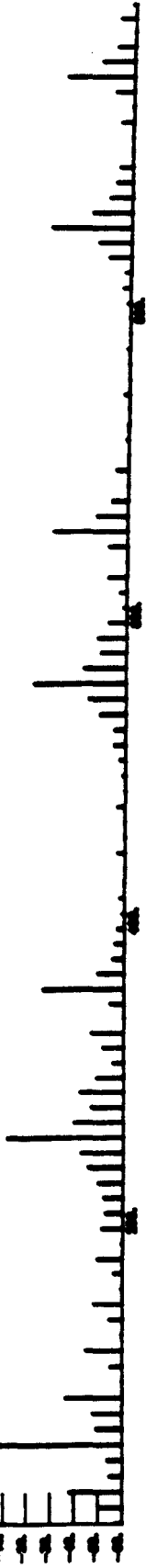
z-1-2

0  
-1  
-2  
-3  
-4  
-5  
-6  
-7  
-8  
-9  
-10



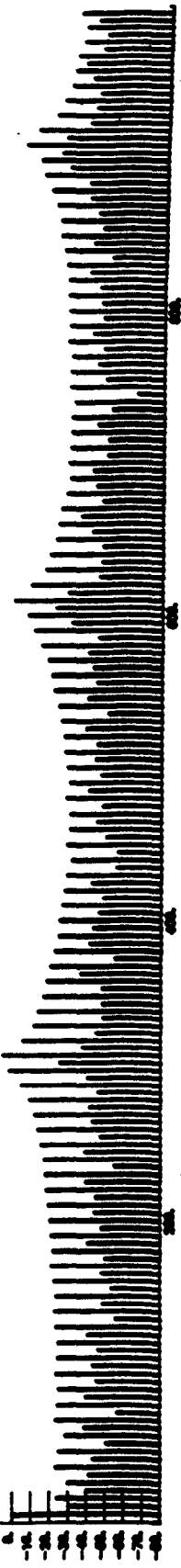
z-1-2

0  
-1  
-2  
-3  
-4  
-5  
-6  
-7  
-8  
-9  
-10



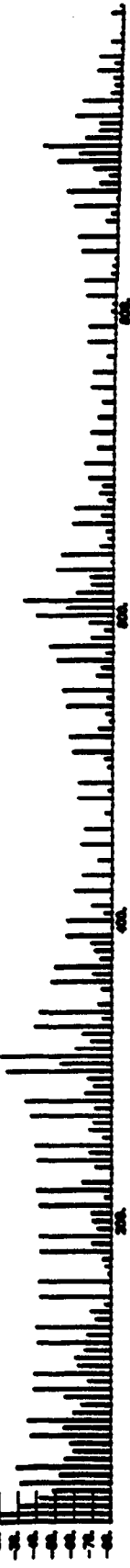
z-1-2

0  
-1  
-2  
-3  
-4  
-5  
-6  
-7  
-8  
-9  
-10



z-1-2

0  
-1  
-2  
-3  
-4  
-5  
-6  
-7  
-8  
-9  
-10



REQ [MODEL 3" 5Hz]

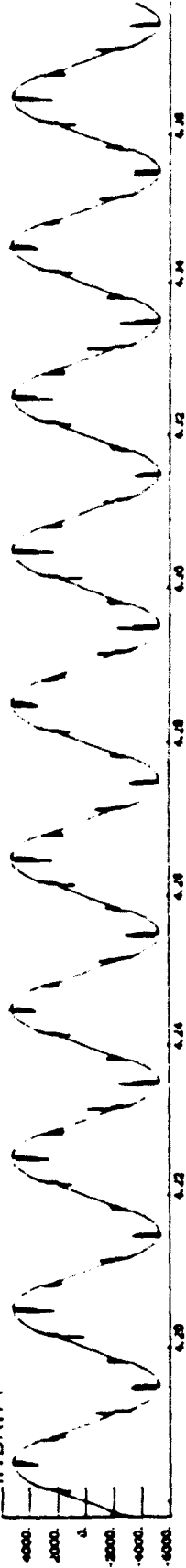
Fig 6.4h Harmonics of system with Model 3



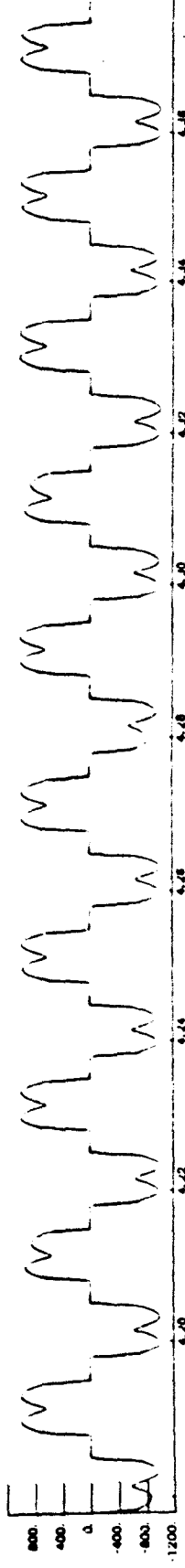
JENG505

ir.DATPP

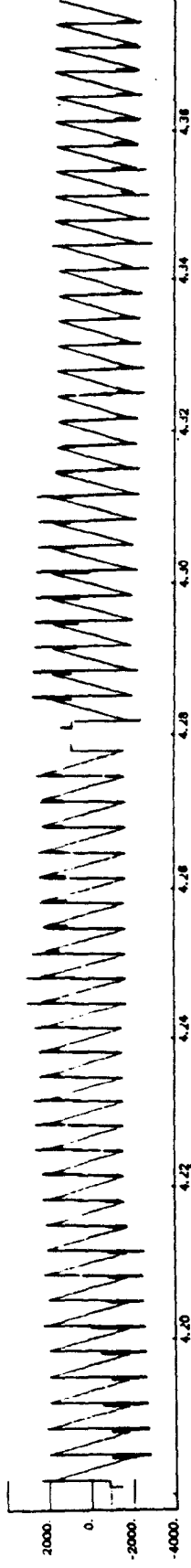
V  
T  
NE



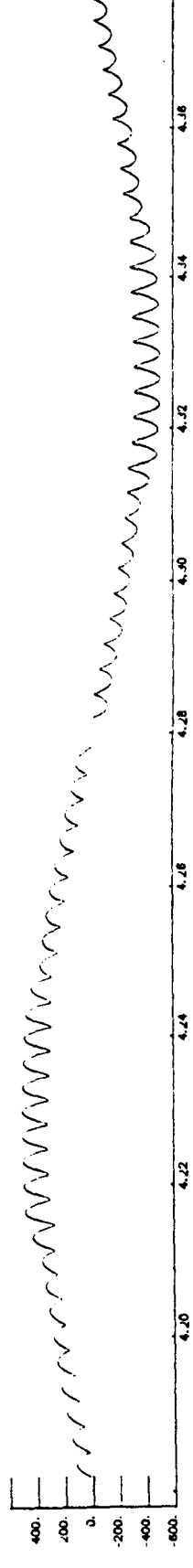
I  
T  
NE



Y  
PCY



I  
PCY



TIME [MODEL 4 5Hz]

Fig 6.4i Waveforms of system with Model 4

JENG505

SDCUR.DATPP

2-10-75

4

12

20

28

36

44

52

60

68

76

84

92

100

108

116

124

132

140

148

156

164

172

180

188

196

204

212

220

228

236

244

252

260

268

276

284

292

300

308

316

324

2-10-75

4

12

20

28

36

44

52

60

68

76

84

92

100

108

116

124

132

140

148

156

164

172

180

188

196

204

212

220

228

236

244

252

260

268

276

284

292

300

308

316

324

2-10-75

4

12

20

28

36

44

52

60

68

76

84

92

100

108

116

124

132

140

148

156

164

172

180

188

196

204

212

220

228

236

244

252

260

268

276

284

292

300

308

316

324

2-10-75

4

12

20

28

36

44

52

60

68

76

84

92

100

108

116

124

132

140

148

156

164

172

180

188

196

204

212

220

228

236

244

252

260

268

276

284

292

300

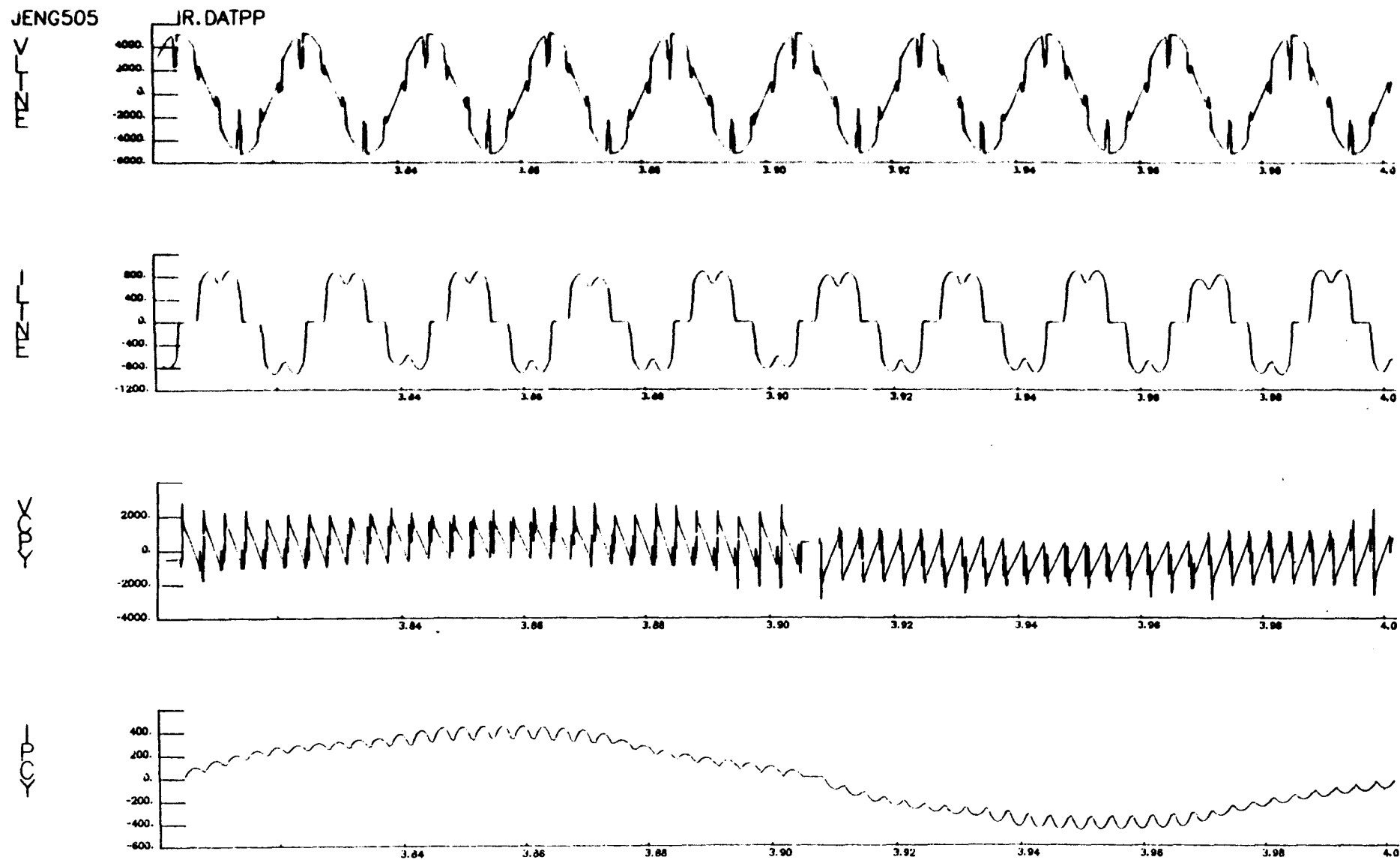
308

316

324

FREQ [MODEL 4 5Hz] Fig 6.4j Harmonics of system with Model 4

JENG505



TIME [MODEL 5  $\mu$ 5 Hz] Fig 6.4k Waveforms of system with Model 5

JENG505

\_SDCUR.DATPP

2-1-73

Δ

-10

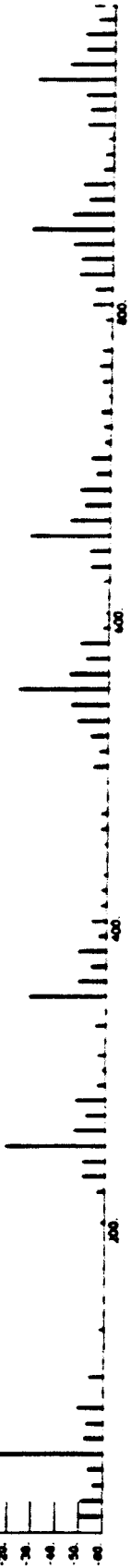
-20

-30

-40

-50

-60



2-1-73

Δ

-10

-20

-30

-40

-50

-60



2-1-73

Δ

-10

-20

-30

-40

-50

-60

-70

-80



2-1-73

Δ

-10

-20

-30

-40

-50

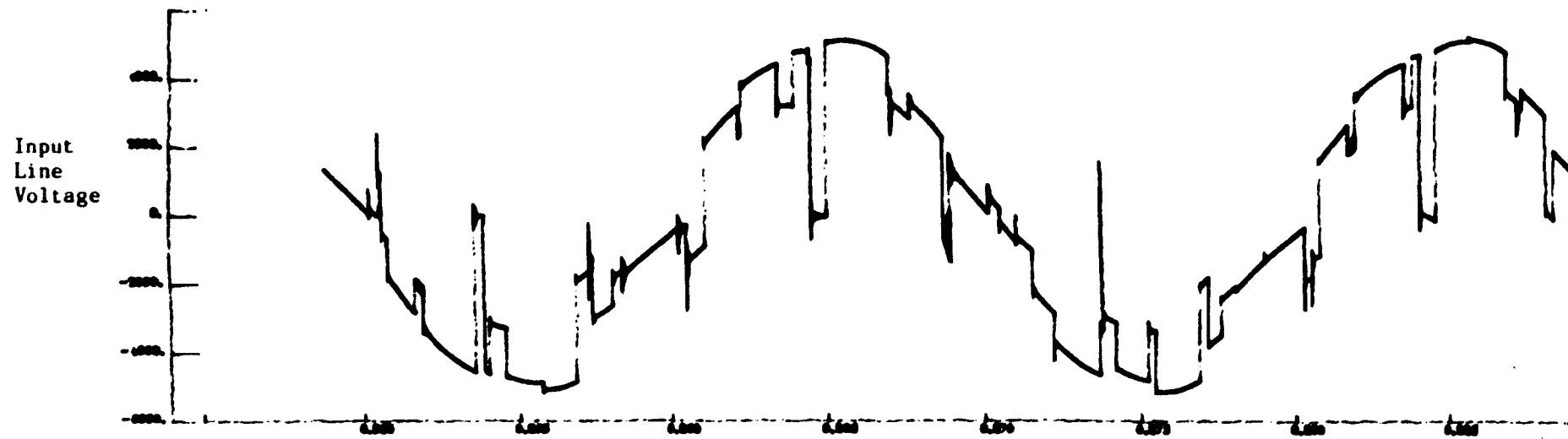
-60

-70

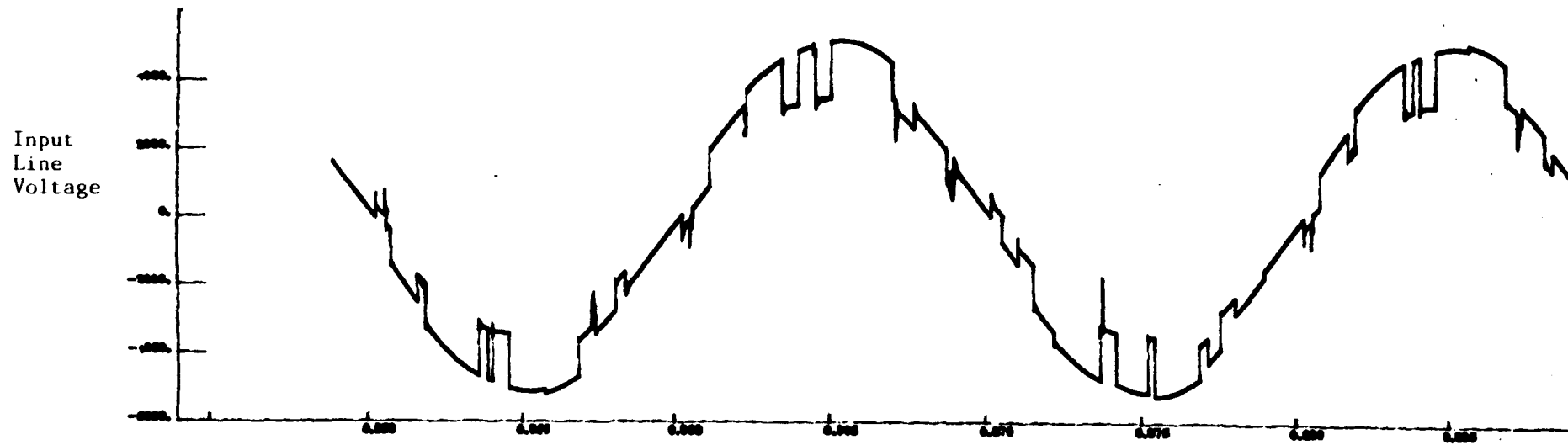
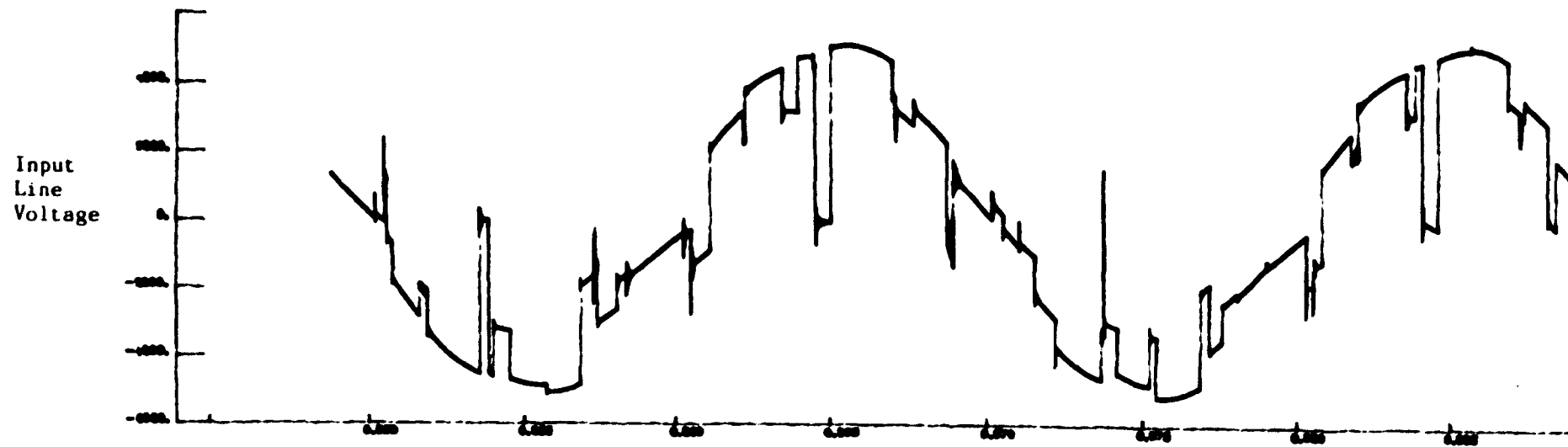
-80



FREQ [MODEL 5" 5Hz] Fig 6.41 Harmonics of system with Model 5



TIME(SECONDS) FREQUENCY 22.5 Fig 6.4m Waveform of typical commutation process



TIME(SECONDS) FREQUENCY 22.5 Fig 6.4n Waveforms of commutation with and without decoupling reactor

**Appendix E**

**Limits for harmonics in the United Kingdom  
Electricity Supply System:**

**Table E1 Permitted harmonic currents for any one  
consumer at the point of common coupling:**

**Table E2 Harmonic voltage distortion limits at any  
point on the system:**

**TABLE 2**

**PERMITTED HARMONIC CURRENTS FOR ANY ONE CONSUMER AT POINT OF COMMON COUPLING  
UNDER STAGE 2 LIMITS**

Supply System Voltage (kV) at Point of Common Coupling	Harmonic Number and Current (A rms)																	
	2	3	4	5	6	7	8	9	10	11	12	13	14	15	16	17	18	19
0.415	48	34	22	56	11	40	9	8	7	19	6	16	5	5	5	6	4	6
6.6 and 11	13	8	6	10	4	8	3	3	3	7	2	6	2	2	2	2	1	1
33	11	7	5	9	4	6	3	2	2	6	2	5	2	1	1	2	1	1
132	5	4	3	4	2	3	1	1	1	3	1	3	1	1	1	1	1	1

0 : A tolerance of +10% or 0.5 A (whichever is the greater) is permissible, provided it applies to not more than two harmonics.

**TABLE 3**

**HARMONIC VOLTAGE DISTORTION LIMITS AT ANY POINT ON THE SYSTEM  
(INCLUDING BACKGROUND LEVELS)**

Supply System Voltage (kV) at Point of Common Coupling	Total Harmonic Voltage Distortion $V_T(\%)$	Individual Harmonic Voltage Distortion (%)	
		Odd	Even
0.415	5	4	2
6.6 and 11	4	3	1.75
33 and 66	3	2	1
132	1.5	1	0.5



REFERENCES

1. Borman J., "Converters for ship propulsion drives" CEGELEC Publication
2. Brown J E, Vas P, Thornton P, "The analysis and computation of a 3-phase cyclo-converter/induction motor drive having isolated output phases"
3. Greer E. J., "Electrical power engineering in modern surface warships", GEC Review, Vol 2, No. 3 1986
4. "Electrical ship propulsion", GEC ALSTHOM EN 44759 a AN
5. Chattopadhyay A S, Janardhara Rao, T, "State-Variable Steady State Analysis of a Phased-Controlled Cycloconverter-Induction Motor Drive. IEE Trans. Ind. Appl., Vol 1A-15, No. 3, pp 313-317 May/June 79
6. Chattopadhyay A. K. and Janardhanara Rao T., "A Generalised Method of Computer Simulation for Induction Motors with Stator Current Discontinuities and its Application to a Cycloconverter-Fed Drive", IEE Transactions on Industry and Applications, IA-16, No. 2, 1980.
7. Cross D. M. and Taylor D. M. "Squirrel Cage Induction Motor Cyclo-Converter Drive at the British Coal Wearmouth Colliery", GEC Review, Vol. 4, No. 3, 1988.
8. R. Le Doruff and Siding, "Study by Digital Simulation of an Induction machine fed by a Three Phased Cyclo-converter", European Conference on Power Electronics, PE2/7.
9. Le Doeuff, Iung, Gudefin "Study by digital simulation of an induction machine fed by a three phased cyclo-converter" International Conference on Electrical Machines 1980, pp 704-11, Vol 2
10. Jacovides L J, "Analysis of a cyclo-converter induction motor drive system allowing for stator current discontinuities" IEEE Trans. Ind. Appl., Vol IA-9, No. 2, pp 206-215.
11. Niiraren Jouko, "Simulation of cyclo-converter fed three and phase synchronous motors during discontinuous stator current", International Conference on the Evolution and Modern Aspects of Synchronous Machines 1991.
12. Susumu Tadakuma and Yoshiaki Tamura, "Current Response Simulation in Six-Phase and Twelve-Phase Cycloconverters". IEEE Transactions, IA-15, No. 4, 1979.

13. Tuncay R.N, Alan I., Brown P.J., "The simulation , analysis and filtering of cycloconverters"  
European Conference on Power Electronics 1987
14. Finney D., "Variable frequency ac motor drive systems", Peregrinus Ltd,  
1988
15. Hancock N H, "Matrix Analysis of Electric Machinery"  
Pogamon Press, 1974.
16. Jones D., "The unified theory of electrical machines",  
Butterworths, 1967.
17. Pelly B. R., "Thyristor phase-controlled converters and cycloconverters", Wiley, 1971.
18. Say M. G., "Alternating Current Machines", Pitman 1976

### **The Test Program**

- Test 1a:** The effect of varying the time interval in the computer program
- Test 1b:** The accuracy of the numerical integration in the computer program
- Test 1c:** Characteristic performance of the Fourier analysis subroutine
- Test 2:** Comparison with results at Wearmouth Colliery
- Test 3:** Comparison with results at Newcastle University
- Test 4:** Monitoring the system behaviour

### **System characteristics and their effects**

- Test 5:** The effect of interbridge delay
- Test 6:** The effect of overlap
- Test 7:** The effect of the supply reactances
- Test 8:** The effect of the decoupling reactances

### **The modelling of complete systems**

- Test 9:** Comparison of Pelly's analytical model and the computer model with a sinewave output
- Test 10:** Comparison of Pelly's analytical mode and the simplified converter and the dq axis model
- Test 11:** Comparison of the simplified model 1 and the complex model 5
- Test 12:** Comparison of the simplified converter and supply reactance model 3, and the complex model 5
- Test 13:** Comparison of the typical industrial model 4, and the simplified model 1
- Test 14:** Comparison of the simplified converter model 1 and the Thevenin motor model 2

## The modelling of complete systems

Definition of the models used in the testing:-

- (a) Model 1    Simplified converter model/dq axis motor  
                  motor  
                  Supply reactance 0 %  
                  Decoupling reactance 0 %  
                  Interbridge delay 0.00 mS  
                  No overlap(reactance 0.0%)  
                  dq axis model motor
- (b) Model 2    Simplified converter model /Thevenin  
                  motor  
                  Supply reactance 0 %  
                  Decoupling reactance 0 %  
                  Interbridge delay 0.00 mS  
                  No overlap(reactance 0.0%)  
                  Thevenin model motor
- (c) Model 3    Simplified converter model including  
                  Supply reactance/dq axis motor  
                  Supply reactance 2.5 %  
                  Decoupling reactance 0 %  
                  Interbridge delay 0.00 mS  
                  No overlap  
                  dq axis model motor
- (d) Model 4    Low reactance Supply  
                  Supply reactance 1 %  
                  Decoupling reactance 2 %  
                  Interbridge delay 0.003 mS  
                  Overlap  
                  dq axis model motor
- (e) Model 5    High Reactance Supply  
                  Supply reactance 2.5 %  
                  Decoupling reactance 5.0 %  
                  Interbridge delay 0.003 mS  
                  Overlap  
                  dq axis model motor